BULGARIAN CHEMICAL COMMUNICATIONS

2020 Volume 52 / Special Issue B

Selected papers from the 10th Jubilee National Conference on Chemistry, Sofia, September 26-28, 2019

Journal of the Chemical Institutes
of the Bulgarian Academy of Sciences
and of the Union of Chemists in Bulgaria

Bulgarian Chemical Communications, Volume 52, Special Issue B (pp. 05-11) 2020 DOI: 10.34049/bcc.52.B.0002

Synthesis and properties of biocomposites based on collagen/ polyurethane

D. I. Zheleva*, L. N. Radev

University of Chemical Technology and Metallurgy - Sofia,
Department Textile and Leather

Received: November 29, 2019; Revised: October 12, 2020

Collagen is the most common protein. It is found in all multicellular organisms in the animal world. It is characterized by good biodegradability and biocompatibility, but with unsatisfactory physico-mechanical properties. Polyurethanes are considered to be the most promising class of polymers for *in vivo* studies, and fulfill all criteria for application to medical practice. These materials are biodegradable, characterized with thermal and mechanical stability but there is some limitation on their use due to the lack of biologically active groups. Therefore, collagen and polyurethane based composites, combining the benefits of natural and synthetic material, would be promising biomaterials for tissue engineering, medicine: drug delivery and other areas. In the present work biocomposites based on polyurethane/collagen were synthesized with different amounts of protein (5 and 10 wt.%) as a filler. An attempt was made to explain the mechanisms of interaction between polyurethane and collagen in the composite. FTIR analysis showed the formation of hydrogen and chemical bonds between collagen and polyurethane, as well as hydrogen bonds between urethane macromolecules themselves. DSC analysis confirmed the higher thermal resistance of the composites. *In vitro* tests revealed the formation of apatite layer, which was also confirmed by microscopic analyzes. This would accelerate the healing process in the human body, increasing the growth of osteoblast cells. Microscopic images showed 3-dimensional morphology, different pores with different sizes are observed, the pores are interconnected, allowing the constant transport of nutrients. Thus, the criteria for application to tissue engineering are fulfilled.

Keywords: biocomposites, collagen, polyurethane, biocompatibility

INTRODUCTION

Collagen is the main scleroprotein that builds the extracellular matrix of connective tissue. It is available in large quantities, especially as waste from slaughterhouses and leather production. Collagen can be used in various biomedical fields, especially in tissue engineering due to its biodegradability and biocompatibility. In the 1980s, collagen became the main biomolecule used in many medical fields, especially in the field of bone implant surgery [1-9]. Unsatisfactory mechanical properties are a major disadvantage of natural biomolecules. Collagen and elastin are two of the key structural proteins studied in the extracellular matrix of many tissues [10-12]. These proteins are important modulators of the physical properties of many skeletal and porous structures that affect cell adhesion and cell growth. Collagen can be obtained in various forms: porous sponges, gels, films and more. It is characterized by porous structure, hydrophilicity, and cellular and tissue adhesion, susceptible to combining with other materials (i.e. synthetic polymers).

The term "composite" means having two or more different parts [9]. Most composites are produced to ensure mechanical properties such as strength, stiffness, toughness and fatigue resistance combined with other necessary qualities: biological functions and biocompatibility.

Polyurethanes are synthetic materials, obtained from isocyanates and hydroxyl-containing components, which are considered the most promising class of polymers for *in vivo* studies. Reasons for this are their non-toxicity, tissue compatibility, high mechanical strength, elasticity and aging resistance. Their properties can be modified and various materials can be obtained: from rigid to elastic, coatings, fibers, foams, films and more. They are very important materials in tissue engineering. The properties and porous structure of the polyurethanes allow bone calcification processes to take place. Another advantage is their biodegradability through absorption, but there is some limitation on their application due to the lack of bioactive groups. Therefore, the key factors for their use as biomaterials include the ways to impart biodegradability and biological activity to polyurethanes. The latter can be modified with biomolecules to enhance their biocompatibility. Therefore, collagen and polyurethane composites combining the benefits of natural and synthetic material would be promising biomaterials for tissue engineering, medicine: drug delivery and other fields.

* To whom all correspondence should be sent:
E-mail: darinajeleva@abv.bg

There are numerous studies on the compatibility of collagen with synthetic polymers and other natural polymers, as well as on its self-application as a biomedical material [1-26].

Radev *et al*. investigated bioactive composites based on collagen-calcium phosphate silicate/ wollastonite [23]. *In vitro* bioactivity studies of hybrids have shown that hydroxyapatite (HA) is formed on the synthesized composite surface. The negatively charged carboxyl groups of the collagen molecule are responsible for the deposition of HA. Hydroxyapatite and other inorganic phosphates have the ability to induce osteoblastic cell growth and consequently bone repair, preventing an inflammatory response.

In our previous study [24], polyurethane (PU)/ bioglass (BG) composite materials were synthesized with different contents of BG (10 and 20 mol.%) as a filler. It has been proved that hydroxyapatite deposition induces osteoblast cell synthesis.

The solubility of collagen in acetic acid enables it to be mixed with other water-soluble polymers [1-3]. The biocomposites based on collagen and water-soluble synthetic polymers have been investigated in medical practice, namely: polyvinylpyrrolidone (PVP); polyvinyl alcohol (PVA); polyethylene glycol (PEG); polyethylene oxide (PEO) [15-22]. The composites can be processed into a variety of forms including porous sponges, thin films, hydrogels, coatings, etc. Other synthetic polymers used are: polyurethanes (PU); polyglycolic acid (PGA), polylactic acid (PLA), poly (DL-lactide-glycolide) (PLGA).

Jianjun *et al*. developed a flexible, biodegradable scaffold structure for cells transplantation in the form of a composite material based on biodegradable poly(esterurethan) urea and collagen type I [16]. Poly(esterurethan) urea was synthesized from poly(caprolactone), 1,4-diisocyanatebutan and putrescine.

The synthesis and properties of a microporous composite based on polyurethane and collagen were investigated (collagen content: 0-15 wt.%). The resulting two-phase structures are characterized by good mechanical properties, pores of the required dimensions and biocompatibility, which are important indicators for biomedical application [17].

Collagen coatings have been successfully applied to numerous hydrophilic polymer scaffolds to improve cell adhesion [18].

The regeneration of damaged or lost tissue requires some functional repair cells to assemble three-dimensionally around and inside the surrounding porous structure [22]. Collagen-based nanofibers and functionalized thermoplastic polyurethane (TPU/collagen) have been successfully obtained by electrospinning technique to produce biomedical material with a porous structure.

A variety of hybrid systems have been developed and optimized to obtain optimal polyurethane structures, some of which serve to aid the healing process, others are applied in the form of implants, others are for drug delivery, for enhancing cell adhesion, cell growth, and more.

The purpose of the present study is to synthesize biocomposites based on polyurethane and collagen, to evaluate the *in vitro* bioactivity of the resulting biocomposites and to analyze application options in tissue engineering and other fields. The other aim is to explain the mechanisms of interaction between collagen and polyurethane in the composite.

EXPERIMENTAL

Materials

Collagen type I (extracted from the skin of bovine lyophilized tissue) was supplied by the Leather-Footwear Research Institute (Bucharest, Romania). Collagen was added as a filler in composite compositions.

The components used for the synthesis of polyurethane foam are as follows: 4,4'-methylenebis (phenylisocyanate) (MDI), from Alfa Aesar, Germany, with a melting point of 40°C, density 1.230 g/cm^3; polypolyol (Lupranol 2095) from BASF - highly reactive trifunctional polyether, molecular weight 4800 g/mol, hydroxyl number 35 and viscosity 850 mPa.s; 1,4-butanediol (BD) as a chain extender; water as a foaming component.

Polyurethane synthesis

The synthesis of polyurethane foam (PUR) was carried out by the reaction of 2-step polyaddition of polyesterpolyol (Lupranol 2095) and 4,4'-methylenebis (phenylisocyanate) (MDI), by extending the chain with 1,4-butanediol, and adding the foaming component.

The process of preparing the polyurethane foam includes two steps: (1) To 10 g of polyol component (Lupranol 2095), a few drops of water are added and the mixture is stirred vigorously. To the polyol mixture a stoichiometrically calculated amount of isocyanate (MDI) - 1 g, is added, followed by vigorous stirring again. The synthesis reaction proceeds at 50°C for 30 min. The next step (2) is the addition of the chain extender (1,4-butanediol) to increase the molecular weight. The

foaming reaction begins seconds after the components are mixed. For PUR synthesis, the reaction with water is important (step 1), in which 2 isocyanate molecules react with 1 molecule of water. The first obtained product is carbamic acid. It is unstable and releases carbon dioxide, which acts as a foaming agent during polycarbamide formation, which leads to the building of the basic macromolecular skeleton. The following process is the reaction of the amine with isocyanate to form urea:

$$R\text{-}NCO + H_2O \longrightarrow R\text{-}NH_2 + CO_2 \xrightarrow{+\ R\text{-}NCO} R\text{-}NH\text{-}CO\text{-}NH\text{-}R$$

The two-step polymerization process is more complex. In the first step, the polyol reacts with excess of diisocyanate, resulting in a prepolymer. This prepolymer is a mixture of elastic segments with terminal isocyanate groups that will form solid segments later. In the second stage, the chain extender is introduced. It reacts with the remaining amount of unreacted diisocyanate, forming solid segments and bonding them to the elastic segments. The material has a two-phase structure, i.e. presence of domains resulting from the agglomeration or crystallization of the various chains. These domains are different for different materials and this predetermines the higher or lower elasticity [25]. In addition to having a two-phase structure, the material also has many functional groups: hydroxyl, ester, ether, urethane -NHCOO-, isocyanate, urea, amide, allophanate, biuret, and hydrogen bonds.

Synthesis of the biocomposites

In the synthesis of PU/Coll (polyurethane/ collagen) composites, collagen was added *in situ* during the polymerization reaction. The reaction proceeds in the same way as for pure polyurethane, except that collagen (Coll) was pre-prepared as an aqueous solution. Collagen in an amount of 5 and 10 wt. % was added to the polyol component. The stoichiometrically calculated amount of isocyanate (MDI) -1 g was then added to the polyol mixture, again followed by vigorous stirring. The synthesis reaction proceeds at 50°C for 30 min. The next step was the addition of the chain extender (1,4-butanediol). The composites are called PU/5Coll and PU/10Coll. In the resulting biocomposite material, in addition to the abundance of polyurethane functional groups, collagen also offers its functional groups: hydroxyl, carboxyl, amide (-NH-CO-), imide (-CO-N=), and polar terminated groups (-COOH, $-NH_2$, -OH).

Bioactivity essay

Bioactivity of the composites obtained was evaluated by examining the apatite formation on their surfaces in SBF solutions. The SBF was prepared from the following salts: NaCl = 11.9925 g, $NaHCO_3$ = 0.5295 g, KCl = 0.3360 g, $K_2HPO_4 \cdot 3H_2O$ = 0.3420 g, $MgCl_2 \cdot 6H_2O$ = 0.4575 g, $CaCl_2 \cdot 2H_2O$ = 0.5520 g, Na_2SO_4 = 0.1065 g, and buffering at pH 7.4 at 36.5ºC with 9.0075 g of *tris* (hydroxymethyl) aminomethane (TRIS) and 1M HCl. A few drops of 0.5% NaN_3 were added to the SBF solution to inhibit the growth of bacteria [27]. After soaking the specimens were removed from the fluid, gently rinsed with distilled water, and then dried at 36.6ºC for 12 h.

In vitro tests of composites in SBF were performed for 7 days under static conditions.

Methods for analysis

Fourier-transform infrared (FTIR) spectroscopy was used for qualitative analysis of the obtained composites. FTIR transmission spectra were recorded by using a Bruker Tensor 27 spectrometer with scanner velocity of 10 kHz. KBr pellets were prepared by mixing ~1 mg of the samples with 300 mg of KBr. Transmission spectra were recorded using MCT detector, with 64 scans and 1 cm^{-1} resolution.

Scanning electron microscopy SEM (Jeol, JSM-35 CF, Japan) was used to ascertain the morphology and chemical constituents of the prepared composites before and after immersion in 1.5 SBF for 7 days at an accelerating voltage of 15 kV.

The differential scanning calorimetry (DSC) method was used to determine the changes in enthalpy, thermal and oxidation stability of the samples. STA PT1600 TG-DTA/DSC (STA Simultaneous Thermal Analyses), Messgeräte GmbH, Germany was used, with a temperature range of 20 ÷ 1550 ºC.

RESULTS AND DISCUSSION

Characterization of the biocomposites before in vitro test in SBF

Figs. 1 and 2 show typical infrared spectra of pure polyurethane (PU) and pure collagen (Coll), which will be compared with the spectra of the biocomposites. In Fig. 1, the spectrum reveals the characteristic bands of PU, the stretching vibrations of the N-H bond at 3392 cm^{-1}, the asymmetric and symmetric vibrations of the CH_2 groups at 2924

cm^{-1} and 2858 cm^{-1}, respectively [29]. The other vibrational bands of CH_2 are positioned at 1410, 1373, and 1303 cm^{-1} [29, 30]. The absorption band of amide I is at 1706 cm^{-1} [29, 31]. Strongly expressed strain δ (N-H) and valence vibrations ν (C-H) are recorded at 1510 cm^{-1} [29] and δ (N-H) + ν (C-N) are recorded at 1237 cm^{-1} [29, 32]. The band at 1450 cm^{-1} is characteristic for the elastic segments of PUR. Absorption at 1183 cm^{-1} and 1100 cm^{-1} refers to the ether bonds [29, 33] and the C-O-C stretching is observed at 1012 cm^{-1} [29, 34]. In addition, the spectrum shows bands at 1776-1597 cm^{-1} that refer to the C=O bond in polyurethane [29]. Moreover, the stretching bands at 1665 cm^{-1} and 1706 cm^{-1} are due to the absorption of hydrogen bonded C=O of urethane linkages [29, 35, 36]. In addition, the isocyanate group absorbs strongly at 2275 cm^{-1} [37]. Many functional groups were registered in the structure of polyurethane.

Fig. 2 shows the FTIR spectrum of collagen. Especially, the amide I, II and III band regions of the spectrum are directly related to the polypeptide conformation [38]. The amide I band, with a characteristic frequency in the range of 1600-1700 cm^{-1}, is mainly associated with the stretching vibrations of the carbonyl groups (C=O bond) along the polypeptide chain and refers to peptide secondary structure [39]. The amide I bands are at 1650-1660 cm^{-1}, 1630-1640 cm^{-1}, and 1680-1700 cm^{-1} in the amide I region of the protein. In our case, the amide I band is centered at 1656 cm^{-1}. In the amide II region of proteins there are bands at 1540-1550 cm^{-1}, 1620-1530 cm^{-1}, and 1520-1545 cm^{-1} [40, 41]. In our case, the amide II is centered at 1553 cm^{-1}. For the amide III band of protein, there are bands centered at 1270-1300 cm^{-1}, 1229-1235 cm^{-1}, and 1243-1253 cm^{-1}. From Fig. 2, the amide III bands were assigned at 1240 and 1281 cm^{-1}. Amide B is centered at 3081 cm^{-1} [39]. The two bands visible at 1399 and 1340 cm^{-1}, can be assigned to the presence of COOH and COO- in the spectrum of pure gelatin and collagen [42].

The spectra of the composites PU/5Coll and PU/10Coll are presented in Figs. 3 and 4. The characteristic bands at 3400 cm^{-1} for N-H bonds are observed. The peak at this absorption band is smaller for pure polyurethane than for PU/Coll. This is an indicator of the occurrence of hydrogen bonds between collagen and polyurethane macromolecules, which leads to strengthening or crosslinking of the structure of the composite. The intensity of the peak of the composite at 1600 cm^{-1} increases, which means that the -OH, $-NH_2$, C=O groups of collagen form hydrogen bonds with the C=O and N-H groups of polyurethane. It can be seen that hydrogen bonds are also formed between urethane macromolecules themselves. The improvement of samples properties even in the presence of small amounts of collagen is confirmed by other assays. It also decreases the peak intensity at 2275 cm^{-1} due to the depletion of the isocyanate groups. This may be explained by the formation of new urethane bonds (-NHCOO-) between the OH groups of collagen and the isocyanate (NCO-) groups of polyurethane.

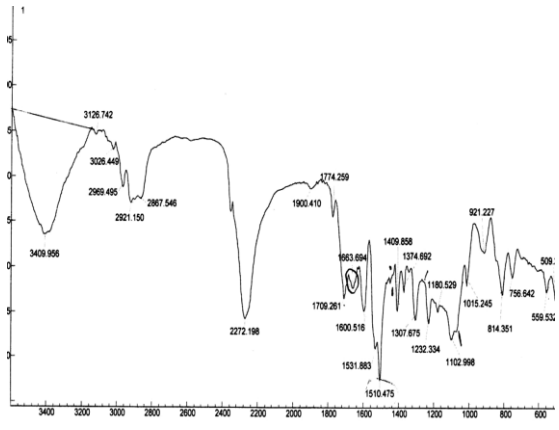

Fig. 1. FTIR spectrum of pure polyurethane (PU)

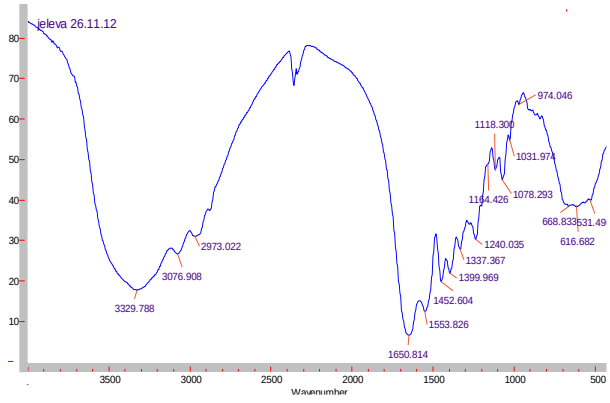

Fig. 2. FTIR spectrum of pure collagen (Coll)

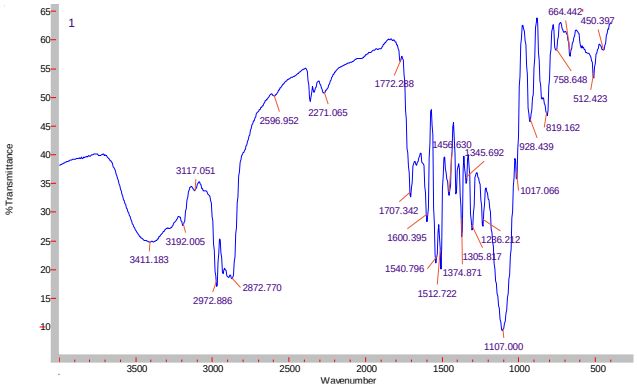

Fig. 3. FTIR spectrum of PU/5Coll composite

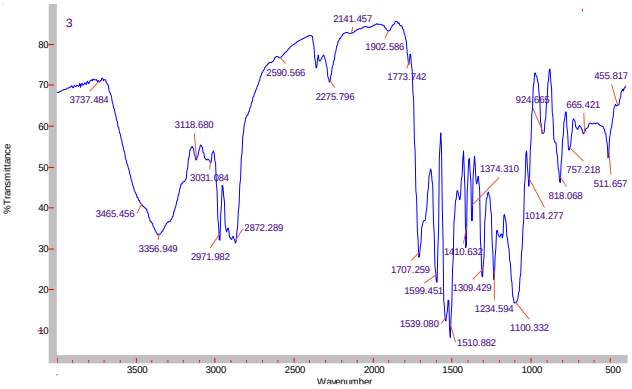

Fig. 4. FTIR spectrum of PU/10Coll composite

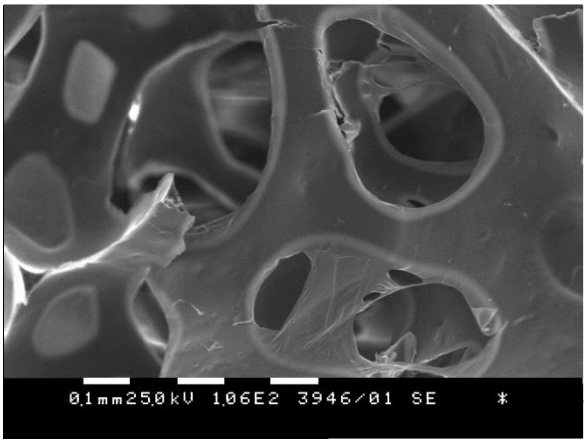

Fig. 5. SEM of PU

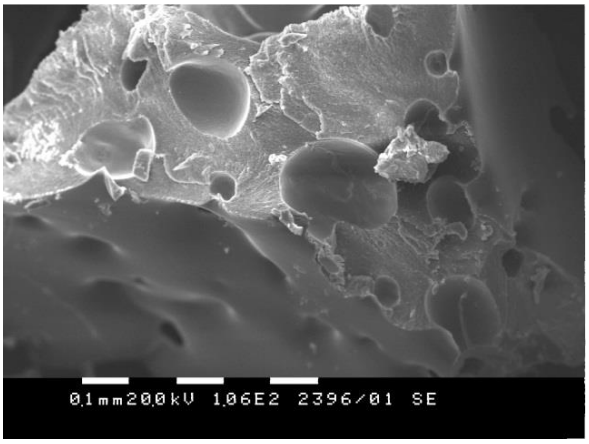

Fig. 6. SEM of the PU/Coll composite

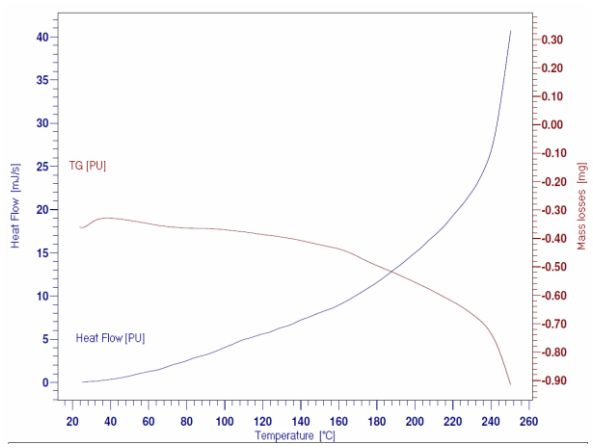

Fig. 7. DSC curves of PU

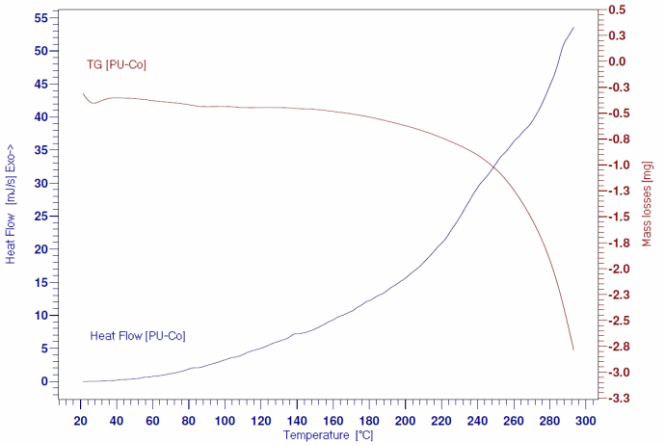

Fig. 8. DSC curves of PU/Coll

The microscopic images (Figs. 5 and 6) show 3-dimensional morphology, interconnected pores with different sizes. The PU/Coll porous scaffolds (Fig. 6) have not only macropores, but also a lot of micropores positioned on the macroporous wall, allowing for the constant transport of nutrients.

The formation of the porous structure can be explained by the gelation mechanism in which the collagen migrates to the surface of the composite films and thus large pores are formed. These pores are randomly distributed and interconnected. The interconnectedness is due to the presence of smaller pores that are adjacent to the collagen fibers. This improves the hydrophilicity of the biocomposites [28].

From the DSC analysis (thermogravimetric curves in Figs. 7 and 8) it can be seen that the transition temperature increases with the addition of the protein and therefore the samples are more thermally stable, increasing the enthalpy. This means that the composites show a higher destruction temperature. Confirmed by other

methods, this is due to the additional cross-linking of structures and the formation of hydrogen and chemical bonds between the molecules of the synthetic and natural polymer. From the thermal analysis, the primary mass loss at 20°C in the TG curve for PU is about ~ 4.5% (Fig. 7) and for the PU/Coll composite it is ~ 1.8% (Fig. 8), which is explained by evaporation of free water and solvents. Between 160-250ºC the mass loss for PU is approximately 8.5% and for PU/Coll between 180 - 300ºC the mass loss is 14%, which also shows the higher thermal destruction of the composite.

Characterization of the biocomposites after in vitro test in SBF

It was observed following feature in each of the samples after soaking in simulated body fluid (SBF). The spectrum of the biocomposite (Fig. 9) shows peaks at 630 cm^{-1} and 560 cm^{-1}, which is an evidence of the formation of hydroxyapatite forms observed in microscopic studies.

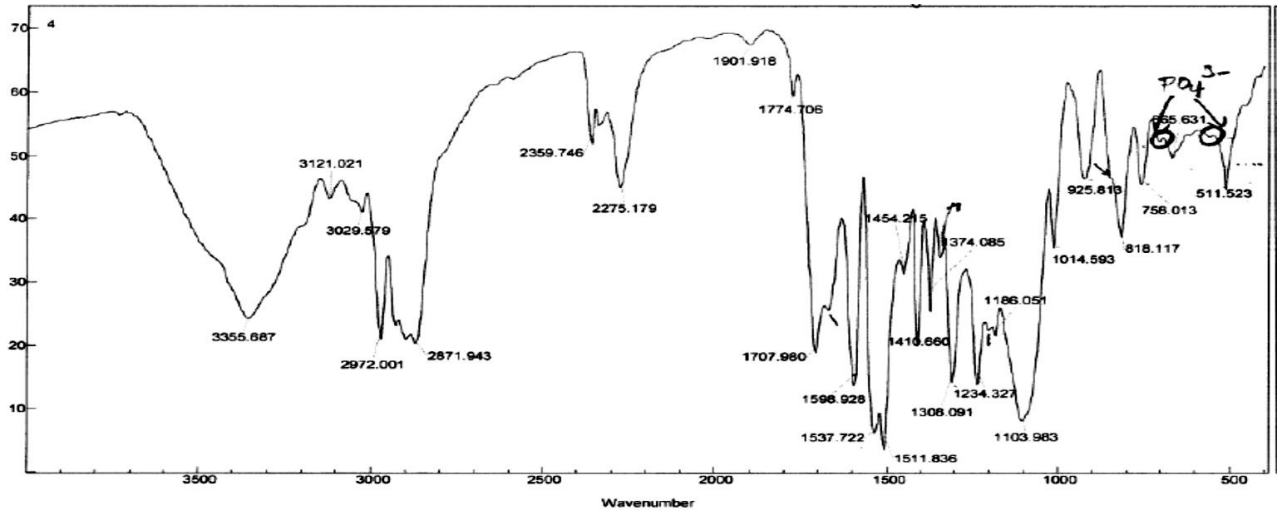

Fig. 9. FTIR spectrum of the PU/Coll composite after *in vitro* test in SBF for 7 days

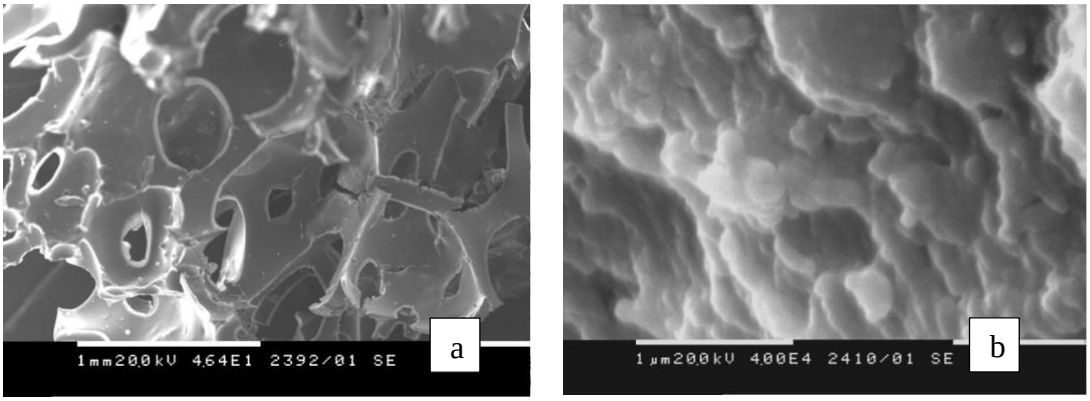

Fig. 10. SEM of the PU/Coll composites after *in vitro* test at different magnifications

The microscopic images (Fig. 10) also show deposition of spherical-sized hydroxyapatite agglomerates after 7-day soaking in SBF. The exact mechanism of calcification is still unclear, but it has been reported that this occurs by the interaction of the polyurethane foam with calcium and phosphorus ions in blood or other body fluid [25, 43]. Bone is a specific form of connective tissue composed of a collagen skeleton impregnated with calcium salts (Ca^{2+}, PO_4^{3-}) [25]. The presence of oxygen is thought to have the greatest influence on calcification. Calcification in hydrophobic polyether urethanes takes place on a surface that is in direct contact with body fluids. In the case of hydrophilic polyether urethanes (as well as our samples), this process takes place both on the surface and through the polymer. For example, acceleration of calcification can be achieved by modification with PEG (polyethylene glycol), which increases the hydrophilicity of PUR [43]. In our composites, collagen, as a natural molecule, increases the hydrophilicity of the biomaterial, imports biological groups, and it would improve cell adhesion and proliferation. PURs swell in the

SBF fluid and increase volume, which increases the direct contact between the material and the tissue [44].

Morphological properties of the PU/Coll samples after soaking in SBF during 7 days, observed by SEM at high magnifications (Fig.10b), show that soaking led to formation of an apatite layer on the surface of the samples. The pores are interconnected to allow continuous flow of nutrients in the scaffold.

CONCLUSION

Biocomposites based on polyurethane/collagen were synthesized with different amounts of protein (5 and 10 wt.%) as a filler. FTIR analysis showed the formation of hydrogen and chemical bonds between collagen and polyurethane, as well as hydrogen bonds between the polyurethane chains. The result is crosslinking and additional reinforcement of the composite structure. *In vitro* tests revealed the formation of hydroxyapatite, confirmed by microscopic analyses. Collagen increases the hydrophilicity of the biomaterial, introduces biological groups, which would lead to improved cell adhesion and proliferation. Microscopic images showed 3-dimensional morphology, different pores with different sizes, and interconnected pores allowing the constant transport of nutrients. Thus, in large part, the criteria for application to tissue engineering are fulfilled. This would accelerate the healing process in the human body, increasing the growth of osteoblast cells.

REFERENCES

1. K. A. Piez, *J. Dent. Res.*, **45**(3), 463 (1966).
2. S. Stegman, S. Chu, R. Armstrong, *J. Dermatol. Surg. Oncol.*, **14**(1), 39 (1988).
3. C. H. Lee, A. Singla, Y. Lee, *Inter. J. Pharm*., **221**(1-2), 1 (2001).
4. I. Chakarska, PhD Thesis, UCTM, Sofia, (2008).
5. J. Heino, *Bioessays*, **29**(10), 1001 (2007).
6. E. Khor, *Biomaterials*, **18**(2), 95 (1997).
7. O. Damink, L. H. H. P. J. Dijkstra, M. Luyn, *J. Mat. Sci*.: *Mat. in Med.*, **17**(8), 765 (1996).
8. Z. Tang, Y. Yue, *A SAIO J.*, **41**, p.72-78 (1995)
9. B. D. Rather, A. S. Hoffman, F. J. Shoen, J. Lemons, Biomaterials Science – an Introduction to Materials in Medicine, USA, 1996, ISBN: 0-12-582460-2.
10. M. Popescu, C. Vasile, D. Macocineschi, *Intern. J. Biol. Macromol.*, **47**, 646 (2010).
11. D. Filip, D. Macocinchi, S. Vlad, *Composites, Part B*, **42**, 1474 (2011).
12. S.-H. Rhee, J. Tanaka, *J. Amer. Ceram. Soc.*, **83**(8), 2100 (2000).
13. E. Jabbari, M. Khakpour, *Biomaterials*, **21**, 2073 (2000).
14. M. N. Huang, J. Wang, J. Luo, *J. Biomedical Sci. Eng.*, **2**, 36 (2009).
15. A. Scotchford, M. G. Cascone, S. Downes, *Biomaterials*, **19**(1-3), 1 (1998).
16. G. Jianjun, J. Stnakus, W. Wagner, *Cell. Transplant.*, **15**, S17 (2006).
17. S. Oprea, *J. Composite Materials*, **44**, 18 (2010).
18. T. Douglas, H. Haugen, *J. Mater. Sci.: Mater. Med.*, **19**, 2713 (2008).
19. C. Huang, R. Chen, Q. Ke, Y. Ke, K. Zhang, X. Mo, *Colloids and Surf. B: Biomaterials*, **82**,307 (2011).
20. R. Chen, C. Uang, Q. Ke, C. He, H.Wang, X. Mo, *Colloids and Surf. B: Biointerfaces*, **79** (2010).
21. T. Masayuki, K. Sasaki, S. Saiton, *J. Oral. Tissue Eng.*, **4**(2), 68 (2006).
22. G. Sarawathy, S. Pal, C. Rose, T. Sastry, *Bull. Mater. Sci.*, **24**(4), 415 (2001).
23. L. Radev, V. Hristov, B. Samuneva, D. Ivanova, *Centr. Eur. J. Chem.*, **7**(4), 711 (2009).
24. L. Radev, D. Zheleva, I. Mihailova, *Centr. Eur. J. Chem.*, **11**(9), 1439 (2013).
25. M. Marzec, J. Kucinska-Lipka, I. Kalaszszynska, H. Janik, *Mat. Sci. Eng., C,* **80**, 736 (2017).
26. M. Zuber, F. Zia, K. Zia, S. Tabasum, M. Salman, *Inter. J. Biol.Macromol.*, **80**, 366 (2015).
27. J. Abe, T. Kokubo, T. Jamamuro, *J. Mater. Sci.: Mater. Med.*, **1**, 233 (1990).
28. A. Bayley, *Mechanism of Aging and Development*, **122**, 735 (2001).
29. A. S. Khan et al., *Acta Biomaterialia*, **4**(5), 1275 (2008).
30. K. Gorna, S. Gogolewski, *Polym. Degrad. Stabil.*, **75**(1), 113 (2002).
31. E. Ayres, R. L. Oréfice, M. I. Yoshida, *Eur. Polym. J.*, **43**(8), 3510 (2007).
32. G. Wang, Ch. Zhang, X. Guo, Zh. Ren, *Spectrochimica Acta Part A: Molecular and Biomolecular Spectroscopy*, **69** (2), 407 (2008).
33. J. Guan, M. Sacks, E. J. Beckman, W. Wagner, *J. Biomed. Mater. Res.* A, **61**(3), 493 (2002).
34. A. Mishra, D. Chattopadhyay, B. Sreedhar, K. Raju, *Prog. Org. Coat*., **55**(3), 231 (2006).
35. L.-F. Wang, *Polymer*, **48**, 894 (2007).
36. Ch. Chen et al., *Polymer*, **46**, 11849 (2005).
37. M. J. Forrest, *Papra Review Reports*, UK, (2001).
38. A. Santos, L. Hemeine, H. Mansur, *Mat. Sci. and Eng. C*, **28**, 563 (2008).
39. J. Payne, A. Vies, *Biopolymers*, **27**, 1749 (1988)
40. S. Krimm, J. Bandekar, *Adv. Protein Chem.*, **38**, 181 (1986).
41. E. Sachlos D. A. Wahl, J. T. Triffitt, J. T. Czernuszka, *Acta Biomaterialia*, **4**, 1322 (2008).
42. M. Chang, C. Ko, W. Douglas, *Biomaterials*, **24**, 2853 (2003).
43. T. Thoma, *J. Biomater. Appl.*, **1**, 449 (1987).
44. J. Podporska-Carrol, J. W. Y. Ip, S. Godolewski, *Acta Biomaterialia*, **10**, 2781 (2014).

Bulgarian Chemical Communications, Volume 52, Special Issue B (pp.12-15) 2020 DOI: 10.34049/bcc.52.B.0003

Bitter vetch seeds (*Vicia ervilia* L.) – a valuable source of nutrients

Zh. Y. Petkova[1*], G. A. Antova[1], M. Y. Angelova-Romova[1], A. Petrova[1], M. Stoyanova[2], S. Petrova[3], A. Stoyanova[2]

[1] *University of Plovdiv 'Paisii Hilendarski', Department of Chemical Technology, 24 Tzar Asen Str., 4000 Plovdiv, Bulgaria*
[2] *University of Food Technologies, 26 Maritza Blvd., 4003 Plovdiv, Bulgaria*
[3] *Institute of Plant Genetic Resources 'Konstantin Malkov', 2 Drouzhba Str., 4122 Sadovo, Bulgaria*

Received: October 31, 2019; Revised: September 11, 2020

The main nutrients of seeds from bitter vetch (*Vicia ervilia* L.) were determined. The seeds were with Russian origin, introduced in Bulgaria. They possessed high carbohydrate (66.2%) and protein (20.1%) content, but their oil content was extremely low (1.4%). The starch and dietary fibers were found to be 20.4 and 3.1%, respectively. The individual composition of water-soluble carbohydrates was determined by high performance liquid chromatography on an Agilent® LC 1220 instrument equipped with a refractive index detector. Total content of water-soluble carbohydrates was found to be 4279.0 mg/100 g. It was established that the only disaccharides in the seeds were sucrose (2649.8 mg/100 g) and cellobiose (149.4 mg/100 g), while the main monosaccharides were glucose (600.9 mg/100 g) and fructose (540.7 mg/100 g). The content of rhamnose and xylose was 198.3 and 140.1 mg/100 g, respectively. Amino acid composition of the seeds from bitter vetch was also determined and 17 amino acids were identified. The major amino acid was phenylalanine (46.2 mg/g), followed by lysine (34.8 mg/g) and histidine (30.0 mg/g). The moisture of the seeds was found to be 9.7% and the ash content was 2.6%. The content of the main nutrients in bitter vetch seeds is relatively high which determines their satisfying energy value – 357 kcal/100 g (1520 kJ/100 g) that corresponds to the energy value of the most commonly used legume seeds.

Keywords: bitter vetch, chemical composition, carbohydrates, amino acids

INTRODUCTION

Legume crops are considered as a very important food group because they are a major source of protein. They are mostly spread in Asia and America, being used as food and for industrial processing. Recently, protein deficiency has been observed in Europe, encouraging the cultivation of legumes that possess high protein content (25-40%) [1]. In Bulgaria, legumes occupy less area than cereals, and the main crops are chickpeas, peas, lentils, beans and soybeans, which are the richest in protein of all legumes. Proteins from leguminous plants are the cheapest and can be used as an additive to increase the protein content of foods for human consumption and feed for animals [2, 3]. Legumes are unique foods because of their rich content of other nutrients such as starch, fiber, oligosaccharides and minerals [1, 4].

Nowadays, there is an increasing interest in new alternative crops that could be a source of valuable nutrients for human consumption. As an alternative to the major legume species bitter vetch (*Vicia ervilia* L.) can be offered [5]. Bitter vetch is an annual crop from the family Fabaceae grown in the Mediterranean region, western and central Asia, North Africa and America [6-9]. The plant is mainly cultivated for forage and yield of seeds. The total protein content of bitter vetch seeds ranges between 20 and 30% [2, 5, 7, 8, 10-16] and their oil content is extremely low (1-2%) [1, 12]. According to Fernández-Fígares *et al.* (1995) [10] the main amino acids in bitter vetch seeds are glutamic acid (18.13 g/kg) and aspartic acid (9.47 g/kg). Sadeghi *et al.*, 2009 [15] also reported that the same amino acids prevailed in the seeds (19.63 and 13.83 g/100 g crude protein, respectively).

The information about the chemical composition of bitter vetch seeds is rather scarce. The previous examinations were mainly focused on their total protein and lipid content, crude fibers, dry matter and ash content, but there was lacking data about total carbohydrates, starch content, energy value of the seeds, as well as the content of water-soluble sugars and amino acid composition. For that reason, the aim of the present study is to perform a thorough determination of the chemical composition of bitter vetch (*Vicia ervilia* L.) seeds with Russian origin introduced in Bulgaria, in order to prove their nutritional value.

* To whom all correspondence should be sent:
E-mail: zhanapetkova@uni-plovdiv.net

MATERIALS AND METHODS

Samples

Bitter vetch seeds, identified as *Vicia ervilia* L., were obtained by the Institute of Plant Genetic Resources "Konstantin Malkov", Sadovo, Bulgaria (crop 2018). The seeds were with Russian origin (var. Krasnografskaya) introduced in the southern part of Bulgaria.

Chemical composition

The oil was extracted from ground seeds using hexane in a Soxhlet apparatus for 8 h [17]. Protein was calculated from the nitrogen content by Kjeldahl method using a factor of 6.25 [18]. The carbohydrate content was calculated by the following formula:

100 – (weight in grams [protein + lipids + water + ash] in 100 g of dry seeds) [19].

The starch content was determined by using BS 13488:76 [20]. Crude fiber, ash content and moisture were determined according to AOAC (2016) [21].

Soluble carbohydrates

The soluble carbohydrates were identified by their extraction with water and were determined by high performance liquid chromatography (HPLC) on an Agilent® LC 1220 (USA) instrument equipped with Zorbax carbohydrate column (150 mm × 4.6 mm, 5μm, Agilent) and Zorbax Reliance Cartridge guard-column (Agilent) and refractive index detector (RID 1260) [22]. The mobile phase was acetonitrile/water (AcN/H_2O) (80/20) at 1.0 mL/min. All standards (individual pure monosaccharides with purity 98%) were purchased from Sigma Chemical Company (USA).

Amino acids

For the hydrolysis of the protein to free amino acids 300 mg of dried seeds were put in a glass ampule with 5 mL of 6N HCl solution. The ampule was thoroughly sealed and left in a drying chamber at 105°C for 24 h. The content of the ampule was transferred to a crystallizer and dried in a vacuum chamber at 40-50°C. After evaporation of the water, the residue was fully dissolved in 10 mL of 20 mM HCl. The solution was filtered through a paper filter and 20 μL of the collected filtrate was derivatized with AccQ-Fluor kit (WATO52880, Waters Corporation, USA). Initially, 60 μL of AccQ-Fluor borate buffer was added to the filtrate and homogenized. Then, 20 μL of AccQ-Fluor reagent was added, and the sample was homogenized again for 30 s. Before injection, the solution was heated in a water bath at 55°C. The resulting AccQ-Fluor derivatives of amino acids were separated by an ELITE LaChrome high performance liquid HPLC chromatograph (HPLC) (Hitachi) equipped with a DAD and a reverse phase C 18 AccQ-Tag (3.9 mm × 150 mm). The volume of injected sample was 20 μL, and the elution was done with a gradient system of two mobile phases: A – buffer (WATO52890, Waters) and B – 60% acetonitrile. Amino acids were detected at 254 nm and column temperature 37°C.

Energy value

The energy value of the seeds was determined following the FAO [19] procedure using the formula:

$$EV = C \times 4 + L \times 9 + P \times 4 \quad \text{(kcal/100 g)},$$

where EV – energy value; C – total carbohydrates, %; L – total lipids, %; P – total proteins, %.

RESULTS AND DISCUSSION

Chemical composition of the examined bitter vetch seeds (*Vicia ervilia* L.) is shown in Table 1.

Table 1. Chemical composition of bitter vetch seeds (*Vicia ervilia* L.)

Composition	Content
Oil content, %	1.4 ± 0.1
Proteins, %	20.1 ± 0.2
Carbohydrates, %	66.2 ± 0.4
Starch, %	20.4 ± 0.2
Fibres, %	3.1 ± 0.2
Ash, %	2.6 ± 0.1
Moisture, %	9.7 ± 0.2
Energy value, kJ/100 g (kcal/100 g)	1520 (357)

Bitter vetch seeds were characterized as a good source of proteins (20.1%) and carbohydrates (66.2%), but possessed low oil content (1.4%). Starch represented about 31% of total carbohydrates. Dietary fibers and ash content were 3.1 and 2.6%, respectively. The moisture of the seeds was found to be 9.7% and corresponded to the results about water content of different seeds [23]. The energy value of bitter vetch seeds was also evaluated – 1520 kJ/100 g (357 kcal/100 g). These results are in agreement with the energy value of different seeds from family Fabaceae such as bean, soybean, peas and chickpeas (337, 446, 326 and 325 kcal/100 g, respectively) [24].

Total protein and lipid content of the examined bitter vetch seeds were in agreement with the

results obtained by previous authors who reported that the oil content of the seeds was between 1.0 and 2.0% [1, 12] and the proteins ranged from 20.0 to 30.0% [2, 5, 7, 8, 10-16]. On the other hand, higher content of crude fat in the seeds was observed by Tabatabaei *et al*. (2000) – 2.43% [16]. The content of the dietary fibers was similar to that reported by Hadjipanayiotou *et al*. (1985) (3.5%) [12], but about twice lower than the results by Tabatabaei *et al.* (2000) (7.75%) [16]. Ash content of the seeds was lower than the results from previous studies where the ash content ranged between 3.20 and 3.97% [12, 15, 16]. Moisture content of the examined seeds was in agreement with previous studies where the dry matter was 92.00 – 94.52 g/100 g [12, 15, 16].

The composition of the soluble carbohydrates of bitter vetch seeds was examined for the first time and determined by high performance liquid chromatography (HPLC) on an Agilent® LC 1220 instrument equipped with a refractive index detector. Their individual composition is presented in Table 2.

Table 2. Composition of soluble sugars in bitter vetch seeds (*Vicia ervilia* L.).

Sugars, mg/100 g	Content
Fructose	540.7 ± 4.9
Glucose	600.9 ± 7.4
Xylose	140.1 ± 15.5
Rhamnose	198.3 ± 7.1
Sucrose	2649.8 ± 82.7
Cellobiose	149.4 ± 22.5
Total	4279.0 ± 111.0

Total content of water-soluble carbohydrates was found to be 4279.0 mg/100 g. It was observed that the main monosaccharides were glucose (600.9 mg/100 g) and fructose (540.7 mg/100 g) while the content of rhamnose and xylose was 198.3 and 140.1 mg/100 g, respectively. Carbohydrates are a major source of energy for the human body and the main representatives of these compounds present in the bitter vetch seeds are oligosaccharides such as sucrose (2649.8 mg/100 g). Other disaccharide found in the seeds was cellobiose (149.4 mg/100 g). High content of sucrose was also observed in soybean (64.2 mg/g), garden pea (62.3 mg/g) and peanuts (81 mg/g) by Kuo *et al.* (1988) [25].

Amino acid composition of bitter vetch seeds (*Vicia ervilia* L.) was also determined by HPLC chromatograph (Hitachi) equipped with a diode array detector (DAD) and a reverse phase C 18 AccQ-Tag (3.9 mm × 150 mm). The results are shown in Table 3.

Table 3. Amino acid composition of bitter vetch seeds (*Vicia ervilia* L.)

Amino acid, mg/g	Content
Aspartic acid	15.7 ± 0.1
Serine	28.5 ± 0.2
Glutamic acid	15.4 ± 0.1
Glycine	15.1 ± 0.1
Histidine	30.0 ± 0.2
Arginine	26.0 ± 0.3
Threonine	19.7 ± 0.1
Alanine	15.5 ± 0.1
Proline	10.0 ± 0.1
Cysteine	10.0 ± 0.2
Tyrosine	16.2 ± 0.1
Valine	23.6 ± 0.1
Methionine	5.6 ± 0.05
Lysine	34.8 ± 0.2
Isoleucine	29.6 ± 0.2
Leucine	4.8 ± 0.1
Phenylalanine	46.2 ± 0.3

Seventeen amino acids were identified in the seeds. The major amino acid was phenylalanine (46.2 mg/g), followed by lysine (34.8 mg/g) and histidine (30.0 mg/g). On the other hand, leucine and methionine were identified with the lowest content – 4.8 and 5.6 mg/g. The contents of the other amino acids were observed to range between 10.0 and 29.6 mg/g. The present results differed from those in previous studies where the authors reported that the main amino acids in bitter vetch seeds were glutamic and aspartic acids [10, 15]. This difference is probably due to the agro-meteorological conditions and the regions where the plants were grown. The relatively high content of lysine and cysteine (10.0 mg/g), which are essential amino acids in the nutrition, suggests that bitter vetch seeds can participate successfully in the human diet.

CONCLUSION

The main nutrients of bitter vetch (*Vicia ervilia* L.) seeds were determined. They possess high carbohydrate and protein content, but their oil content is extremely low. Total content of water-soluble carbohydrates was relatively low and the only disaccharides in the seeds were sucrose and cellobiose, while the main monosaccharides were glucose and fructose. Seventeen amino acids were identified in the seeds and the major ones were phenylalanine, lysine and histidine. The content of the main nutrients in bitter vetch seeds was observed to be relatively high which determined their satisfying energy value that corresponds to the

energy value of the most commonly used legume seeds.

Overall, bitter vetch seeds have a high nutritional value and could be successfully used as a valuable source of nutrients.

Acknowledgements: *This work was supported by the Bulgarian National Science Fund (BNSF), Ministry of Education and Science, projects of junior basic researchers and postdocs – 2018 [grant number КП-06-М29/2, 01.12.2018].*

REFERENCES

1. A. Bakoglu, E. Bagci, H. Ciftci, *J. Food Agric. Environ.*, **7** (2), 343 (2009).
2. A. Abdullah, M. M. Muwalla, R. I. Qudsieh, H. H. Titi, *Trop. Anim. Health Prod.*, **42**, 293 (2010).
3. S. G. Haddad, *Livest. Sci.*, **99**, 221 (2006).
4. M. E Ukhun, *Cell. Mol. Life Sci.*, **42**(6), 948 (1986).
5. Gh. Sadeghi, A. Samie, J. Pourreza, H.R. Rahmani, *Int. J. Poult. Sci.*, **3**, 522 (2004).
6. A. Arabestani, M. Kadivar, M. Shahedi, S. A. H. Goli, R. Porta, *Int. J. Biol. Macromol.*, **57**, 118 (2013).
7. A. Larbi, A. M. A. El-Moneim, H. Nakkoul, B. Jammal, S. Hassan, *Anim. Feed Sci. Tech.*, **165**, 278 (2011).
8. E. Pastor-Cavada, R. Juan, J. E. Pastor, M. Alaiz, J. Vioque, *J. Food Sci.*, **76**, 1118 (2011).
9. G. H. Sadeghi, *Trop. Anim. Health Prod.*, **43**, 259 (2011).
10. I. Fernández-Fígares, L. Pérez, R. Nieto, J. F. Aguilera, C. Prieto, *Anim. Sci.*, **60** (3), 493 (1995).
11. J. González, S. Andrés, *Anim. Res.*, **52**, 17 (2003).
12. M. Hadjipanayiotou, S. Economides, A. Koumas, *Annales de Zootechnie, INRA/EDP Sciences*, **34** (1), 23 (1985).
13. K. Kökten, A. Koçak, E. Bağci, M. Akçura, S. Çelik, *Grasas Aceites*, **61** (4), 404 (2010).
14. E. Ramos-Morales, M. R. Sanz-Sampelayo, E. Molina-Alcaide, *J. Anim. Physiol. Anim. Nutr.*, **94**, 55 (2010).
15. Gh. Sadeghi, J. Pourreza, A. Samie, H. Rahmani, *Trop. Anim. Health Prod.*, **41**, 85 (2009).
16. M. A. Tabatabaei, H. Aliarabi, A. Nik-Khah, S. R. Miraei-Ashtiani, *Iran. J. Agric. Sci.*, **31** (3), 601 (2000).
17. ISO 659:2014. Oilseeds. Determination of oil content (Reference method).
18. American Oil Chemists Society (AOAC) Official methods of analysis of AOAC International, method 945, 18-B, "Kjeldahl's method for protein determination in cereals and feed", 16th edn., Washington, DC, 1996.
19. Food and Agriculture Organization of the United Nations. Food energy — Methods of analysis and conversion factors (FAO Food and Nutrition Paper, Report of a Technical Workshop, Vol. 77), Rome, ISSN 0254-4725, 2003.
20. BS 13488:1976. Grain. Method for determining the starch content.
21. American Oil Chemists Society (AOAC) - Association of Official Analytical Chemists Official methods of analysis, 20th edn., Washington, DC, 2016.
22. Y. Georgiev, M. Ognyanov, I. Yanakieva, V. Kussovski, M. Kratchanova, *J. BioSci. Biotechnol.*, **1** (3), 223 (2012).
23. A. Stoyanova, M. Perifanova-Nemska, E. Georgiev, Raw Material Science about glyceride and essential oils, Agency 7D Publishing, Plovdiv, 2006.
24. T. Tashev, G. Shishkov, Tables for composition of Bulgarian food products, Meditzina i fizkultura Publ., Sofia, 1975.
25. T. M. Kuo, J. F. Van Middlesworth, W. J. Wolf, *J. Agric. Food Chem.*, **36**, 32 (1988).

Bulgarian Chemical Communications, Volume 52, Special Issue B (pp. 16-21) 2020 DOI: 10.34049/bcc.52.B.0004

Comparison of seasonal and spatial phycotoxin profiles of mussels from South Bulgarian coast

Z. V. Peteva[1*], B. Krock[2], M. D. Stancheva[1], St. K. Georgieva[1]

[1]*Medical University - Varna, Department of Chemistry, Tsar Osvoboditel Blvd. 84, 9000 Varna, Bulgaria*
[2] *Alfred-Wegener-Institut Helmholtz-Zentrum für Polar- und Meeresforschung, Chemische Ökologie, am Handelshafen 12, 27570 Bremerhaven, Germany*

Received: December 21, 2019; Revised: April 2, 2020

Phycotoxins (marine algal toxins) are toxic metabolites released by certain phytoplankton species. They can be responsible for seafood poisoning outbreaks because filter-feeding mollusks, such as mussels, can accumulate these toxins throughout the food chain and present a threat for consumers' health. A wide range of symptoms, from digestive to nervous, are associated to human intoxication by biotoxins, characterizing different and specific syndromes, called shellfish poisoning. The aim of this study is to compare the seasonal and spatial phycotoxin profiles of mussels (wild and farmed) harvested from South Bulgarian coast in the period 2017-2018. Analyzed were 57 samples by different analytical techniques - liquid chromatography tandem mass spectrometry (LC-MS/MS) and high-performance liquid chromatography with fluorescent detection followed by postcolumn derivatization. Domoic acid (DA), yessotoxin (YTX), pectenotoxin-2, PTX-2sa/ epi-PTX-2sa and gonyautoxin-2 (GTX2) were detected in the studied samples. Results revealed huge seasonal variations in the phycotoxin profiles of the mussels investigated. Spring 2017 profile is dominated by domoic acid present in 67% of the samples and reaching highest level of 618.9 ng. g^{-1}. In summer 2017 samples YTX is prevalent (60%) reaching a level of 8.3 ng.g^{-1}. No phycotoxins were detected in samples from fall 2017. The epimer pair PTX-2sa/ epi-PTX-2sa was with highest seasonal abundance in winter-spring 2018 – 47%. Its maximum detected level was 7.1 ng.g^{-1}. No statistically significant differences in mean phycotoxin levels of different sampling locations were determined. Generally, the herein reported marine toxins levels are comparable or even lower than in other European studies and much lower than legislative limits set in EU. Nevertheless, the huge seasonal variations in the phycotoxin profile show that for protection of consumers' health a further surveillance on marine toxins content in edible mussels is required.

Keywords: marine biotoxins**,** Black Sea, domoic acid, yessotoxin, shellfish poisoning

INTRODUCTION

The growth of aquaculture is mainly due to the increase in the human population and the general overexploitation of the fisheries [1]. Additionally, recreational harvesting has been documented to be very popular along the coast of numerous countries [2]. An important fraction of these two activities in Bulgaria is focused on mollusks and more specifically on mussels. For instance, in 2018 the commercial catch of Black Sea mussels has increased by 24% compared to 2017, becoming 13.11 tons and aquaculture production of the same species was exceeding 3000 tons [3].

Bivalves feed on the organic matter suspended in the seawater. Phytoplankton is the main component of this matter but some phytoplanktonic species can produce potent toxins (phycotoxins) which can be accumulated by mussels. Intoxications caused by consumption of contaminated mollusks are categorized according to their symptoms. The main ones are paralytic (PSP), diarrhetic (DSP) and amnesic (ASP) shellfish poisoning [4]. In Europe, the legislated groups of phycotoxins consist of six different chemical groups - paralytic toxins (saxitoxin and derivatives) (PSTs), domoic acid (DA), yessotoxins (YTXs), azaspiracids (AZAs), pectenotoxins (PTXs), and okadaic acid (OA) and its derivatives - the dinophysistoxins (DTXs). For these toxins, levels found in shellfish for human consumption must be lower than 180 μg eq STX kg^{-1}, 20 mg DA kg^{-1}, 3.75 mg eq YTX kg^{-1}, 0.16 mg eq AZA kg^{-1}, and 0.16 mg eq OA kg^{-1} (for the OA and PTX toxin group) [5, 6].

To reduce and prevent the potential risk of intoxication many studies have emphasized the importance of seasonal and spatial monitoring of phycotoxin levels in mussels intended for human consumption. Ujević *et al.* (2010) [7] found great variations in the levels of ASP causing toxin - domoic acid - in mussel samples from Adriatic Sea. Within a single winter season DA level ranged from not detected to 6.5 μg g^{-1}. The detected levels were much lower than the permissible limit and authors conclude that mussel consumption was not found to endanger human health.

In mussels purchased from Lugo (Galicia, Spain), belonging to five commercial brands of different

* To whom all correspondence should be sent:
E-mail: zlatina.peteva@mu-varna.bg

origins, Otero *et al.* (2018) [8] determined that the DSP causing toxins OA and DTX-2 are the main risk in harvested mollusks. Their levels varied greatly within the investigated period 2018-2019. In the positive samples the toxicity was determined between 3.6 and 234.1 μg OA eq kg^{-1} and three samples even exceeded the legal limit of 160 μg kg^{-1}. Therefore, authors conclude that DSP toxins are the major cause for concern in local mollusks and it is necessary to monitor phycotoxins levels to check future risks derived from mussel consumption.

Given the increase in reports of fluctuations of phycotoxins levels, coupled with a high demand on Bulgarian mussels, further investigations into a potential consumer risk caused by phycotoxins is required. The aim of this study is to compare the phycotoxin profiles of mussels harvested from South Bulgarian coast in the period 2017-2018.

EXPERIMENTAL

Field samples

Cultivated mussel samples (N=41) were collected manually every two weeks and more often directly from cultivation ropes from farming areas. Wild mussel samples (N=16) were collected manually from rocks in locations used for recreational harvesting. The study area covers the south Bulgarian coast from Nessebar to Tsarevo. Samples were collected in spring, summer and fall 2017, as well as in winter and spring of 2018.

All mussel samples were drained with distilled water to discard algae and sand. Thereafter the shells were removed. The digestive glands of minimum 0.5 kg of mussels (without shells) were dissected, homogenized and used for paralytic toxins, domoic acid and lipophilic toxins analysis.

Domoic acid and lipophilic toxins analysis

Each homogenate of digestive glands (~4 g) was subjected to methanol extraction. The procedure is in detail described by Peteva *et al*. (2017) [9]. An aliquot (~ 1000 μl) of each extract was analyzed by LC-MS/MS according to Krock *et al.* (2008) [10] for presence of DA and the lipophilic toxins - OA, DTXs, YTX and PTXs. Mass spectrometric experiments were performed on a triple quadrupole mass spectrometer (model API 4000 QTrap, SCIEX, Darmstadt, Germany), equipped with a TurboSpray® interface coupled to a liquid chromatograph (model 1100, Agilent, Waldbronn, Germany). The limits of detection (LOD) for the investigated lipophilic toxins and DA (Table 1) were determined based on 3:1 signal-to-noise ratio for each series of measurements.

Table 1. Limits of detection (LOD) of lipophilic toxins and DA for samples from fall 2017 and winter-spring 2018

Analyzed phycotoxins	LOD, $ng.g^{-1}$
DA	0.250
YTX	3.178
OA	4.975
DTX1	5.800
DTX2	2.375
PTX2	2.125

Paralytic shellfish poisoning toxins (PSTs) analysis

Each homogenate of digestive gland (~2 g) was subjected to acetic acid extraction. The procedure is briefly described by Peteva *et al.* (2019) [11]. An aliquot (~ 1000 μl) of each extract was analyzed by reverse-phase ion-pair liquid chromatography coupled to a post-column derivatization system according to Krock *et al.* (2007) [12]. The limits of detection of the investigated PSTs (Table 2) were determined for each series of measurements.

Table 2. Limits of detection of the investigated PSTs

Analyzed phycotoxins	LOD, $ng.g^{-1}$	
	Spring and summer 2017 samples	Fall 2017 and winter-spring 2018 samples
C1/2	2.15	3.57
GTX 4	20.70	25.69
GTX 1	26.75	32.71
dc-GTX2	0.86	1.13
dc-GTX 3	0.90	1.16
GTX 2	1.06	1.40
GTX 5	5.67	1.84
GTX 3	1.29	6.78
Neo STX	10.55	14.71
dc-STX	1.56	2.46
STX	0.89	1.54

Calculations

As there is no reference material for PTX-2sa/ epi-PTX-2sa, their levels are given as PTX2 equivalents.

Statistical analysis

SPSS 16 was used for statistical processing of the results. Descriptive statistical analysis was applied using tabulated graphical method, mean values, distribution values, etc. Using the MS Excel 2016 descriptive statistics feature, the bar indicates the standard deviation (in absolute value) within each group. Statistical hypothesis test (t-test) was applied to establish the existence of a statistically significant difference between the mean values of toxins by type of samples and depending on the sampling location and the sampling season. Results were reported by p-values. The groups for which we proved statistically significant difference $p \leq 0.05$ are indicated with *.

RESULTS AND DISCUSSION

In this investigation, wild and cultivated mussels (N=57) were collected from eight locations on the south Bulgarian coast including important areas of mussel farming and recreational harvesting. Domoic acid and the lipophilic toxins were extracted from the digestive glands of mussels because this is the known organ where these toxins accumulate [13, 14]. Although PSTs are hydrophilic compounds [15] there is evidence that they are also concentrated in this organ [16, 17].

DA, GTX2/3, YTX, PTX2 and the epimeric pair PTX2sa/ epi-PTX2sa were detected in the samples analyzed (Table 3). OA and DTXs were not detected in the samples. Domoic acid was detected in the samples from spring 2017 and in only one sample from 2018 with a huge difference in its level. YTX was detected in spring 2017 and summer-fall 2017 samples characterized by a wide content range for both seasons. Highest level (24.559 $ng.g^{-1}$) was registered in May 2017. This level is much lower than the regulatory limit of 3.75 $mg.kg^{-1}$ [5]. PTX2 was only detected in spring 2017 samples whereas its level within the season increases up to 30 times to reach a maximum of 59.79 $ng.g^{-1}$. Comparison with legislative limit -160 μg OA $eq.kg^{-1}$ [6] showed that no risk for human health is expected. Surprisingly, at the end of the investigated period (spring 2018) PTX-2sa/ epi-PTX-2sa appeared in the studied samples. GTX2/3 was determined in a small number of samples. Few samples containing PSTs were also reported in other Bulgarian studies [18, 19].

Table 3. Levels of detected phycotoxins in mussel samples

Detected phycotoxins	Spring 2017		Summer-fall 2017		Winter-spring 2018	
	Wild mussels	Cultivated mussels	Wild mussels	Cultivated mussels	Wild mussels	Cultivated mussels
Domoic acid number of positive samples	5	9	+0	0	0	1
Domoic acid content range, $ng.g^{-1}$	247.36-576.04	108.3-618.9	<LOD	<LOD	<LOD	0.3
YTX, number of positive samples	0	9	2	7	0	0
YTX, content range, $ng.g^{-1}$	<LOD	0.009-24.559	1.596-3.926	1.606-14.806	<LOD	<LOD
PTX2, number of positive samples	3	2	0	0	0	0
PTX2, content range, $ng.g^{-1}$	1.85-59.79	0.6-1.8	<LOD	<LOD	<LOD	<LOD
PTX2sa/ epi-PTX-2sa, number of positive samples	0	0	0	0	2	5
PTX2sa/ epi-PTX2sa, content range, ng PTX2 $eq.g^{-1}$	<LOD	<LOD	<LOD	<LOD	3.0-3.3	3.1-7.1
GTX2/3, number of positive samples	1	1	0	1	0	0
GTX2/3, content range, $ng.g^{-1}$	2.63	1.79	<LOD	2.59	<LOD	<LOD

Comparison of phycotoxin profiles of the studied wild and cultivated mussels (Fig. 1) showed the presence of all detected toxins in both types of samples. In cultivated mussels YTX was dominating, followed by domoic acid and PTX-2sa/ epi-PTX-2sa. The phycotoxin profile of wild mussels was characterized prevalently by domoic acid, followed by PTX2. Morton *et al.* (2009) [20] also investigated the presence of toxins in mussels from the Black Sea. The authors found the dominance of PTX2 and PTX-2sa/ epi-PTX-2sa in the phycotoxin profile. Another study from the Black Sea [21] showed that the majority of the toxin load is due to YTX and its analogues. To characterize the change of the phycotoxin profile in the three studied seasons, the ratio between the detected toxins was calculated (Fig. 2). In spring 2017 the richest variety of toxins - DA, YTX, PTX2 and GTX2/3 was registered. The dominating toxin was domoic acid, followed by YTX and PTX2. DA and PTX2 were determined in the samples until the beginning of May, while YTX was detected throughout the whole season. The presence of GTX2/3 in the samples of both seasons was scarce.

As domoic acid was only detected in spring 2017, a comparison of mean DA levels (t-test) was reasonable. It showed a statistically significant difference (Fig. 3) ($p=0.014 \leq 0.05$) between the mean levels in cultivated (181.1 ± 209.5 ng.g^{-1} hp) and in wild mussels (396.8 ± 119.7 ng.g^{-1} hp). The large standard deviations are explained by the variation in DA level throughout the season, as well as with the number of negative samples.

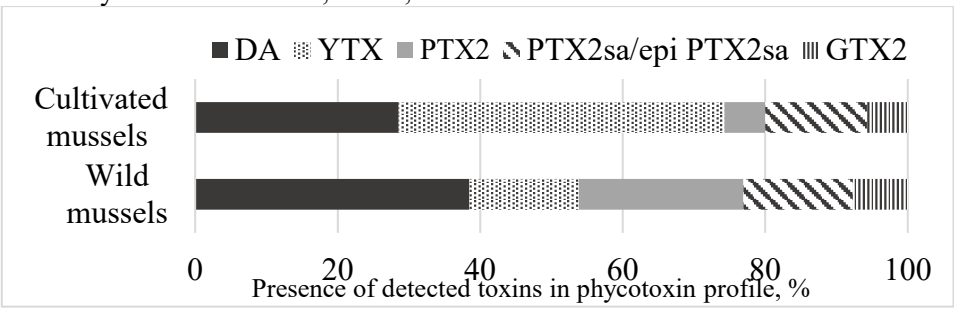

Figure 1. Phycotoxin profile of wild and cultivated mussels

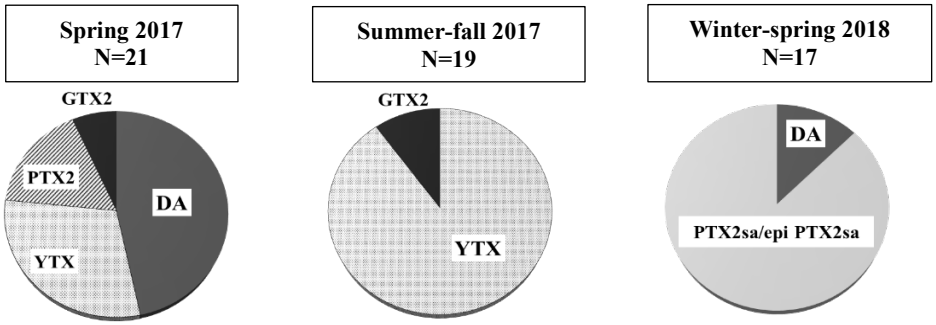

Figure 2. Seasonal phycotoxin profiles of investigated mussel samples

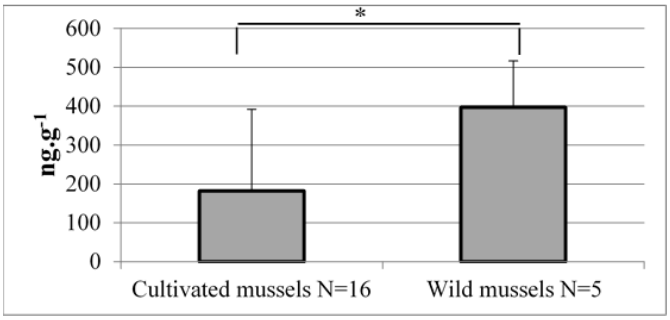

Figure 3. Comparison of domoic acid levels in mussel samples from spring 2017

In summer-fall YTX was the prevalent toxin. Its highest level (14.806 $ng.g^{-1}$ hp) was registered in July 2017. The only toxin that appeared in the samples from two subsequent seasons – spring and summer-fall 2017 was YTX. The range of YTX levels in spring 2017 was much wider than in summer-fall 2017, but the *t-test* showed no statistically significant difference between the mean seasonal levels (Fig. 4) ($p = 0.93 \geq 0.05$). But a large standard deviation of YTX levels was determined, which is due to fluctuations in the YTX level throughout the season and the YTX levels below the LOD. Only results of cultivated mussels were subjected to statistical processing because in these samples more positive results were registered (Table 3).

Interestingly, in the third studied period- winter-spring 2018, a new toxin emerged in the samples - the epimeric pair PTX2sa/ epi-PTX2sa and domoic acid in only one sample. Since there is evidence of PTX2 presence in plankton samples from other investigation seasons [9] and conversion of PTX2 to PTX2sa is well documented in the literature [22-24], it is reasonable to assume that PTX2sa/ epi-PTX2sa also resulted from PTX2 through metabolic conversion in mussels. A comparison of the spatial differences between the phycotoxin profiles was also made (Fig. 5). Although there were much more samples from Sozopol than from Ravda and Primorsko/Tsarevo, sampling was performed throughout the whole investigated period at both locations. Results from Primorsko and Tsarevo were combined due to their close proximity.

It is obvious that phycotoxin diversity is higher in samples from Sozopol. All detected toxins were determined in the samples from this location. The quantities of DA, YTX and PTX2sa/ epi-PTX2sa were similar. In contrast, the phycotoxin profile of samples from Ravda only contained DA and YTX. In samples from Primorsko/Tsarevo predominant were also YTX and DA, but in some samples also PTX2 was registered.

DA and YTX are the phycotoxins that were determined in the samples from the three locations (Fig. 6). Mean DA level in samples from Sozopol was much lower than in the other two locations, whereas mean YTX level was decreasing from north to south. Nevertheless, no statistically significant differences ($p \geq 0.05$) were established between the mean concentrations for both DA and YTX for the three sampling sites.

CONCLUSION

Phycotoxin profiles of investigated mussel samples contained DA, YTX, PTX2, PTX2sa/ epi-PTX2sa and GTX2/3. The temporal profile changed each season, whereas only in Spring 2017 all the toxins were detected in the samples. The spatial profile differs at the sampling locations. The samples from Sozopol contained all the detected toxins. In the current perspective of climate change, any variation in the environmental factors could contribute to a change of the toxin load. Although hereby reported levels are much lower than the legislative limits further surveillance on phycotoxins content in mussels is required in order to protect consumers' health.

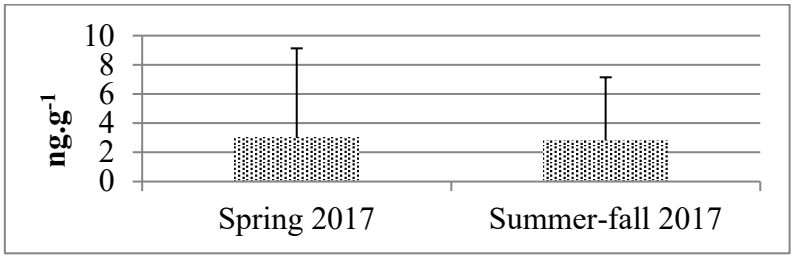

Figure 4. Comparison of mean seasonal YTX levels of cultivated mussels

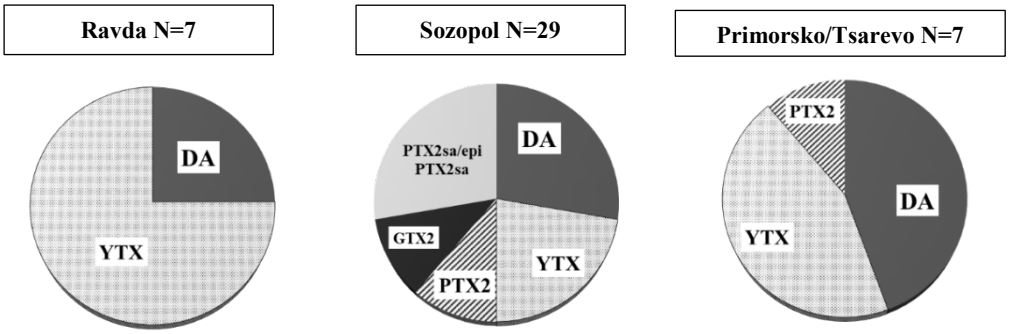

Figure 5. Spatial phycotoxin profiles

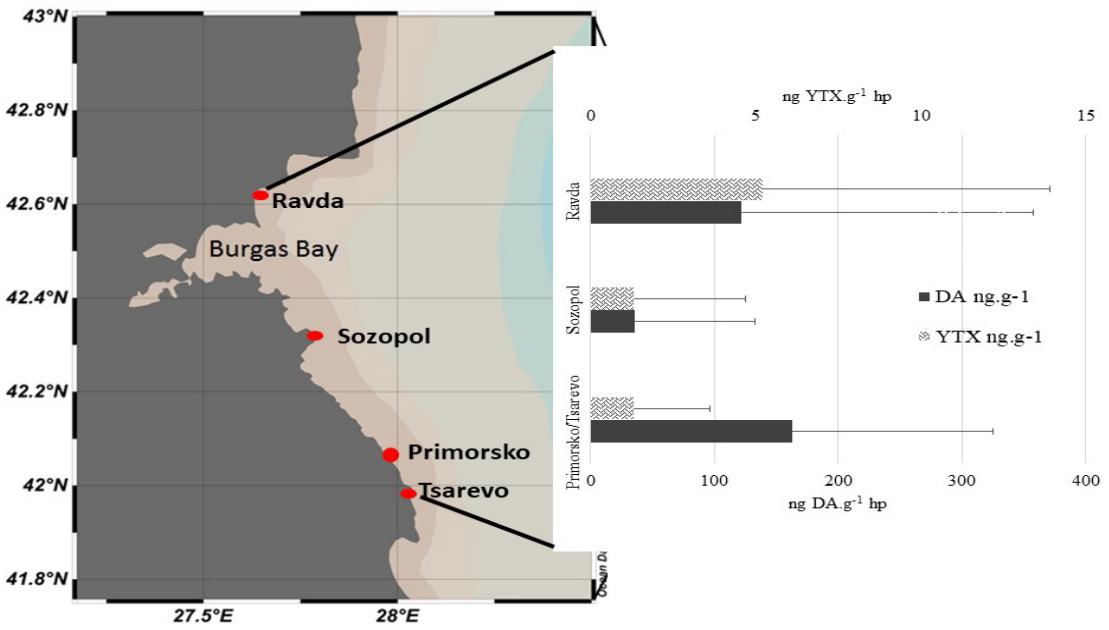

Figure 6. Spatial distribution of DA and YTX

REFERENCES

1. J. Blanco, Á. Moroño, M.L. Fernández, *Revista Galega dos Recursos Mariños (Monog)*, **1**, 70 (2005).
2. J. G. Sutinen, R. J. Johnson, *Marine Policy*, **27**, 471 (2003.
3. Bulgarian Agency for Fisheries and Aquaculture (BAFA), Situation-perspective analysis Fish and other aquatic organisms in 2017 and perspectives for 2018, Sofia, Ministry of Aqriculture, Food and Forest, 2018.
4. G. M. Hallegraeff, in: Manual of Harmful Marine Microalgae, G. M. Hallegraeff, D. M. Anderson, A. D. Cembella (eds.), UNESCO Publishing, 1995.
5. European Commission (EC). Commission Regulation (EU) No 786/2013 amending Annex III to Regulation (EC) No 853/2004 of the European Parliament and of the Council as regards the permitted limits of yessotoxins in live bilvalve molluscs, 2013.
6. European Commission (EC). Commission Regulation (EU) No 853/2004 of the European parliament of the council laying down the specific hygiene rules for the hygiene of foodstuffs, 2004.
7. I. Ujević, Ž. Ninčević-Gladan, R. Roje, S. Skejić, J. Arapov, *Molecules*, **15,** 6835 (2010).
8. M. Otero, E. Cebrian, P. Francour, B. Galil, in: Monitoring marine invasive species in Mediterranean marine protected areas (MPAs). Malaga: IUCN Centre for Mediterranean Cooperation, 2013.
9. Z. Peteva, B. Krock, St. Georgieva, M. Stancheva, *SSRG,* **5**, 3 (2018).
10. B. Krock, U. Tillmann, U. John, A. D. Cembella, *Anal. Bioanal. Chem*., **392(**5), 797 (2008).
11. Z. V. Peteva, G. N. Kalinova, B. Krock, M. D. Stancheva, S. K. Georgieva, *Bulg. Chem. Commun*., **51**(D), 233 (2019).
12. B. Krock, C. G. Seguel, A. D. Cembella, *Harmful Algae*, **6**(5),734 (2007).
13. L. L. Mafra Jr., D. Lopey, V. C. Bonilauri, H. Uchida, *Mar. Drugs*, **13(**6), 3920 (2015).
14. L. MacKenzie, P. Holland, P. Mcnabb, V. Beuzenberg, *Toxicon*, **40**,1321 (2002).
15. B. A. Suarez-Isla, in: Marine and Freshwater Toxins, Toxinology, P. Gopalakrishnakone (ed.), Springer Science, Dordrecht, 2015.
16. R. W. M. Kwong, W.-X. Wang, P. K. S. Lam, P. K. N. Yu, *Aquatic Toxicology*, **80**, 82 (2006).
17. Z. Amzil, M. A. Quilliam, T. Hu, J. L. C. Wright, *Natural Toxins*, **7(**6), 271 (1999).
18. G. Krumova-Valcheva, G. Kalinova, *Acta Microbiologica Bulgarica,* **33(**1), 30 (2017).
19. G. Kalinova, P. Mechkarova, M. Marinova, *Trakia Journal of Sciences*, **13**, 303 (2015).
20. S. L. Morton, A. Vershinin, L. L. Smith, T. A. Leighfield, S. Pankov, M. A. Quilliam, *Harmful Algae*, **8**, 629 (2009).
21. A. Vershinin, S. Morton, S. Pankov, L. Smith, M. Quilliam, J. Ramsdell, *African Journal of Marine Science*, **28**, 209 (2006).
22. Z. Amzil, M. Sibat, F. Royer, N. Masson, *Mar. Drugs,* **5(**4), 168 (2007).
23. J. Blanco, G. Alvarez, E. Uribe, *Toxicon,* **471**, 710 (2007).
24. P. Ciminiello, C. Dell'Aversano, E. Fattorosso, M. Forino, L. Tartaglione, *Toxicon*, **55**, 280 (2010).

Bulgarian Chemical Communications, Volume 52, Special Issue B (pp. 22-27) 2020 DOI: 10.34049/bcc.52.B.0014

Detection of marine biotoxin in plankton net samples from the Bulgarian coast of Black Sea

Z. V. Peteva[1*], B. Krock[2], T. Max[2], M. D. Stancheva[1], S. K. Georgieva[1]

[1]*Medical University - Varna, Department of Chemistry, Tsar Osvoboditel Blvd., 84, 9000 Varna, Bulgaria*
[2]*Alfred-Wegener-Institut Helmholtz-Zentrum für Polar- und Meeresforschung, Chemische Ökologie, am Handelshafen 12, 27570 Bremerhaven, Germany*

Received: December 21, 2019; Revised: April 2, 2020

Some diatoms and dinoflagellates can produce marine toxins, which can accumulate in, e.g. filter-feeding bivalves, posing a potent treat to seafood consumers. In this study, concentrated net plankton samples were collected from mussel cultivation regions (Kavarna bay) and zones for wild catch (Varna bay) in two periods - winter to fall 2018 and spring 2019. A method using liquid chromatography-tandem mass spectrometry (LC-MS/MS) was employed to analyze domoic acid (DA), okadaic acid, dinophysistoxins, yessotoxin, pectenotoxin-2 (PTX2), gymnodimine A (GYM), 13-desmethyl spirolide C (SPX1), and goniodomin A (GDA). Paralytic shellfish toxins (PSTs) were investigated by high performance liquid chromatography with post-column derivatization and fluorescence detection. Results indicated the presence of DA, PTX2, SPX1 and GDA reaching maximum levels of 1.4 $ng.NH^{-1}.m^{-1}$ DA, 115.5 $ng.NH^{-1}.m^{-1}$ PTX2, 0.2 $ng.NH^{-1}.m^{-1}$ SPX1 and 8.6 $ng.NH^{-1}.m^{-1}$ GDA. No PSTs were detected in the investigated samples. The maximum toxin load of the samples was due to the presence of PTX2. Detection of DA, PTX2, SPX1 and GDA in the samples points to the possible toxigenic nature of phytoplankton species along the Bulgarian coast. These data may be used to evaluate the probability of potential risks to local aquaculture and seafood from wild catch.

Keywords: Black Sea, domoic acid, PTX2, SPX1, goniodomin A, LC-MS/MS, HPLC-FLD

INTRODUCTION

Natural toxins are harmful organic compounds that have a biogenic origin. Some of them are also bio-contaminants – they are produced by microorganisms and may accumulate in food and food products. Among them are mycotoxins, bacterial toxins and marine biotoxins. Mycotoxins are a chemically diverse group of compounds that are secondary metabolites of fungi. They have a strong capacity to produce acute toxicity in animals and humans. Bacterial toxins are proteins produced by a large variety of bacterial pathogens. They can act, e.g. as primary virulence factors. Marine biotoxins are produced mostly by certain freshwater and marine microalgae. They find their way to humans through the food chain causing severe illness when exceeding certain levels.

Scientific interest on the occurrence of natural toxins in Bulgaria is not persistent. Just in 1996, the first survey on the natural occurrence of *Fusarium* mycotoxins in Bulgarian wheat was published [1], although the breeding of these crops has long tradition in Bulgaria [2]. More standing but still not contemporary is the investigation on the possible role of mycotoxins for the development of endemic nephropathy by the rural population [3-5]. Lately, an approach based on the immunosensor quantification of aflatoxins was proposed [6].

More recent are studies on genetics [7, 8] and occurrence [9-11] of toxin-producing bacteria. Even more, Stratev *et al.* (2016) [12] proved a risk to human health through consumption of fish and fish products due to the presence of *A. hydrophila* strains that form different virulence factors.

In 2017 Stoyneva-Gärtner *et al*. [13] published a summary of results on the assessment of cyanoprokaryote blooms and of cyanotoxins (freshwater phycotoxins) in Bulgaria in a 15-years period (2000-2015), incl. drinking-water reservoirs, recreational lakes and sites of nature conservation importance, indicating a particular scientific activity in this field. Furthermore, a hygienic assessment of some water reservoirs based on determination of cyanotoxins was also made [14].

Marine biotoxins were investigated in seafood within the national monitoring program [15-17] and by our scientific team by means of human exposure estimation [18-20]. Due to the bioaccumulation processes, chemical levels in marine biota (e. g. mussels) are by orders of magnitude larger than in

* To whom all correspondence should be sent:
E-mail: zlatina.peteva@mu-varna.bg

water. Even more, some marine toxins undergo chemical changes through the food chain transfer [21, 22]. Additionally, the evidence of potentially toxigenic microalgae on the Bulgarian coast [23-25] and other parts of the Black Sea [26] is increasing.

Therefore, to better understand the origin of marine toxins, a research down to the lowest trophic levels is required. The aim of this study is to determine the phycotoxin levels in plankton net samples from the Bulgarian coast.

EXPERIMENTAL

Sampling and extraction procedure

Sampling area covered Kavarna and Varna bays, situated on the north Bulgarian coast, and the two periods - winter to fall 2018 and spring 2019. Plankton samples (N = 37) were collected by horizontal net tow hauls with a 20-μm mesh and an aperture of 40-cm diameter. Net haul concentrates were adjusted to a defined volume of 500-1000 mL (depending on the net tow volume) using 20 μm filtered seawater. The samples were separated into two aliquots. Each aliquot was filtered on 0.45 μm Whatman® nylon membrane filters. Filters were then washed with 200-1000 μL of 100% methanol for domoic acid and lipophilic toxins and with 200-1000 μL of 0.03M acetic acid for paralytic toxins.

The methanolic and acetic acid suspensions were then sonicated (40 Hz, 15 min) and centrifuged at 4000 × g for 10 min at 10 °C. The supernatants were filtered through syringe filters (0.45 μm pore size, ⌀ 25 mm, Minisart, Sartorius, Germany). Filtrates (150-1000 μL) were transferred into chromatographic vials and kept at -20 °C until further analysis.

Chromatographic analysis

The hydrophilic paralytic toxins were determined by HPLC-FLD with post-column derivatization according to Krock *et al.* (2007) [27] on a LC1100 series liquid chromatograph (Agilent, Waldbronn, Germany) coupled to a PCX 2500 post-column derivatization system (Pickering Laboratories, Mountain View, CA, USA) and dual monochromator fluorescence detector (G1321A) as described in detail in our previous study (Peteva *et al.* 2019). Briefly, the mobile phase contained two eluents: A – 6 mM octanesulfonic acid, 6 mM heptanesulfonic acid and 40 mM ammonium phosphate and B - 13 mM octanesulfonic acid and 50 mM phosphoric acid maintained by isocratic elution program (flow rate was 1 mL min^{-1}). As stationary phase a 250 mm × 4.6 mm i.d., 5 μm, Luna C18 reversed-phase column (Phenomenex, Aschaffenburg, Germany) equipped with a Phenomenex SecuriGuard pre-column was used.

Post-column derivatization constituted of oxidation of the eluate with 10 mM periodic acid dissolved in 555 mM ammonium hydroxide followed by an acidification with 0.75 M nitric acid. Detection was performed on following wavelengths - λex 333 nm; λem 395 nm. Calculated limits of detection (LOD) are reported in Table 1. The hydrophilic domoic acid (DA) and lipophilic toxins – gymnodimine A (GYM), 13-desmethyl spirolide C (SPX1), okadaic acid (OA), dinophysistoxins-1 and -2 (DTX1,2), pectenotoxin-2 (PTX2), goniodomin A (GDA), yessotoxin (YTX) and azaspiracid-1 (AZA1) were analyzed according to Krock *et al.* (2008) [28] on an LC-MS/MS system. It consists of Agilent model 1100 LC coupled to an API-Sciex 4000 QTrap triple-quadrupole mass spectrometer (Sciex, Darmstadt, Germany) equipped with a Turbo Spray interface. Measurements were carried out in positive-ion mode by selected reaction monitoring (SRM) experiments. Toxins were separated by reverse-phase chromatography on an analytical column (50 × 2 mm) packed with 3 mm Hypersil BDS 120 Å (Phenomenex, Aschaffenburg, Germany). Gradient elution was performed with two eluents, where eluent A was water and B was acetonitrile/water (95:5v/v), both containing 2.0 mM ammonium formate and 50 mM formic acid. Calculated limits of detection are presented on Table 1.

The quality control was performed by regular analysis of procedural blanks and certified reference material (National Research Council, Canada). Quantification of detected toxins was done by integration of the areas of the chromatographic peaks.

Calculations

Toxin contents are expressed as nanograms per net tow and meter (ng. NT^{-1} m^{-1}).

RESULTS AND DISCUSSION

With the aim to determine the qualitative and quantitative composition of marine biotoxins in plankton net samples a variety of toxins were analyzed, where DA, PTX2 (Table 2), SPX1 and GDA were detected.

Domoic acid is a hydrophilic marine biotoxin that represents a pyrrolidine carboxylic acid and belongs to a group of amino acids called kainoids [29]. DA was detected in the samples from winter-spring 2018. The highest concentration of 1.4 $ng.NH^{-1}.m^{-1}$ was registered in a sample from April 2018. This value is much lower than the concentrations detected

by Almandoz *et al.* (2017) [30] – 97 – 5041 ng.NT^{-1} in Argentinian Sea during a summer expedition. Still, it should be considered that this difference could be due to variation in salinities of both Argentinian and Black Sea.

Domoic acid was determined in plankton net samples from Marmara Sea [31], as well as in Tyrrhenian [32] and North Sea [33], which was always associated with the presence of a natural population of the toxic diatom *Pseudo-nitzschia*. As also on the Bulgarian coast there is an evidence of the same genus [23-25], the presence of this toxin in plankton samples was expected. Spirolides and gymnodimines are cyclic imines. Structure elucidation of SPX1 showed that it contains a 6-5-5-polyether ring system in addition to a heptacyclic imine ring [34, 35]. Production of SPX1 is linked to *A. ostenfeldii* [36, 37]. This species is also recorded in the Black Sea [38, 39]. Often along with SPX1 also paralytic toxins and gymnodimines are present in the plankton samples [40-42]. There are also studies reporting that in geographical isolates either GYMs or SPX1 [43] are detected. Our investigation showed that SPX1 was registered in the samples from summer-fall 2018. Highest value (0.245 ng.NH^{-1}.m^{-1}) was determined in a sample from July 2018.

Table 1. Limits of detection (LOD) of analyzed marine biotoxins

HPLC- FD method		LC-MS/MS method	
Paralytic toxins analyzed	LOD, ng.NH^{-1}.m^{-1}	Marine toxins analyzed	LOD, ng.NH^{-1}.m^{-1}
C1/2	2.1	DA	1.1
GTX 4	20.1	GYMA	0.2
GTX 1	26.0	SPX1	0.1
dc-GTX2	0.8	OA	1.5
dc-GTX 3	0.9	DTX2	1.1
GTX 2	1.0	DTX1	20.3
B1	5.5	PTX2	1.0
GTX 3	1.3	GDA	4.6
Neo STX	10.3	YTX	3.8
dc-STX	1.5	AZA1	0.3

Table 2. Levels of detected phycotoxins in mussel samples

Period studied	Detected toxins – positive concentration range, ng.NT^{-1}.m^{-1}		
	DA	*PTX2*	*SPX1*
Spring-Fall 2018	0.5-1.4	1.3-115.5	0.054-0.245
Spring 2019	nd	69.8-109.1	nd

It is lower than the SPX1 levels (0.5 - 143.6 ng.NT^{-1}) detected in the northern Patagonian shelf in the Argentinian Sea by Guinder *et al.* (2018) [36].

The samples were also analyzed for paralytic toxins by HPLC-FLD, but all were negative. The absence of paralytic toxins is in agreement with our previous study on plankton samples from the same area in 2017 [18], where no paralytic toxins were detected in the plankton samples as well.

Gymnodimines are the smallest molecules of the group of cyclic imines. The chemical structures of GYM A, 12-methyl GYM A [44], GYM B, GYM C, GYM D [45], 16-desmethyl GYM D and GYM E [46] have been structurally elucidated by now. All GYM analogues have a six-membered imino ring. Their macrocycle contains 16 carbon units and one ether bridge [47].

The investigation on GYMs showed that some samples from spring-summer 2018 were near but below the LOD.

In two samples from summer-fall 2018 a putative gymnodimine A-like compound was detected. The difference in mass of this compound (*m/z* 540/522, RT 3.21 min) to GYM A (*m/z* 508/490, RT 3.02 min) is 32 Da which could be a variant with two additional water molecules. However, abundances were too low for confirmatory analysis. Calculated concentrations of this putative gymnodimine A-like compound are 1.1 and 3.0 ng.NH^{-1}.m^{-1}.

Gymnodimines are not often reported in field samples. GYM-A and its analogues are mostly detected in isolates and cultures of the species from, e.g. the Netherlands [46], the Baltic Sea [45], etc. Detected concentrations in the Bulgarian samples were much lower than the reported by Kremp *et al.*, (2019) [48] for Limfjord (up to 590 ng.NT^{-1}) and the North Sea (up to 100 ng. NT^{-1}). Goniodomin-A

(GDA) is a linear polyether macrolide. GDA was detected in two samples from summer 2018 with values of 8.6 and 5.5 ng.NH^{-1}.m^{-1}. GDA is known to be produced by species with a wide abundance like *A. pseudogonyaulax* [49, 50] and the two rare species *A. monilatum* and *A. hiranoi* [51, 52]. These species were also registered in the Black Sea [53-55] and even on the Bulgarian coast [56]. Nevertheless, to our knowledge SPX1 and GDA have never been detected in plankton samples from the Black Sea.

Pectenotoxins are also linear polyether compounds. Their common structural features include a spiroketal group, three oxolanes, a bicyclic ketal and a six-membered cyclic hemiketal [57]. The most dominant lipophilic toxin was PTX2 (Table 2), which was detected in 67 % of the samples from April-July 2018, as well as in single samples from August and September 2018 and from March and April 2019 (Fig. 1). In 2018 the highest value (115.5 ng.NH^{-1}.m^{-1}) was detected in a sample from July. This value is close to the highest value registered in spring 2019 (109.1 ng.NH^{-1}.m^{-1}). In July 2018 the PTX2 concentrations were higher compared to the other investigated season when the toxins were detected in single samples.

The PTX2 concentration ranges of 2018 and 2019 are comparable with PTX2 levels reported by Guinder *et al.* [36] (2018) in Argentinian Sea.

Okadaic acid (OA), dinophysistoxins (DTXs) (also known as diarrhetic shellfish toxins) and pectenotoxins are toxic polyether compounds produced by planktonic species of the genus *Dinophysis* and benthic species of *Prorocentrum* [58,59]. These toxins very often cooccur [60-62], but also only PTX2 containing isolates are reported [63]. Hereby, the toxin profile of plankton net samples also includes only the PTX2, which could be due to a geographical specification of the producing species. Neither OA, DTXs nor YTX and AZA1 were detected in the samples.

Investigation on the toxin load of the samples showed that only eight samples, all from 2018, contained more than one toxin (Fig. 2).

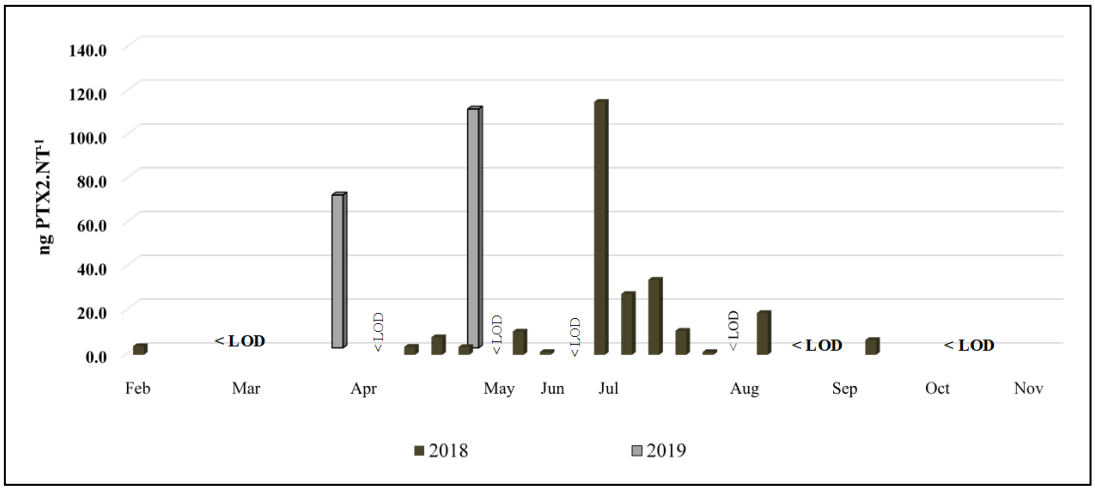

Figure 1. Distribution of PTX2 in plankton samples

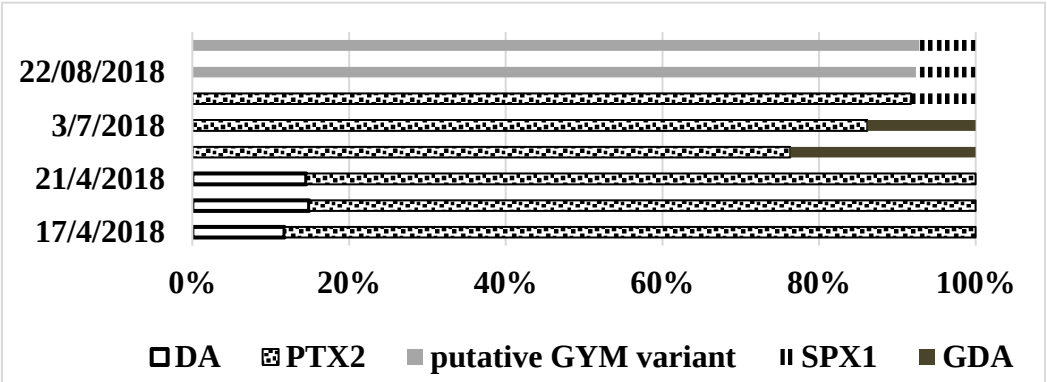

Figure 2. Toxin load of multitoxin plankton samples

The major contribution in the toxin content of the samples is due to the presence of PTX2 (6 samples) and in two samples to the availability of the "putative GYM variant". However, two pairs of samples are

collected on the same time; no seasonal variation could be concluded. Still, as domoic acid is present in only three multitoxin samples and in one more sample and no paralytic toxins were detected, it is reasonable to conclude that the toxin profile of plankton net samples is based on the presence of lipophilic toxins.

CONCLUSION

During a sampling campaign in 2018 and 2019 the marine algal toxins – PTX2, SPX1, DA and GDA were detected in phytoplankton net samples from North Bulgarian coast. The maximum toxin load was due to the presence of PTX2. This is the first report for the SPX1 and GDA in plankton samples from Bulgarian Black Sea coast.

Acknowledgement: *This study was partially funded by the Science Fund of Medical University Varna, Project Incoming number 16012/2016 and by the Helmholtz-Gemeinschaft Deutscher Forschungszentren through the research program "Polar regions and Coasts in the changing Earth System" (PACES II) of the Alfred-Wegener-Institut Helmholtz-Zentrum für Polar- und Meeresforschung.*

REFERENCES

1. T. Vrabcheva, R. Geßler, E. Usleber, E. Märtlbauer, *Mycopathologia*, **136(**1), 47 (1996).
2. Z. Uhr, G. Rachovska, G. Delchev, *Agricultural Science and Technology***6**(2), 152 (2014).
3. T. Petkova-Bocharova, M. Castegnaro, *Food Additives & Contaminants*, **2(**4), 267 (1985).
4. T. Petkova-Bocharova, M. Castegnaro, *IARC Scientific Publications*, **115**, 135 (1991).
5. P. G. Mantle, K. M. McHugh, *Mycological Research*, **97(**2), 205 (1993).
6. M. P. Slavova, R. T. Georgieva-Nikolova, M. M. Nikolova, R. K. Hadjiolova, *Bulg. Chem. Commun*., **48(**4), 689 (2016).
7. R. Popova, I. Sirakov, I. Alexandar, T. Strateva, H. Daskalov, I. Mitov, *Acta Microbiologica Bulgarica*, **33(**1), 17 (2017).
8. R. Gergova, I. Sirakov, I. Mitov, T. Strateva, *Comptes rendus de l' Académie bulgare des Sciences*, **69**(8), 1073 (2016).
9. R. T. Gergova, V. S. Tsitou, I. I. Gergova, A. A. Muhtarova, I. G. Mitov, *African Journal of Clinical and Experimental Microbiology*, **20**(4), 280 (2019).
10. T. Ivanova, E. Gergova-Mehmedova, H. Daskalov, *Bulgarian Journal of Agriculture Science*, **23(**1), 159 (2017).
11. V. Urumova, M. Lyutzkanov, V. Petrov, *Macedonian Veterinary Reviews*, **38(**1), 21 (2015).
12. D. Stratev, E. Gurova, I. Vashin, H. Daskalov, *Bulgarian Journal of Agriculture Science*, **22(**2), 308 (2016).
13. M. P. Stoyneva-Gärtner, J. P. Descy, A. Latli, B. A. Uzunov, V. T. Pavlova, Z. Bratanova, P. Babica, B. Maršálek, J. Meriluoto, L. Spoof, *Advances in Oceanography and Limnology*, **8(**1), 131 (2017).
14. V. Georgieva, V, Pavlova, Z. Bratanova, *Bulgarian Journal of Public Health*, **7(**4), 3 (2015)
15. G. Krumova-Valcheva, G. Kalinova. *Acta Microbiologica Bulgarica*, **33(**1), 30 (2017).
16. G. Kalinova, P. Mechkarova, M. Marinova *Trakia Journal of Sciences*, **13**, 303 (2015).
17. V. Peneva, Y. Gogov, G. Kalinova, A. Slavova, in: Proceedings Jubilee Scientific Session 110 Years NDNIVMI, 2011.
18. Z. V. Peteva, G. N. Kalinova, B. Krock, M. D. Stancheva, S. K. Georgieva, *Bulg. Chem. Commun*., **51(**D), 233 (2019).
19. Z. V. Peteva, M. Stancheva, S. Georgieva, B. Krock, A. Gerasimova, *Food Science and Applied Biotechnology*, **2(**2), 166 (2019)
20. M. Stancheva, Z. Peteva, B. Krock, *Scripta Scientifica Medica*, **51(**1), 24 (2019).
21. C. O. Miles, A. L. Wilkins, R. Munday, M. H. Dines, A. D. Hawkes, L. R. Briggs, M. Sandvik, *Toxicon*, **43(**1), 1 (2004).
22. R. W. M. Kwong, W.-X. Wang, P. K. S. Lam, P. K. N. Yu, *Aquatic Toxicology*, **80**, 82 (2006).
23. N. Dzhembekova, S. Moncheva, P. Ivanova, N. Slabakova, S. Nagai, *Biotechnology & Biotechnological Equipment*, **32(**6), 1507 (2018).
24. N. Dzhembekova, I. Atanasov, P. Ivanova, S. Moncheva, in: Surveying Geology & Mining Ecology Management, Proc. International Multidisciplinary Scientific Geoconference: SGEM, 2017, 17, p. 889.
25. N. Dzhembekova, S. Urusizaki, S. Moncheva, P. Ivanova, S. Nagai, *Harmful Algae*, **68**, 40 (2017).
26. Ö. Baytut, C. T. Gürkanli, E. Deniz, İ. Öycoǫ, A. Gönülol, *Turkish Journal of Botany*, **40**, 546 (2016).
27. B. Krock, C. G. Seguel, A. D. Cembella. *Harmful Algae*, **6(**5), 734 (2007).
28. B. Krock, U. Tillmann, U. John, A. D. Cembella, *Analytical Bioanalytical Chemistry*, **392(**5), 797 (2008).
29. M. A. Quilliam, in: Manual on harmful marine microalgae, G. M. Hallegraeff, D. M. Anderson, A. D. Cembella (eds.), UNESCO Publishing, Paris, 2004, p. 247.
30. G. O. Almandoz, E. Fabro, M. Ferrario, U. Tillmann, A. D. Cembella, B. Krock, *Harmful Algae*, **63**, 45 (2017).
31. F. Dursun, T. Yurdun, S. Ünlü, *Bulletin of Environmental Contamination and Toxicology*, **96(**1), 70 (2016).
32. R. Congestri, L. Micheli, G. Palleschi, *American Journal of Plant Science*, **8(**6), 1077 (2017)
33. A. Delegrange, A. Lefebvre, F. Gohin, L. Courcot, D. Vincent, *Estuarine, Coastal and Shelf Science*, **214**, 194 (2018).
34. B. Krock, A. D. Cembella, in: Proc. Sixth International Conference on Molluscan Shellfish Safety, 2007, 316.

35. S. L. MacKinnon. J. A. Walter, M. A. Quilliam, A. D. Cembella, P. Leblanc, I. W. Burton, W. R. Hardstaff, N. I. Lewis, *Journal of Natural Products*, **69**, 983 (2006).
36. V. A. Guinder, U. Tillmann, B. Krock, A. L. Delgado, T. Krohn, J. E. Garzón-Cardona, K. Metfies, C. L. Abbate, R. Silva, R. Lara, *Frontiers in Marine Science*, **5** (2018).
37. R. M. Van Wagoner, I. Misner, C. R. Tomas, J. L. Wright, *Tetrahedron Letters*, **52**, 4243 (2011).
38. P. J. Mudie, F. Marret, K. N. Mertens, L. Shumilovskikh, S.A.G. Leroy, *Marine Micropaleontology*, **134**, 1 (2017).
39. Yu. V. Bryantseva, A. F. Krakhmalnyi, V. N. Velikova, O. V. Sergeeva, *International Journal on Algae*, **18(**1), 21 (2016).
40. H. Martens, U. Tillmann, K. Harju, C. Dell'Aversano, L. Tartaglione, B. Krock, *Microorganisms*, **5(**2), 29 (2017).
41. E. Fabro, G. O. Almandoz, M. E. Ferrario, U. John, U. Tillmann, K. Toebe, B. Krock, A. D. Cembella, *Journal of Phycology*, **53(**6), 1206 (2017).
42. A. Kremp, P. Tahvanainen, W. Litaker, B. Krock, S. Suikkanen, *Journal of Phycology*, **50(**1), 81 (2014).
43. P. Salgado, P. Riobó, F. Rodríguez, J. Franco, I. Bravo, *Toxicon*, **103**, 85 (2015).
44. R. M. Van Wagoner, I. Misner, C. Tomas, J. L. C. Wright, Tetrahedron Letters, **52**(33), 4243 (2011).
45. K. Harju, H. Koskela, A. Kremp, S. Suikkanen, P. de la Iglesia, C. O. Miles, B. Krock, P. Vanninen, *Toxicon*, **122**, 68 (2016).
46. C. Zurhelle, J. Nieva, U. Tillmann, T. Harder, B. Krock, J. Tebben, *Marine Drugs*, **16(**1), 446 (2018).
47. EFSA, *EFSA Journal*, **8(**6), 1628 (2010).
48. A. Kremp, P. J. Hansen, U. Tillmann, H. Savela, S. Suikkanen, D. Voß, F. Barrera, H. H. Jakobsen, B. Krock, *Harmful Algae*, **87** (2019).
49. H. Zmerli Triki, M. P. Laabir, N. Moeller, O. Chomérat, *Toxicon*, **111,** 91 (2016).
50. B. Krock, U. Tillmann, Y. Wen, P. J. Hansen, T. O. Larsen, A. J. C. Andersen, *Toxicon*, **155,** 51 (2018).
51. T. Kita, Y. Fukuyo, *Bull. Plankton Soc. Jpn.*, **35(**1), 1 (1988).
52. M. Murakami, K. Makabe, K. Yamaguchi, S. Konosu, M. R. Walchli, *Tetrahedron Lett.*, **29(**10), 1149 (1988).
53. L. M. Terenko, *International Journal on Algae*, **8**(4), 345 (2006).
54. D. A. Nesterova, L. M. Terenko, G. V. Terenko, in: The northwestern Black Sea: biology and ecology, Y. P. Zaytsev, B. G. Alexandrov (eds.), Naukova Dumka, Kiev, 2006, p. 557
55. T. A. Shiganova, E. I. Musaeva, T. A. Lukasheva, A. N. Stupnikova. N. Zas'ko, L. L. Anokhina, A. E. Sivkovich, V. I. Gagarin, Yu. V. Bulgakova, *Russian Journal of Biological Invasions*, **3(**4), 255 (2012)
56. S. Moncheva, S. Gorinstein, G. Shtereva, F. Toledo, P. Arancibia-Avila, I. Goshev, S. Trakhtenberg, *Hydrobiologia*, **501(**1-3), 23 (2003).
57. J. S. Allingham, C. O. Miles, I. Rayment, *Journal of Molecular Biology*, **371(**4), 959 (2007).
58. T. Yasumoto, M. Murata, *Chemical reviews*, **93(**5), 1897 (1993).
59. T. Yasumoto, Y. Oshima, W. Sugaware, Y. Fukuyo, H. Oguri, T. Igarashi, N. Fujita, *Bull. Jpn. Soc. Sci. Fish*., **46**, 1405 (1980).
60. E. Fux, J. L. Smith, M. Tong, L. Guzmán, D. M. Anderson, *Toxicon*, **57(**2), 275 (2011).
61. L. Maranda, S. Corwin, S. Dover, S.L. Morton, *Harmful Algae*, **6**, 632 (2007).
62. T. Kamiyama, T. Suzuki, *Harmful Algae*, **8**, 312 (2009).
63. M. L. Fernández, B. Reguera, S. González-Gil, A. Míguez, *Toxicon*, **48(**5), 477 (2006).

Bulgarian Chemical Communications, Volume 52, Special Issue B (pp. 28-34) 2020 DOI: 10.34049/bcc.52.B.0009

Analysis of color reproduction accuracy of digital printing systems

I. Spiridonov[1], R. Boeva[1], S. Yordanov[1*], G. Vladić[2], G. Delić[2], T. Bozhkova[1]

[1] *Department of Pulp, Paper and Printing Arts, University of Chemical Technology and Metallurgy, 8, Kl. Ohridski Blvd., 1756 Sofia, Bulgaria*

[2] *Department of Graphic Engineering and Design, University of Novi Sad, Faculty of Technical Sciences, Novi Sad, Serbia*

Received: November 30, 2019; Revised: October 13, 2020

In the last 10 years, the new generation of state of art digital printing technology has become a significant driver of technical development, and it has become increasingly important in all areas of imaging science, packaging, and printing industry. The new printing technologies offer better color reproduction accuracy, fewer color deviations in the printing run, higher speeds, reduced material and energy consumption, reduced machine preparation time. A large number of various indicators related to the quality of digitally printed output are considered in this study. In the experimental part of this research color difference ΔE, gray balance, color gamut evaluation, tone value, tone value increase, etc., were investigated. These indicators are directly related to the printing process and the possibility of its continuous optimization to achieve a high quality of printing output and the ability to meet international ISO printing standards and requirements. Quality of densitometric and colorimetric characteristics of different types of print media production was investigated. Digital printouts from different manufacturers were used in the media. ICC profiles were generated, and 2D and 3D visualizations were made for visual comparison with international ISO standards. Color quality and accuracy of Pantone colors reproduction was assessed. The Pantone color reproduction is very important for wider spreading out of digital printing processes in packaging, where the color accuracy demands are higher. From the results we can derive how important it is to keep as much as possible recommendations and ISO standards so that we can optimize and maintain print quality to meet the customer's high demands on the end product. This is especially important when printing packages, labels, and more.

Keywords: Printing Quality, Color Reproduction Accuracy, Digital Print, Color Difference, Tone Value Increase

INTRODUCTION

Digital print is a new generation technology in comparison to all known methods of printing information on paperback or any other type of carrier. With the development of information technologies, the application of this printing method also increases. It picks up style in the Graphic industry, as the tendency is for it to go into full industrial use for the production of packages and labels in small and medium circulations. [2]

This paper is the first part of a series of researches, which are focused on different classes of digital printing machines as the latter are used in a variety of applications, such as “Commercial Printing”, “Outdoors Advertisement”, “Packaging and Label” and so on.

EXPERIMENTAL

Reaching the set goals was aided by the use of different measurement tools – densitometer, spectrophotometer, which served to examine the accuracy and quality of tonal and color reproduction in digital printing machines. In order to maintain result reproducibility, a specialized test form was developed and used.

The test form consists of:

- ECI 2002 test chart with 1485 patches for colorimetric assessment and generating of ICC profiles [6];
- Test charts with 0, 5, 10, 20 to 100% for all process colors and their double overlays;
- Positive and negative lines of different width and number of colors for assessment in order to detect the thinnest lines, which could be reproduced from the given material by the examined printing systems;
- Test images for visual analyses;
- Small positive and negative texts of different size;

A multitude of colorimetric and densitometric methods were used [7-9].

The goal of this paper is to render examination results on the accuracy and quality of tonal and color reproduction in ink-jet and electrophoto-graphical digital print as a multitude of assessment methods related to tonal and color reproduction accuracy were selected regarding the Pantone coloring system, color characteristics of solid primary colors, tone value increase, assessment

* To whom all correspondence should be sent:
E-mail: simeon.jordanov@gmail.com

of 3D and 2D color gamut shape and values, visual analyses of images, reproduction of thin positive and negative line art and lines, as well as fonts with small size in one, two and more colors [3]. The following digital machines were used to carry out the experiment: Canon IPF 9400 – ink-jet printer with water-based inks; media used to perform the experimental analyses were: glossy photo paper – 190 g/m^2.

RESULTS AND DISCUSSION

Due to the large dataset obtained from the thorough research on the precision and quality of tonal and color reproduction for ink-jet and electrophotographical digital print, this paper will only include the results obtained during the experiments with Canon IPF 9400 loaded with photo paper. The examination included assessment of color characteristics of test prints, simulating specially selected Pantone colors. Also there was a measurement of the color coordinates as per the CIE Lab system with included calculation and comparison of ΔE_{76} and ΔE_{00} according to ISO 12647-2:2013 [4]. A dedicated software product was used to render the 2D and 3D visualization and a comparison between the color gamut of the examined media was made with a standard ICC profile FOGRA47 and FOGRA51 [6].

In order to compare the quality of tonal and color reproduction of catalogue and selected Pantone system colors, one must calculate the color difference ΔE for a set number of colors. In order to calculate ΔE, one must first obtain the color coordinates of all colors according to the CIE Lab system. The reference values are the color coordinates as per ISO 12647-2:2013 [4].

Process control for the production of half-tone color

Color differences were derived using the following formulas:

color difference ΔE_{76}:

$$\Delta E^*_{76} = \sqrt{(L^*_1 - L^*_2)^2 + (a^*_1 - a^*_2)^2 + (b^*_1 - b^*_2)^2} \quad (1)$$

color difference ΔE_{00}:

$$\Delta E^*_{00} = \sqrt{\left(\frac{\Delta L'}{K_L S_L}\right)^2 + \left(\frac{\Delta C'}{K_C S_C}\right)^2 + \left(\frac{\Delta H'}{K_H S_H}\right)^2 + R_T \frac{\Delta C'}{K_C S_C} \frac{\Delta H'}{K_H S_H}} \quad (2)$$

where: L – lightness/brightness; C – saturation; H – hue.

The measurements of color coordinates are made using a spectrophotometer under the following conditions:

- standard light illuminant - D50;
- 2° standard observer;
- no polarization filter;
- aperture – 4 mm;
- white backing.

Investigation of color reproduction accuracy of digital printing systems and calculation of ΔE for Pantone colors

In order to examine the reproduction precision of the fundamental Pantone colors, the color coordinates (Lab) for the media listed above were measured. Figure 1 represents the basic Pantone colors.

In order to examine the reproduction precision of the basic Pantone colors, the color coordinates (Lab) for the media listed above have been measured. Figure 1 represents a selection of Pantone colors.

Due to the extensiveness of the measurements and the multitude of obtained results, this paper presents only an excerpt there to concerning the stated printing machine and the printing media, used in conjunction with it. Tables 1 and 2 show all results derived from ΔE calculations.

Fig. 1. Selection of Pantone colors used in the experiment

Table 1. Experimental results for color reproduction accuracy obtained for selected Pantone colors

Selected Pantone colours			ΔE76			Count of colours corresponding to the average limitations (total of 13)			ΔE00			Count of colours corresponding to the average limitations (total of 13)		
№	Digital machine	Media	ΔE avg.	ΔEmin	ΔEmax	ΔE<3	ΔE<5	ΔE>5	ΔE avg.	ΔEmin	ΔEmax	ΔE<3	ΔE<5	ΔE>5
1	HP Latex 370	polypropylene	7,16	1,42	23,94	2	4	7	3,30	0,48	6,21	7	3	3
2	HP Latex 370	Self-adhesive PVC	7,21	2,31	24,17	2	3	8	3,36	1,25	6,40	8	2	2
3	Agfa Anapurna M2540	Vinil	7,34	2,31	22,03	3	3	7	3,44	1,43	8,47	8	2	3
4	HP Latex 370	Jetcoat paper	7,44	2,03	24,30	2	3	8	3,48	1,18	7,44	7	3	3
5	HP Indigo 5500	Matte coated paper	7,59	1,69	18,68	2	2	9	3,83	1,49	5,95	4	7	2
6	Canon IPF9400	Photo paper	8,28	3,72	21,07	0	3	10	4,18	1,99	7,15	5	3	5
7	HP Indigo 5500	Glossy coated paper	8,63	2,41	19,65	1	1	11	5,00	2,15	16,07	4	7	2
8	HP Indigo 5500	Offset uncoated paper	11,49	3,76	21,39	0	1	12	6,49	3,25	9,68	0	4	9

Table 2. Results obtained from measuring the color differences with ΔE_{76} and ΔE_{00} and comparing Pantone colors with ISO 12647-2: 2013 for photo paper printed on the Canon IPF 9400

Selected Pantone Colors									
Photo Paper Media		Canon IPF 9400			ISO (coated)			ΔE_{76}	ΔE_{00}
№	color	L	a	b	L	a	b		
1	Pantone 7420	32.92	48.29	7.9	36	51	15	8.20	4.45
2	Pantone 429	72.67	-1.18	-9.23	70	-2	-3	6.83	5.47
3	Pantone 431	39.36	-2.91	-10.79	44	-3	-6	6.67	5.45
4	Pantone 151	62.34	37.58	64.44	67	51	80	21.07	6
5	Pantone 314	46.39	-38.05	-38.13	46	-43	-37	5.09	2.1
6	Pantone 618	66.46	-3.64	55.29	67	-4	49	6.32	1.99
7	Pantone 659	63.89	-6.58	-36.35	62	-3	-35	4.27	3.2
8	Pantone 318	82.25	-14.63	-13.81	84	-25	-11	10.89	7.15
9	Pantone 7465	72.99	-26.26	-5.33	71	-42	-5	15.87	6.57
10	Pantone 680	68.97	30.63	-14.33	68	24	-8	9.22	4.28
11	Pantone 348	46.31	-53.01	26.06	47	-57	23	5.08	2.22
12	Pantone 876	46.89	16.37	18.83	48	17	23	4.36	2.61
13	Pantone 4685	84.92	6.3	9.41	84	6	13	3.72	2.81
					ΔEavg			8.28	4.18

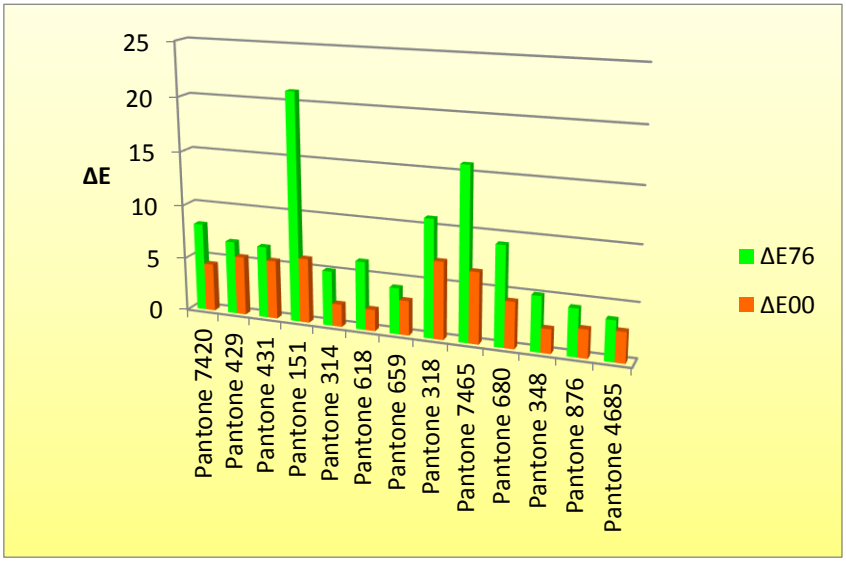

Fig. 2. Comparison of the color differences, according to CIE Lab, between the selected Pantone colors with ΔE_{76} and ΔE_{00} for glossy photo paper printed through Canon IPF 9400

Figure 2 shows the comparative graphs for comparison of the color differences according to CIE Lab, between the selected Pantone colors with ΔE_{76} and ΔE_{00} for glossy photo paper printed through Canon IPF 9400.

Investigation of tone value increase for digital printing systems on glossy photo paper

The tone value increase is an indicator which defines tone and color reproduction and under certain conditions it influences the image depth field. This is one of the most important measured values, serving to control the printing process and is directly linked to the quality of the printed image [1]. In order to define the tone value increase for the separate prints, one performs densitometric measurements of tonal fields in the interval between 5% and 100%.

Figure 3 depicts the relationship between the set and measured raster tone for photo paper, which is the gradation characteristic of reproduction in the four primary colors (CMYK). The figure shows that for all four colors (cyan, magenta, yellow and black) we have a substantially uniform increase. Only the black color from 0% to 15% has slightly higher measured values than the other colors.

Figure 4 shows the relationship between the reference tone value and the tone value increase of cyan, magenta, yellow and black printed on photo paper compared to standard curves according to ISO 12647-2: 2013. The graph shows that the experimental curves of the four primary colors have varying values, in light medium and dark tones. In cyan there is a slight decrease in the values from 20% to 35%, after which in the average tones from 40% to 70% we have approximately the same values compared to the reference (A-E) accepted in ISO 12647-2: 2013.

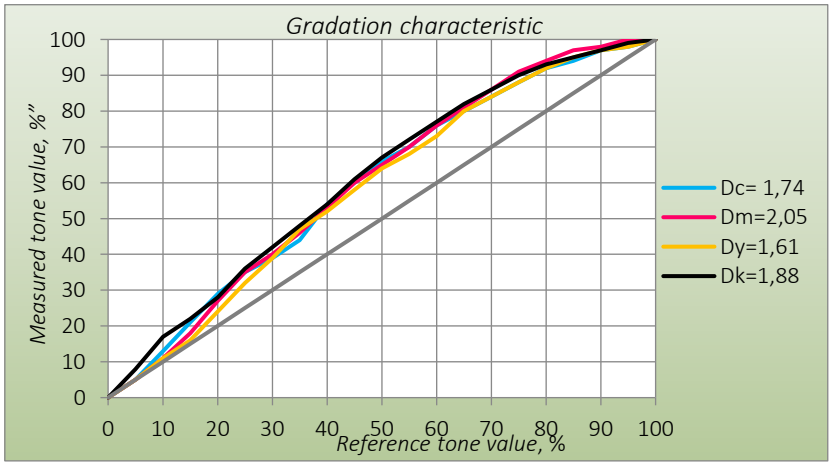

Fig. 3. Dependency between the reference and measured tone value (gradation characteristic) for glossy photo paper printed through digital printer Canon IPF 9400

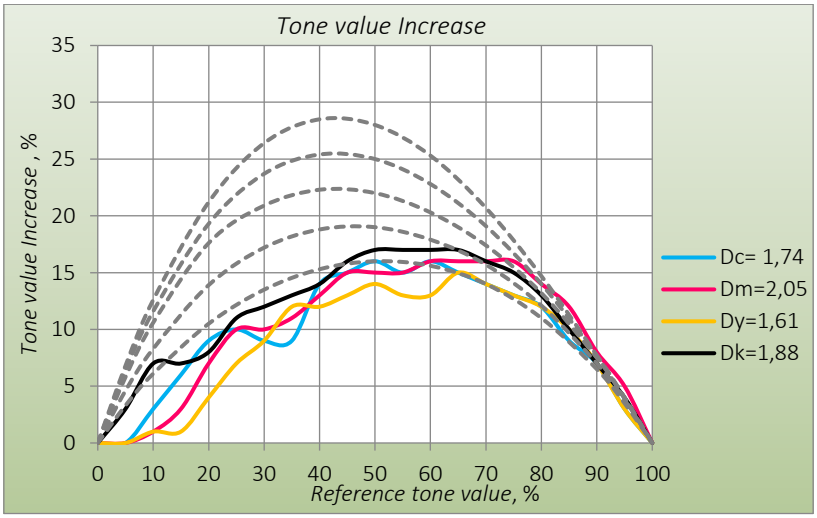

Fig. 4. Tone value increase for the four primary colors and standard curves as per ISO 12647-2:2013 for glossy photo paper printed through digital printer Canon IPF 9400

With magenta from 0% to 40%, the results obtained are lower than the standard values, at 50% and 60% the data obtained are closest to the standard values, and then in the dark tones we have slightly higher values. For the black color from 0% to 10%, the obtained data are approximately the same as the reference values, and then it can be seen that it has lower measured values than the standard values up to 45%. In the color yellow from 0% to 15%, significantly lower results are observed, followed by a smoother increase to medium tones, and between 50% and 60% a slight decrease occurs in the measured data. Yellow has the lowest values compared to the others. This graph shows no shift in the peak of growth, despite varying results in all four colors. These results can also lead to inaccuracies in tone and color reproduction.

Investigation of color gamut volumes and comparison of 2D and 3D color gamut of different digital printing systems

One important function which is used to visualise the colors, as reproduced by any given machine, is the 2D and 3D representation of the respective color gamut. This paper also uses 2D and 3D representations. The 2D representation of color gamut with different cross-sections along the L-axis of the CIE Lab color space allows for good visual comparison of colors in light, mid and dark tones, as well as comparison of a large number of color gamut at once [7]. The 3D representation of color gamut allows a complex visual assessment for the 3D body of the color gamut. It is appropriate for the visualization and comparison of one or two color gamuts.

In order to perform the comparison for the color gamut of the examined prints from the corresponding digital printing presses – HP Indigo 5500, Agfa Anapurna M2540, Canon IPF9400 and HP Latex 370 it is necessary to provide a 3D visualization with a standard ICC profile FOGRA 47 for uncoated papers and FOGRA 51 for coated papers with the ultimate goal to achieve visual representation for the color gamut. The 3D visualization of the ICC color profiles was performed using the software PROFILE MAKER 5.10. To compare the color gamut on offset uncoated paper, a standard ICC profile FOGRA 47 was used.

From Figure 5 it can be seen that the color range of FOGRA 51 is significantly larger than the color range of photo paper printed on the Canon IPF9400. It is observed that in certain areas the color range of the digital machine under study may produce colors that FOGRA 51 cannot.

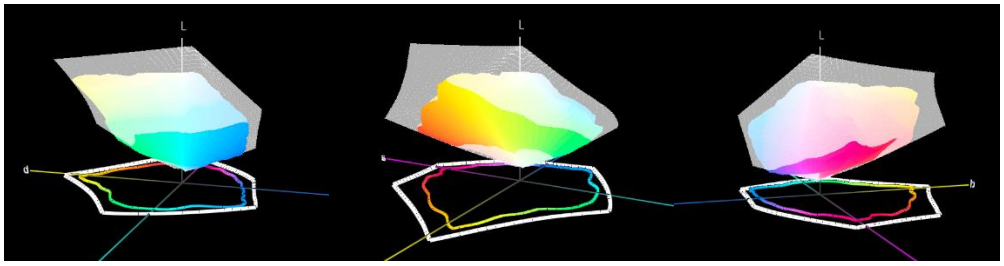

Fig. 5. 3D visualization (Lab system) of an ICC profile of glossy photo paper printed through Canon IPF 9400 and FOGRA 51

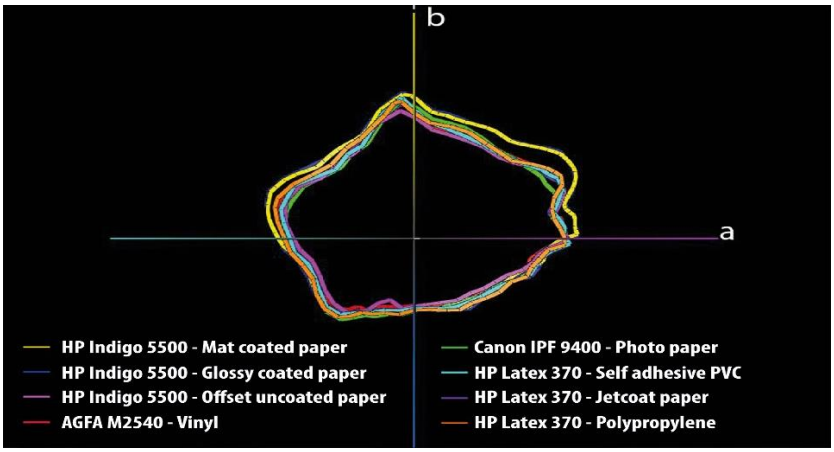

Fig. 6. 2D visualization of the color range of all types of media used within the scope of the experiment

It can be seen that with photo paper we have better color reproduction in the medium tones of the yellow-red area and in the light tones of the blue-green area. While with FOGRA 51 we have better color reproduction in dark tones and light tones in the yellow-green area.

Figure 6 depicts a 2D visualization of the color gamut of the tested media. The data shows that the most accurate tone and color reproduction occurs on matte and glossy papers printed through HP Indigo 5500, as they coincide in all areas. The smallest color gamut occurs with offset paper printed through the same machine. This phenomenon is due to the fact that offset paper is considered an uncoated print medium and has more porous structure, thus causing more ink intake in comparison to coated media.

Table 3. Volume of the color gamut.

№	Machines	Used media	Volume of the color gamut ΔE^3
1	HP Indigo 5500	Offset uncoated paper	202 479
2	HP Indigo 5500	Matte coated paper	293 021
3	HP Indigo 5500	Glossy coated paper	314 299
4	Agfa Anapurna M2540	Vinyl	244 498
5	Canon IPF 9400	Glossy photo paper	246 780
6	HP Latex 370	Paper “Jetcoat”	236 614
7	HP Latex 370	Polypropylene	254 321
8	HP Latex 370	Self-adhesive PVC	244 983

CONCLUSIONS

Based on the experimental results obtained in this paper, the following conclusions were drawn:

1. Color reproduction accuracy is an ever more important factor provided by the increasing usage of digital printing systems, especially in the production of packages, labels and other. In spite of the extended color gamut in most digital printing systems some of the fundamental problems originate from the insufficient color reproduction accuracy – especially with Pantone. After printing 240 Pantone colors, colorimetric measurement and appropriate analyses it was established that:

- The average color difference in ascending order between the set Pantone colors and the measured prints is:
  a. $\Delta E_{00\ avg.}$ HP Indigo 5500 varies between 3.83 and 7.06 ($\Delta E_{76\ avg.}$ from 7.59 to 23.33);
  b. $\Delta E_{00\ avg.}$ HP Latex 370 varies between 3.30 and 8.48 ($\Delta E_{76\ avg.}$ from 7.16 to 25.98);
  c. $\Delta E_{00\ avg.}$ Canon IPF9400 varies between 4.18 and 7.40($\Delta E_{76\ avg.}$ from 8.28 to 25.37);
  d. $\Delta E_{00\ avg.}$ Agfa Anapurna M2540 varies between 3.44 and 8.26 ($\Delta E_{76\ avg.}$ from 7.34 to 25.87).
- The minimal color difference in ascending order is ΔE_{00} = 0,48 (HP Latex 370) up to 4,10 (HP Indigo 5500)
- The maximal color difference in ascending order is ΔE_{00} = 5,95 (HP Indigo 5500) up to 26,06 (HP Latex 370)

From the obtained results one may conclude that the highest color reproduction accuracy of the Pantone colors is achieved while using the machine HP Indigo 5500 followed by all the other examined printing systems. Therefore, the present paper focuses mainly on its results as closest to ISO12647-2:2013. However, the average color difference ΔE is relatively high and could be the source of some inaccurate perception, especially with pretentious customers who often insist on a maximal tolerance of ± 1÷2 ΔE. For some of the Pantone colors, one obtains very good and low values of ΔE such as ΔE_{00} = 0.48 (HP Latex 370).

2. Color gamut and its volume is of special significance when the print quality is defined. The largest color gamut was obtained with HP Indigo 5500 (ΔE^3 =314 299), followed by HP Latex 370 (ΔE^3 =254 321), Canon IPF9400 (ΔE^3 =246 780) and Agfa Anapurna M2540 (ΔE^3 =244 498). The standard color gamut of FOGRA52 was best met by the HP Indigo 5500, followed by HP Latex 370 and Agfa Anapurna M2540.

3. The tone value increase and color characteristics of primary colors are important for the research of comparable visual results of digital print compared to the conventional printing processes. The experiment established that the TVI curves of digital printing systems differ significantly from their standardized counterparts. For the most cases, the curves follow the standards for light and dark hues and differ in the mids.

From the presented graphic material depicting the dependency between the reference and

measured color tone, representing the gradation characteristics, one may observe a uniform increment of the color tone for the four primary colors with all tested media.

For the most part of the tested media, one observes that within the first 5% of the reference there is 0% increase of the color tone for some of the colors. Another interesting fact which becomes apparent from these graphics, is that with most media, the obtained values during the primary colors measurements are slightly lower in the light and mid hues – up to the 60% mark. On the one hand this does not lead to any significant increase of the color tone, but the very fact that there are lower values obtained for the CMYK across most of the media could also lead to some inconsistencies in tonal and color reproduction. From the results obtained herein, one could begin to understand how important it is to adhere as much as possible to the recommendations of the ISO standards in order to be able to optimize and to maintain the print quality so that the customer's highest requirements with respect to the end product are fully met. This is especially important with the print of packages, labels and other.

REFERENCES

1. N. Kachin, I. Spiridonov, *Cellulose Chemistry and Technology*, **39**(3-4), 255 (2004).
2. N. Kachin, I. Spiridonov, Printing Processes, Part 1, Theoretical bases, Pleiada, Sofia, 2000.
3. H. Kipphan, Handbook of Print Media, Encyclopedia, Springer, 2001(ISBN 3-540-67326-1).
4. ISO 12647-2:2013 Graphic technology - Process control for the production of half-tone color separations, proof and production prints - Part 2: Offset lithographic processes.
5. https://www.fogra.org/.
6. http://www.eci.org/.
7. I. Spiridonov, M. Shopova, *Journal of the University of Chemical Technology and Metallurgy*, **48** (3), 247 (2013).
8. I. Spiridonov, M. Shopova, R. Boeva-Spiridonova, *Optica Applicata*, **42** (3), 627 (2012).
9. T. Bozhkova, I. Spiridonov, K. Shterev, *Bulgarian Chemical Communications*, **49**, 195 (2017).

Bulgarian Chemical Communications, Volume 52, Special Issue B (pp. 35-39) 2020 DOI: 10.34049/bcc.52.B.0010

Investigation of physical and mechanical properties changes of papers during thermal ageing

R. Boeva[1*], I. Spiridonov[1], S. Đurđević[2], Ž. Zeljković[2]

[1]*Department of Pulp, Paper and Printing Arts, Department of Physical Chemistry, University of Chemical Technology and Metallurgy, 8, Kl. Ohridski Blvd., 1756 Sofia, Bulgaria*
[2]*Department of Graphic Engineering and Design, University of Novi Sad, Faculty of Technical Sciences Novi Sad, Serbia*

Received: November 30, 2019; Accepted: October 13, 2020

The papers and boards are the main used materials for printing industry. Therefore, it is very important to know their characteristics and peculiarities and to know in advance, how their properties would change all over the time it is used and stored. Over the time all papers and boards change their physical, mechanical and chemical properties – called papers ageing processes. The ageing is an irreversible process. As much slower the process of ageing, as longer life of paper is expected. The papers examined in this research, are chosen for their wide use and popularity in the world printing industry. The aim of the present study is to investigate the influence of artificial thermal ageing at 105ºC on the basic physical, mechanical and optical properties of all types of investigated papers. Various structural and dimensional properties, as well as physical, mechanical and optical properties were determined before, during and at the end of the artificial thermal ageing process. From the results obtained it is clear that the different fibrous composition and the storage conditions have a great influence on the ageing of the paper. All investigated parameters take changes in specific and different ways, but all of them decreasing in the ageing process.

Keywords: thermal ageing**,** physical-mechanical and optical properties of papers, papers and boards

INTRODUCTION

Each paper changes its physical, mechanical and chemical properties over time - paper ageing - and the process is irreversible. With long-time natural ageing, the fibers in the paper lose their elasticity [1, 2]. Paper ageing is a complex process whose nature is still poorly understood as it is influenced by many factors [2]. Most important is the action of light and heat. There are two types of ageing of fibrous materials - thermal and photo ageing. Thermal ageing is in most cases due to oxidation processes under the action of oxygen from air and hydrolysis under the action of humidity. The durability of the paper is its ability to retain certain physico-mechanical, optical and chemical properties unchanged over time [3, 4]. The most commonly used conditions for artificial thermal ageing are:

• temperature of 105 ± 2°C in a dry air circulation chamber (ISO 5630-1: 1991) and temperature of 80°C at 65% relative humidity (ISO 5630-3: 1996).

For these parameters, it is assumed that treatment over 3, 6, 12 or 24 days corresponds, respectively, to 25, 50, 100 or 200 years of natural ageing of the paper. Under the direct influence of light (solar or artificial), new papers quickly turn yellow and become fragile [5, 6].

EXPERIMENTAL

The international standard ISO 12647-2: 2004 lists the main types of paper for sheet and roll printing used most widely in practice [5-9]. The following paper types were used for the experiment: LWC (Light Weight Coated) and NP (Newspaper). The papers examined in this research were chosen for their wide use and popularity in the world printing industry.

Structural-dimensional properties of the studied papers determined:

- Humidity (EN 20287: 1996);
- Type of fibrous material (microscopic analysis) (EN 8658-71);
- Weight (g/m^2) (EN ISO 536: 1998);
- Thickness and density (EN ISO 534: 2006).

Microscopic analysis of the fiber structure of the examined papers was made.

Basic physical-mechanical properties determined:

- Tensile index (EN ISO 1924-2: 2000);
- Tear index (EN ISO 21974: 2001);
- Burst index (EN ISO 2758: 2005).

* To whom all correspondence should be sent:
E-mail: : r_boeva@abv.bg

Optical properties determined:

- Brightness (R457);
- Yellowness (ISO 2470:2007).

A spectrophotometer (SpectroEye) was used under measurement conditions: light source D65, observer angle 10°. The change in artificial ageing was monitored before and after 6, 12, 24, 36, 48 hours of ageing.

RESULTS AND DISCUSSION

Determination of structural-dimensional properties of the studied papers

The following analyses were made on both types of paper as shown in Table 1.

Table 1. Structural-dimensional properties of the studied papers

Type of paper	Weight, (g/m^2)	Thickness, (μm)	Density, (kg/m^3)	Humidity, (%)
LWC	89	1.1	80	4.37
NP	45	1	45	7.73

Picture 1. LWC

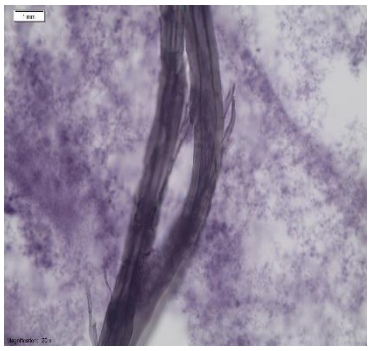

Picture 2. NP

Microscopic analysis of the fiber structure of the examined papers

The microscopic analysis was performed on an apparatus OLYMPUS BX 53. Different fiber materials were used in the production of many types of paper in a certain proportion. The microscopic pictures show the fiber composition of the papers examined. Picture 1 shows that the LWC paper contains hardwood and softwood pulps. Picture 2 (NP) shows that the newsprint is made up of a considerable groundwood pulp. Non-uniform fibers characteristic of the high-yield fibrous materials are observed. These tears are most likely caused by grinding, as well as by subsequent chemical treatment of the wood during boiling. Characteristic vessels with open edges that have extensions characteristic of deciduous wood are observed. From the pictures, the main types of fibers used in the structure of the papers under study are clearly visible.

Investigation of the basic physical and mechanical properties of the two types of papers

Figures (1-3) show the changes in the values of the basic physical-mechanical parameters of the studied papers. They determine the basic and important properties for all types of papers and cardboards.

The formation of the physical-mechanical properties of paper is influenced by a number of factors that affect the strength of the paper; they ultimately exert their effect through three main factors, and it can be said that the strength depends primarily on them. These are:

- The bonding forces between the fibers and the surface on which they act;
- The strength, elasticity and dimensions of the fibers themselves;
- Laying the fibers in the paper sheet.

Figure 1 shows the tensile index values for both types of paper and the changes that occur in the process of artificial thermal ageing at 105°C.

The tensile index depends primarily on the bonding forces between the fibers and less on the length and strength of the fibers themselves. Figure 1 shows that the largest changes in the tensile index are observed with newsprint (12.92), which is due to the fiber composition of the test paper. The changes for LWC are smaller (9.39). This indicator is most influenced by the bonding forces between the fibers and less by the length and strength of the fibers themselves. Figure 2 shows the variations in the burst index values for the paper being tested. This indicator is a complex function of the tensile index and the elongation of the paper before it tends to grow as they increase. This indicator depends on both the length of the fibers and the bonding forces between them. The biggest changes occur with the LWC, but the changes in the other paper are identical. The tendency of the studied papers is: faster changes during the first hours of the artificial thermal ageing to about 6 – 12 h and smoother decrease with the process progressing up to 24 h. Figure 3 shows the values of the test papers for the tear index. This is one of the most important properties of paper that characterizes the dynamic strength. This indicator can be used to judge the stretchability of the paper. The tear index is determined by the structure of the paper (mass, density, fiber orientation), as well as by the length and strength of the fibers, and depends only to a minimum on the bonding forces between them. The tendency to decrease this indicator is identical for all the papers examined. The fastest is the reduction again at the beginning of the ageing process to about 12 h. The largest changes (Fig. 3) in this indicator were observed in newsprint (5) and in LWC (around 4).

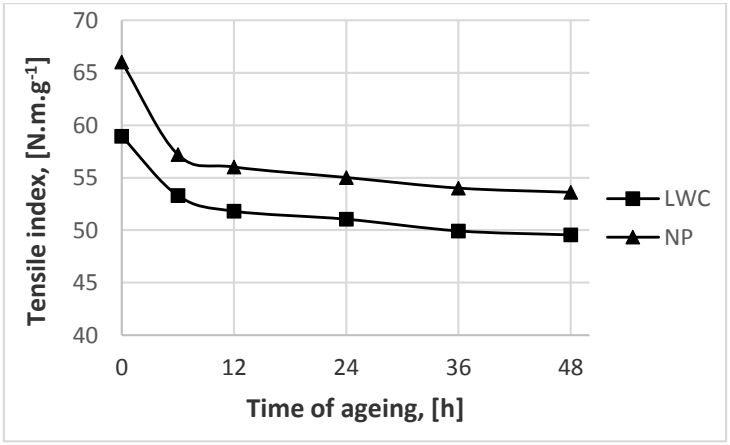

Fig. 1. Change of the tensile index of the test papers before and after artificial ageing at 105ºC

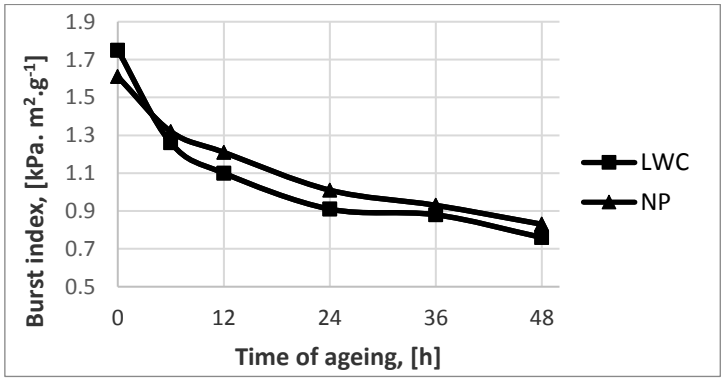

Fig. 2. Change of the burst index of the test papers before and after artificial ageing at 105ºC.

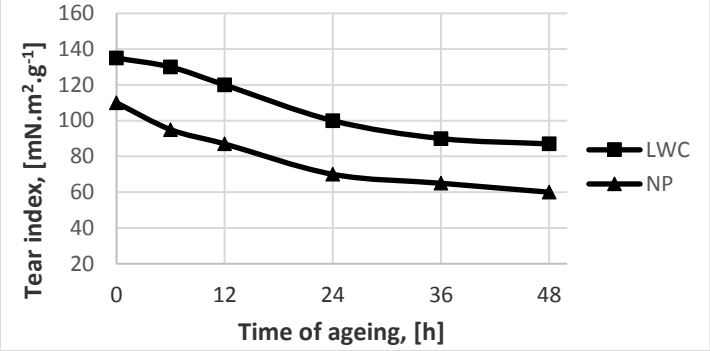

Fig. 3. Change of the tear index of the test papers before and after artificial ageing at 105ºC.

Investigation of the optical properties of the papers

The optical properties of the paper depend on the contrast of the image, the accuracy of color rendering in multicolor, the quality and appearance of the print as a whole. Some of the most important optical properties are: those related to the reflection of light – brightness, yellowness, gloss and matte. Figure 4 shows the values of the brightness change over time in the process of artificial thermal ageing at 105°C. For the first 6 hours and anywhere up to about 12 h the decrease in brightness (Fig. 4) is most dramatic, after which it becomes smoother. At least the brightness decreased with newsprint, but it had a lower initial brightness (58.88%). Figure 5 shows the changes in the degree of yellowing in the process of artificial ageing. Yellowing of the paper is a pretty important indicator for writing and printing papers. The reason for its increase is the influence of light, increase of temperature and humidity of the environment, harmful gases in the atmosphere (mainly SO_2), the type of fibrous materials used and the ways of their production. Figure 5 shows that the largest changes are the yellowness values for LWC paper (24.15) and smaller for NP due to the fiber composition. Both papers are characterized by the fastest change up to 6 – 12 h from the start of the ageing process and the subsequent tendency to gradually decrease by the end of the studied ageing period. It is seen that in the course of ageing, with the passage of time, the brightness decreases and the yellowness increases with the studied papers.

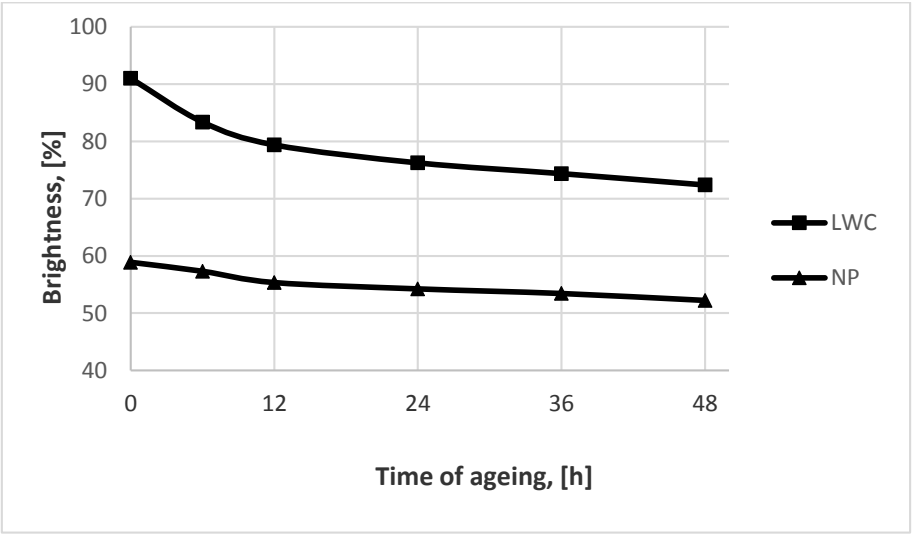

Fig. 4. Change in the brightness of the test papers in the process of artificial ageing at 105ºC.

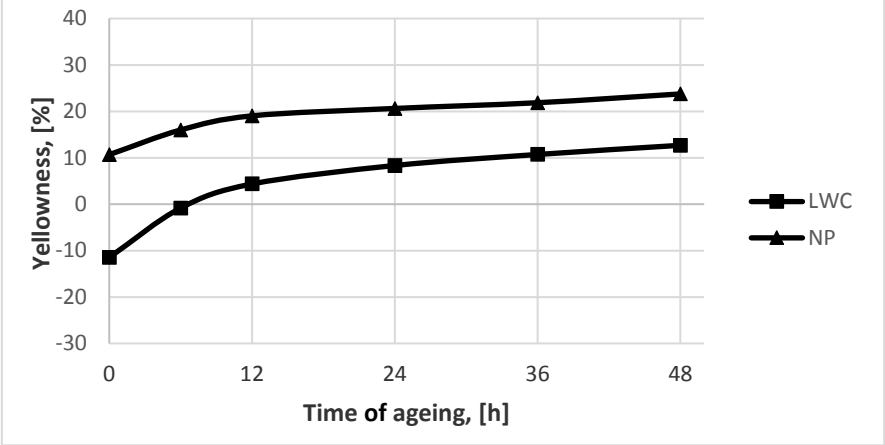

Fig. 5. Changes in the yellowness of the test papers in the process of artificial ageing at 105ºC.

CONCLUSIONS

The largest changes in the tensile index are observed for newsprint (12.92), which is due to the fiber composition of the test paper. The changes for LWC are smaller (9.39). The tear index decreases most rapidly at the beginning of the ageing process to about 12 h. Major changes in this indicator were observed in newsprint (5) and smaller changes in LWC (around 4). The biggest changes in the burst index occur at the LWC, but the changes for the other paper are identical. The trend in the papers studied is: faster changes in the first hours of artificial ageing up to 6 – 12 h and subsequent gradual decrease with the progress of the process up to 24 h. It is seen that in the course of ageing, with the passage of time, the brightness rate decreases and the yellowness rate increases with the studied papers. The brightness decreased with newsprint, but it had a lower initial brightness (58.88%).

Acknowledgements: *The authors thank the Scientific Research Centre (contract №11888) at the UCTM Sofia for the financial support of these investigations.*

REFERENCES

1. R. Zou, J. Hao, R. Liao, IEEE 20th International Conference on Dielectric Liquids (ICDL), 2019.
2. M. Nedelcheva, Chemistry and technology of the paper, Sofia, 1992.
3. M. Valkova, Conservation and restoration of works of art on paper, 2016.
4. M. Area, H. Cheradame, *Bioresources*, **6**, 5307 (2011).
5. B. Lajić, I. Majnaric, I. Bolanča Mirković, *Nordic Pulp and Paper Research Journal*, **28**(1), 101 (2013).
6. A. Munajad, C. Subroto and Suwarno, *Energies*, **10**, 1857 (2017).
7. M. El-Sakhawy, *Polymer Degradation and Stability*, **87**, 419 (2005).
8. B. Havlínová, D. Babiaková, M. Brezová, V. Ďurovič, M. Novotná, F. Belányia, *Dyes and Pigments*, **54**(2), 173 (2002).
9. M. Karlovits, D. Gregor-Svetec, *Acta Polytechnica Hungarica*, **9**(6) (2012).

Bulgarian Chemical Communications, Volume 52, Special Issue B (pp. 40-43) 2020 DOI: 10.34049/bcc.52.B.0011

Cytotoxic effect of dimethyl sulfoxide (DMSO) on hematopoietic stem cells: Influence of the temperature and the incubation time

I. D. Tonev[1*], S. H. Hristova[2,3], A. M. Zhivkov[3], M. S. Mincheff[1]

[1]*National Specialized Hospital for Active Treatment of Hematological Diseases, Plovdivsko pole Str. 6, Sofia 1756, Bulgaria*

[2]*Department of Medical Physics and Biophysics, Medical Faculty, Medical University – Sofia, Zdrave Str. 2, Sofia 1431, Bulgaria*

[3]*'Rostislaw Kaishew' Institute of Physical Chemistry, Bulgarian Academy of Sciences, Acad. G. Bonchev Str., Bl. 11, Sofia 1113, Bulgaria*

Received: November 28, 2019; Accepted: November 15, 2020

The cryoprotection is crucial for the preservation of haematopoietic stem cells, which allows postponing of their transplantation after the isolation, without significant decrease of the cell viability even after years. Dimethyl sulfoxide (DMSO) is a widely used intracellular cryoprotectant. Its small amphiphilic molecule fast penetrates through the cytoplasmic membrane. It is known that DMSO is toxic above 4°C but its effect on the hematopoietic stem cells is insufficiently studied. The purpose of this investigation is to analyze the influences of the duration and the temperature of incubation in a 5 % solution of DMSO in saline on the viability of the hematopoietic stem cells, using trypan-blue exclusion test. The results show out that at 4°C DMSO has a low cytotoxic effect even after 24 hours of incubation. At room temperature the viability decreases by 67% for the same time of treatment; and at 37°C the 24-hour incubation leads to 100% cell mortality.

Keywords: DMSO cytotoxicity, cryoprotection, stem cells

INTRODUCTION

Hematopoietic stem cell (HSC) transplantation is widely used in the therapy of benign and malignant hematological diseases and the number of autologous and allogeneic transplantations rises every year [1-3]. The hematopoietic stem cells from bone marrow, peripheral blood or cord blood are with intensive metabolism, therefore, their storage time at a temperature between +2 and +24°C is limited [4, 5]. The storage of stem cells between +4ºC and +8ºC is accepted as safe for up to 5 days, after which their viability drops markedly [6-8], so their longer storage until the day of transplantation is possible only in a frozen state. The cryoprotection is crucial for the freezing of living cells, as intracellular cryoprotectants should penetrate the cell membrane not allowing dehydration that causes osmotic injury [9]. Dimethyl sulfoxide (DMSO) is a widely used intracellular cryoprotectant [10] for haematopoietic stem cells. Its small amphiphilic molecule quickly penetrates through the cytoplasmic membrane. Despite slower passage through cell membrane in comparison with water [11], the membrane permeability P of DMSO is 0.157 μm/s for model membranes [12] and 0.13 μm/s for red blood cells [13], which is approximately three times faster than this of glycerol. The presence of negatively charged atoms like sulfur and oxygen, determines the dipole and nucleophilic character of its molecule, thus making DMSO proton acceptor in hydrogen bonds generation. The hydrogen bonds, generated between DMSO and two water molecules, are 1.3 times stronger than the hydrogen bonds between water molecules themselves. Resulting from this, DMSO disturbs the water molecules organization and impedes ice formation inside the cell during freezing [14]. Additionally, the use of this intracellular cryoprotectant leads to widening of the temperature diapason of the dehydration, so the cell has more time for response to changes in osmotic pressure [15].

A major requirement for the cryoprotectants, in addition to their protective role during cell freezing, is to be nontoxic for the cells at high molar concentration necessary for prevention of extreme ice formation [9]. The cytotoxicity of DMSO depends on its concentration [13, 16, 17] and the type of the treated cells. It is known that DMSO is toxic above 4°C but its effect on the hematopoietic stem cells is insufficiently studied. The temperature of incubation, ranging from 4°C to 37°C at low DMSO concentration for short periods does not affect cytotoxicity. For instance, neonatal human dermal fibroblasts retain their viability after 30-min incubation in 5% DMSO at temperatures of 4°C, 25°C and 37°C [18].

* To whom all correspondence should be sent:
E-mail: ivanton@mail.bg

Similar effect is observed in human chondrocytes, where the incubation at temperatures of 4°C, 22°C and 37°C does not change the cell viability with 1M (approximately 8%) DMSO for 120 min [19]. Low dose cytotoxicity is observed in retinal ganglion cells after 24-hour incubation with 4% DMSO [20].

Despite the fact that DMSO is a widely used intracellular cryoprotectant for different animal cells, including stem cells, the effect of incubation temperature on DMSO cytotoxicity after longer incubation periods is not explored in detail. The purpose of our work is to study the correlation between incubation temperature and cytotoxicity on human hematopoietic stem cells after exposure to 5% DMSO for up to 24 hours.

MATERIALS AND METHODS

Hematopoietic stem cells from peripheral blood of stimulated donors and patients were collected using a cell separator. The cell suspension was concentrated by removing the plasma. A cryoprotective solution was added so that the final concentration of DMSO was 5%; of hydroxyethyl starch (HES) 450 kg/mol 3.6% and of human serum albumin (HSA) 3%. The viability of the stem cells mixed with cryoprotective solution, was tested by trypan-blue exclusion after incubation at 4°C, room temperature and 37°C for 30 min, 1 hour and 24 hours. Trypan-blue test is based on the different membrane permeability of living and dead cells for dyes. Trypan blue is a large, hydrophilic, tetrasulfonated anionic dye. The intact lipid bilayer of the cell membrane is an impermeable barrier for this relatively large and negatively charged molecule. Thus, the living cells remain uncolored, while the dye penetrates in the dead cells and they are colored in intensive blue.

RESULTS

At the lowest temperature, the number of dead cells (colored in blue) practically does not change, while at higher temperatures their number significantly increases with the incubation time. On Figure 1 are presented microscopic pictures of HSC suspension incubated with 5% DMSO at different temperatures and stained with trypan blue after 30, 60 min and 24 hours (Fig. 1A at 4°C, Fig. 1B at 20°C, and Fig. 1C at 37°C).

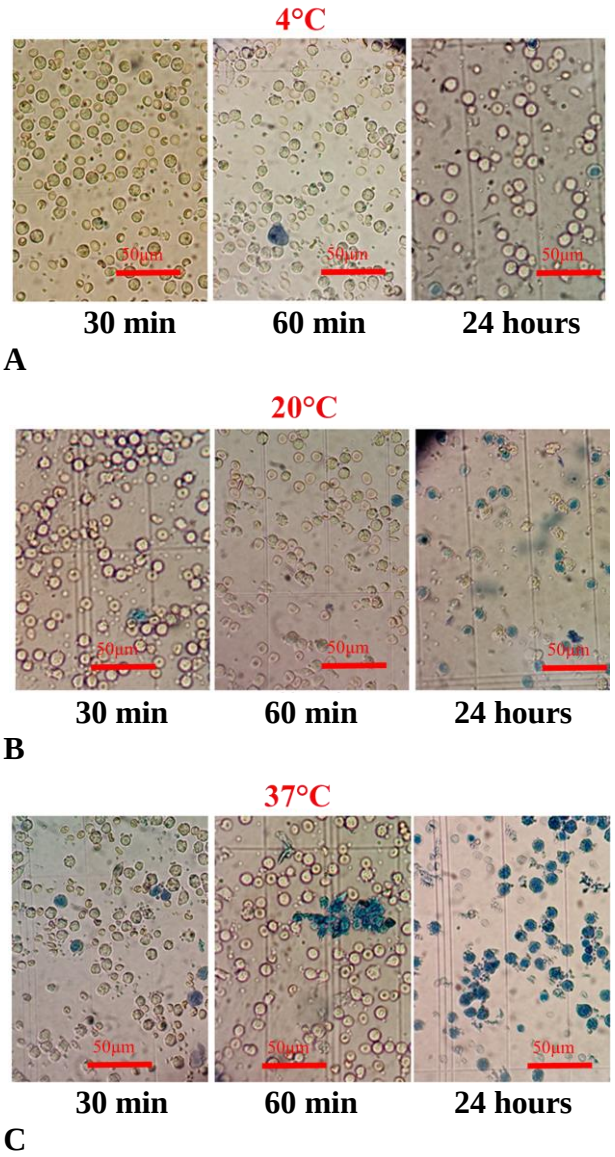

Fig. 1. Microscopic pictures of trypan-blue test for stem cell viability at 4°C (A), 20°C (B) 37°C (C) temperature of incubation. The dead cells are colored in blue.

The percentage of viable stem cells, shown after incubation at different temperatures with a standard cryoprotective solution, used for hematopoietic stem cell freezing, can be seen on Figure 2. The viability of the stem cells, when incubation periods are short, is much less affected by DMSO and its cytotoxic action is practically seen only at 37°C. One-hour incubation of peripheral blood stem cells leads to insignificant viability changes in comparison with 30-min incubation (Fig. 2B).

The influence of the temperature on the cytotoxic action of DMSO becomes apparent on the 24th hour of incubation of the stem cells with standard cryoprotective solution (Fig. 2C). At 4 °C the viability still remains very high – 99% and DMSO cytotoxicity is practically not seen. At room temperature the one-day incubation decreases the cell viability to 33%, and incubation at 37 °C leads to complete loss of cell viability.

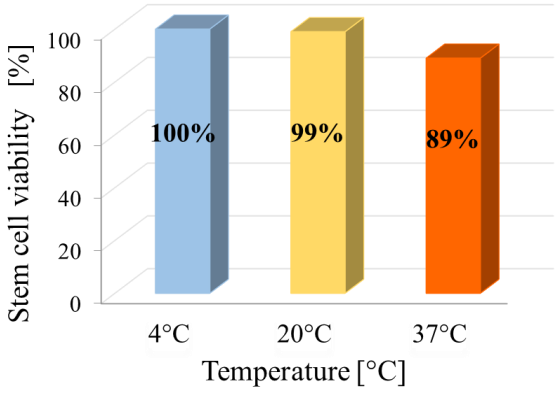

A

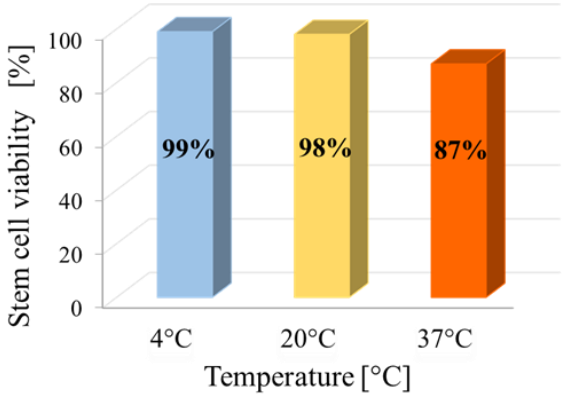

B

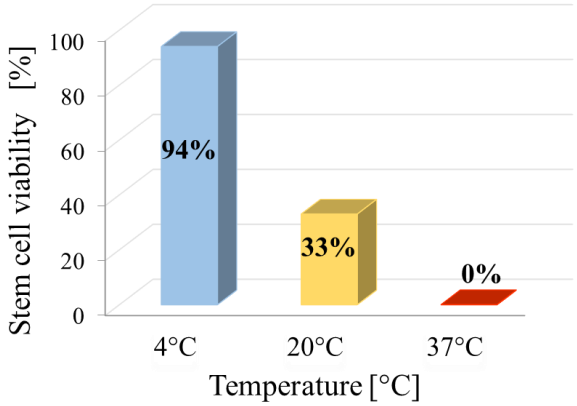

C

Fig. 2. Stem cell viability after 30 min (A), 60 min (B) and 24 hours (C) of incubation in cryoprotective solution with 5% DMSO. The standard deviation did not exceed 5%.

The influence of incubation temperature on DMSO cytotoxicity on the 24th hour is so apparent, that the changes in the hematopoietic stem cell suspension in standard cryoprotective solution can be seen macroscopically by the change of its color (Fig. 3). We suppose that this macroscopic change in the coloration of the sample results from the connection of the hem ring of the red blood cells which are part of the cell suspension, and the change in its electronic structure, changing its absorption spectrum.

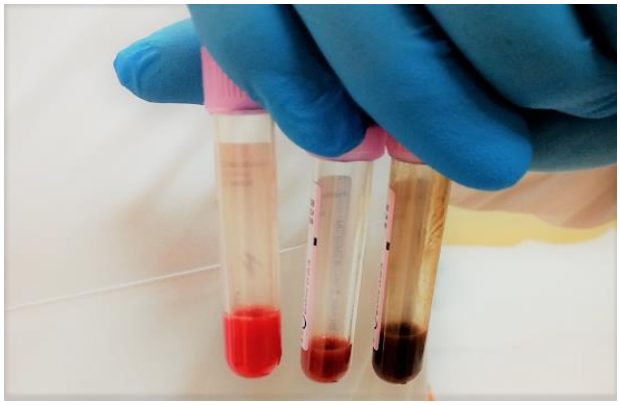

Fig. 3. Macroscopic picture of stem cell suspension after 24 hours of incubation in cryoprotective solution. The cells, incubated at 37ºC, are with darkest color.

DISCUSSION

DMSO causes major alterations in structure and function of mammalian cell membranes, proteins and nucleic acids. Membrane lipids are subjected to peroxide oxidation with injury resulting in mitochondrial membrane potential reduction, proteins are denaturated and the structure of the nucleic acids is changed. Time of incubation and DMSO concentration are important factors. Our results show that the temperature of exposure is also important for DMSO cytotoxicity. Exposure of cells to DMSO at low concentation (less than 10%) even at 37°C for 1 hour does not result in a gross loss of viability. For practical purposes, this would imply that addition of cryoprotectants that have low DMSO concentration can be performed sucessfully at ambient (22°C) room temperature.

CONCLUSIONS

Five percent DMSO is toxic for hematopoietic stem cells after long periods (more than 1 hour) and high (above 22°C) temperature of incubation. After 24 hours of incubation at room temperature, the viability decreases much faster and at 37°C 100 % cell loss is registered. The cell viability decreases after 1 hour only at a temperature higher than 20°C. DMSO cytotoxicity is low even after 24 hours of incubation. Currently, cryoprotectants are cooled to

4°C prior to addition to the cell suspension and the cells are frozen as soon as possible. Our results show that manipulation of cells (addition of cryoprotectant solution) at ambient temperature for a short period of time (up to 60 min) is also safe and will not result in additional loss of viability.

Acknowledgement: *This work is supported by the Bulgarian Ministry of Education and Science under the National Program for research "Young Scientists and Postdoctoral Students".*

REFERENCES

1. R. Munker, The BMT Data Book Including Cellular Therapy, Cambridge Univ. Press, London, 2013.
2. F. R. Appelbaum, *N. Engl. J. Med.*, **357,** 1472 (2007).
3. H. Baldomero, M. Gratwohl, A Tichelli, D. Niederwieser, A Madrigal, K. Frauendorfer, *Bone Marrow Transplant.*, **46**, 485 (2011).
4. FACT-JACIE International Standards for Cellular Therapy Product Collection, Processing, and Administration Accreditation Manual, 2015.
5. D. C. Hutchins, R. Fisher, S. Gordon. World Marrow Donor Association. Guidelines for couriers and the transportation of haematopoietic progenitor cells, 2011.
6. V. Antonenas, F. Garvin, M. Webb, M. Sartor, K. F. Bradstock, D. Gottlieb, *Cytotherapy*, **8**, 158 (2006).
7. G. Hechler, R. Weide, J. Heymanns, H. Koppler, K. Havemann, *Ann Hematol.*, **72**, 303 (1996).
8. . J. Ruiz-Arguelles, A. Larragina-Diez, B. Perez-Romano, A. Marin-Lopez, A. Larregina-Diez, M. G. Apreza-Molina, *Am. J. Hematol.*, **48**, 100 (1995).
9. H. T. Meryman, *Cryobiology*, **8**, 173 (1971).
10. E. M. Kang, E. M. Areman, V. David-Ocampo, C. Fitzhugh, M. E. Link, E. J. Read, S. F. Leitman, G. P. Rodgers, J. F. Tisdale, *Blood*, **92**, 850 (2002).
11. C. J. Hunt, *Transfus. Med. Hemoth.*, **46**, 134 (2019).
12. K. K. Fleming, E. K. Longmire, A. Hubel, *J. Biomech. Eng.*, **129**, 703 (2007).
13. B. P. Best, *Rejuvenation Res.*, **18**, 422 (2015).
14. C. F. Brayton, *Cornell. Vet.*, **76**, 61 (1986).
15. R. Spindler, W. F. Wolkers, B. Glasmacher, *Cryo Letters*, **32**, 148 (2011).
16. H. Kloverpris, A. Fomsqaard, A. Handley, J. Ackland, M. Sullivan, P. Goulder, *J. Immunol. Methods*, **356**, 70 (2010).
17. A. B. Trivedi, N. Kitabatake, E. Doi, *Agric. Biol. Chem.*, **54**, 2961 (1990).
18. X. Wang, T. C. Hua, D. W. Sun, B. Liu, G. Yang, Y. Cao, *Cryobiology*, **55**, 60 (2007).
19. H. Y. Elmoazzen, A. Poovadan, G. K. Law, J. A. Elliott, L. E. McGann, N. M. Jomha, *Cell Tissue Bank*, **8**, 125 (2007).
20. J. Galvao, B. Davis, M. Tilley, E. Normando, M. R. Duchen, M. F. Cordeiro, *Faseb J.*, **28**, 1317 (2014).
21. L. J. Fry, S. Querol, S. G. Gomez, S. McArdle, R. Rees, J. A. Madrigal, *Vox Sang*, **109**, 181 (2015).

Bulgarian Chemical Communications, Volume 52, Special Issue B (pp. 44-47) 2020 DOI: 10.34049/bcc.52.B.0012

Complex transformation of acid hydrolysates of primary and secondary biomass to bioenergy

P. G. Velichkova*, T. V. Ivanov, I. G. Lalov

Department of Biotechnology, University of Chemical Technology and Metallurgy - Sofia, 8 Kliment Ohridski Blvd., 1756 Sofia, Bulgaria

Received: February 27, 2019; Revised August 27, 2020:

In the current paper a comparative study of bioenergy (biofuels) yields from models of primary and secondary biomass - grass and potato peels is done. Acidic hydrolysis was used as a pre-treatment of these raw materials. The pre-treatment of the two types of biomass was conducted by autoclaving for 20 min at 121 °C in the presence of 1M HCl. The hydrochloric acid hydrolysates obtained from both biomasses had basic parameters for the grass hydrolysate 0.23 g reducing sugars/ g dry matter and COD 45.76 g O_2/ L, and for potato peels – 0.59 g reducing sugars/ g dry matter and COD 35.74 g O_2/ L. Both hydrolysates were found to be suitable substrates for bioethanol generation, where 12.48 mg ethanol/g dry matter was produced from grass hydrolysate and 180 mg ethanol/g dry matter from potato peels hydrolysate. The potential of both hydrolysates to biomethane generation was also studied. From the grass hydrolysate 0.196 L CH_4/ g dry biomass was obtained and from potato peels - 0.41 L CH_4/ g dry biomass. The results demonstrated the higher energy potential of potato peels compared to grass biomass. This was probably due to the high starch content typical for this type of waste.

Keywords: BMP, grass, potato peels, bioenergy, bioethanol, hydrolysis

INTRODUCTION

The conversion of lignocellulosic biomass into biofuel requires three steps, including pre-treatment, hydrolysis and fermentation [1]. Biofuels currently provide approximately 1.5 % of the global transport fuel as a result of the rapidly increasing production over the last decade [2].

Pre-treatment is usually used before anaerobic digestion to increase biodegradability of biomass. Therefore, various methods based on biodegradation and dissolution of lignin and hemicelluloses have been developed to achieve efficient hydrolysis and facilitate biogas production [3]. Pre-treatment should overcome the structural limitations of lignocellulose and its polymers (cellulose and hemicellulose), making them susceptible to microbiological treatment, leading to increased biomass and biogas yield [4]. The most commonly used methods are biological, chemical, physical or mixed.

Compared to other methods, chemical pre-treatment is considered much more promising. These methods can be quite effective in degrading more complex structured substrates. Major reactions during alkaline pretreatment include dissolution of lignin and hemicellulose and deesterification of intermolecular ester bonds. Dilute acids (< 4 % w / w) are usually used in acid pre-treatment. Often these methods are combined with high temperatures (> 100 °C).

Concentrated acids are not preferred because they are corrosive and need to be recovered to make pre-treatment economically viable [5, 6].

Potatoes are starchy crops that do not require complex pre-processing. Although a high-quality crop, 5 % to 20 % of the potatoes grown remain as by-products that can be used to produce bioethanol. In addition, during potato processing, especially in potato chip production, approximately 18 % is generated as waste. Therefore, potato waste can be used as a growth medium (economically viable carbon source) for fermentation processes in ethanol production, as it has high starch content. In particular, it has great potential for bioethanol production due to the high starch content. The most used are potato pulp, potato processing water, peels and waste potato pulp [7]. In addition to producing bioethanol, potato peels are used in the production of biogas.

The sustainable use of forest biomass for fuels and chemicals, instead of fossil fuels and petroleum products, can significantly reduce carbon dioxide emissions. The conversion of wood and non-wood lignocelluloses into biofuels and renewable intermediates was investigated. In conventional ethanol fermentation, yeast or bacteria can only ferment hexoses (C6 sugars). Various bacteria are capable of metabolizing and fermenting both hexoses and pentoses, but all produce a mixture of fermentation products. Biogas can be derived from

* To whom all correspondence should be sent:
E-mail: poliv1989@gmail.com

lignocellulosic biomass by its degradation [8].

According to the literature, hydrochloric acid is usually used for complete hydrolysis of the plant origin carbohydrates to simple reducing sugars, with no adverse effects on the material [9]. Chemical pretreatment is considered much more promising, as these methods can be quite effective in degrading more complexly structured substrates. Cellulose and hemicellulose, which are polymers of various sugar monomers, can be separated from lignin and extracts and hydrolyzed to their monomer units by acidic, alkaline or enzymatic hydrolysis.

The aim of this study was to compare the production of bioethanol and biogas (mainly biomethane) from model primary and secondary biomass - grass and potato peels. Acid hydrolysis with hydrochloric acid was used for pretreatment of these raw materials.

MATERIALS AND METHODS

Substrates

Fresh grass mix (perennial ryegrass *Lolium perenne* and cocksfoot *Dactylis glomerata*) was collected at Park Studentski in Sofia and then was cut to small pieces. The potatoes *Solanum tuberosum* were purchased from a large grocery store and were washed, peeled and blended.

Preparation of hydrolysates

The pre-treatment of both types of biomass was conducted by autoclaving them for 20 min at 121 °C with 1M HCl. For further analyses, the resulting hydrolysates were centrifuged and filtered using a 0.45 μm pore size filter. After separation the solid residues (53.1% for grass and 21.4% for potato peels) were discarded and only liquid fractions were used in the study. The obtained solutions were then refrigerated at 4 °C.

Methanogenic consortia

Methanogens were obtained as activated sludge from a factory producing bioethanol "Almagest", Verinsko village, Bulgaria.

Analytical methods

The chemical oxygen demand (COD) was determined according to APHA, 1992 [10]. Reducing sugars were determined as glucose using dinitrosalicylic acid (DNS) reagent by the method described by Miller, 1959 [11]. Gas production rate measurements were performed using a manual constant pressure liquid displacement system. The biogas composition was estimated using the absorptive method as was described previously by Lalov *et al.*, 2015 [12] and using the gas analyzer Optima 7 biogas, MRU-Germany. Biochemical methane potential was determined by the batch process described by Velichkova *et al*., 2017 [13].

Ethanol fermentation

Hydrolysates obtained by both substrates (grass and potato peels) were subjected to ethanol fermentation by *Saccharomyces cerevisiae* under anaerobic agitated conditions in a 250 ml Erlenmeyer flask with fermentation trap. Forty milligrams of lyophilized yeast were hydrated with 2 ml of distilled water at a temperature about 30 °C for 20-30 min. They were then added to 50 ml of hydrolysate. The process conditions were: temperature around 25 °C, fermentation time 4-5 days (or lack of new bioethanol produced).

Calculation of biochemical methane potential (BMP)

The obtained results were used in the final determination of the real energy potential of grass and potato peels hydrolysates. BMP was determined according to the following eq. (1):

$$BMP = \frac{V_{biogas} \cdot C_{methane}}{V_{sub} \cdot COD_{sub}} \quad (1)$$

where:

BMP – biochemical methane potential, LCH_4 / gCOD; V_{biogas} – volume of produced biogas, L; $C_{methane}$ – methane concentration, %; V_{sub} – volume of the substrate used in the BMP-test, L; COD_{sub} – chemical oxygen demand of substrate, gO_2 / L.

RESULTS AND DISCUSSION

Characteristics of the obtained hydrolysates

In order to characterize the obtained hydrolysates as substrates for a bio-refinery platform and to study their full energy potential, the most important characteristics were examined - content of reducing sugars and chemical oxygen demand. The results are summarized in Table 1.

Table 1. Main characteristics of the obtained hydrolysates

	Reducing sugars, g / g dry matter	COD, g O_2/ L
Grass hydrolysate (GH)	0.23	45.76
Potato peels hydrolysate (PPH)	0.59	35.74

The data in Table 1 show that the amount of reducing sugars is higher in potato peels hydrolysate (PPH) *vs*. grass hydrolysate (GH). This is also a prerequisite for the higher production of bioethanol from PPH. The COD shows an inverse relationship. However, the values are very close. The results show that hydrolysates from both biomasses have a good potential for liquid (bioethanol) and gaseous (biomethane) biofuels production. This potential was then explored by biomethanation and fermentation.

Biogas production and BMP determination

The methane content under the conditions of biogas collection reached 93% for GH and 95% for PPH, respectively. The biochemical methane potential of the obtained hydrolysates was then determined by equation 1 and recalculated per gram of dry biomass. A batch process of biomethanation at 35°C was repeated three times. The results are summarized in Figure 1.

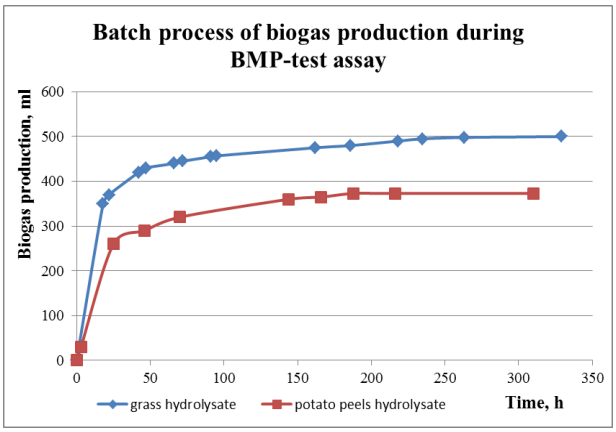

Figure 1. Batch process of biogas production from grass and potato peels hydrolysates.

BMP for PPH was 0.410 L CH_4 / g dry biomass and for GH – 0.196 L CH_4 / g dry biomass. The amount of biogas produced is higher for GH compared to PPH but the potential of potato peels as a feedstock for biomethane generation is higher. Maybe that's because they contain starch which degrades more readily than cellulose in the grass by acid hydrolysis. Potato peels waste can produce biogas about 0.55 L / g of dry matter according to the literature [14], which corresponds to our results.

Bioethanol production

The treated primary and secondary raw materials were fermented. Bioethanol with concentration 12.48 mg ethanol/g dry matter from GH and 180 mg ethanol/g dry matter from PPH was produced. Such a significant difference in the amount of bioethanol produced (compared to the amount of reducing sugars found in the different hydrolysates) can be explained mainly by the difference in the composition of the two raw materials. It is well known that the main product of the acid hydrolysis of a starch-containing raw material such as potato peels will be glucose. This compound can be easily and almost completely transformed into ethanol by the yeast culture used in the process. On the other hand, the typically high content of hemicelluloses in the composition of lignocellulosic raw materials usually leads to the formation of a broad spectrum of products, especially monosaccharides other than glucose (xylose, arabinose, galactose, mannose, etc.). Of course, such monosaccharides will increase the amount of the "reducing sugars" detected in the hydrolysate but they are non-fermentable (cannot be converted into ethanol) under the conditions of our process. Furthermore, acid hydrolysis of lignocellulosic biomass can result in formation of some inhibitory compounds such as furfural that is key derivative of xylose for example [15].

Generally, it can be assumed that the results prove once again the advantage of starch-containing raw materials over those of lignocellulosic composition.

CONCLUSION

Both hydrolysates (PPH and GH) were found to be suitable substrates for bioethanol production and had good potential for biomethane generation. The results demonstrated the higher potato peels energy potential compared to grass biomass. This was due to the high starch content typical for this type of waste. Combining the two bioenergy generation methods (biogas and bioethanol production) would expand the spectrum of generated fuels.

Acknowledgement: *This work was financially supported by Bulgarian National Science Fund (scientific project № KP-06-H27/4 from 12.2018).*

REFERENCES

1. P. Tantayotai, P. Pornwongthong, C. Muenmuang, T. Phusantisampan, M. Sriariyanun, *Energy Procedia*, **141**, 180 (2017).
2. D. Kumari, R. Singh, *Renewable and Sustainable Energy Reviews*, **90**, 877 (2018).
3. L. Li, X. Kong, F. Yang, D. Li, Z. Yuan, Y. Sun, *Appl. Biochem. Biotechnol.*, **166**, 1183 (2012).
4. S. Achinas, V. Achinas, G. J. W. Euverink, *Engineering*, **3**, 299 (2017).
5. S. R. Paudel, S. P. Banjara, O. K. Choi, K. Y. Park, Y. M. Kim, J. W. Lee, *Bioresource Technology*, **245**, 1194 (2017).
6. V. B. Agbor, N. Cicek, R. Sparling, A. Berlin, D. Levin, *Biotechnology Advances*, **29**, 675 (2011).
7. G. Izmirlioglu, A. Demirci, *Fuel*, **202**, 260 (2017).

8. K. Melin, M. Hurme, *Cellulose Chem. Technol*, **44** (4-6), 117 (2010).
9. D. Arapoglou, Th. Varzakas, A. Vlyssides, C. Israilides, *Waste Management*, **30 (10),** 1898 (2010).
10. APHA, WPCF, AWWA Standard methods for examination of water and wastewater, 18th edn. Washington, American Public Health Association, 1992.
11. G. L. Miller, *Anal. Chem.*, **31**(3), 426 (1959).
12. I. G. Lalov, M. N. Kamburov, T. V. Ivanov, P. G. Velichkova, *Scientific Books of University of Food Technologies*, **LXII**, 540 (2015).
13. P. G. Velichkova, T. V. Ivanov, I. G. Lalov, *Bulg. Chem. Commun.*, **49**, Special Issue L, 74 (2017).
14. D. Wu, *Procedia Environmental Sciences*, **31**, 103 (2016).
15. A. Mamman, J. Lee, Y. Kim, I. Hwang, N. Park, Y. Hwang, J. Chang, J. Hwang, *Biofuels, Bioprod. Bioref.*, **2**, 438 (2008).

Bulgarian Chemical Communications, Volume 52, Special Issue B (pp. 48-52) 2020 DOI: 10.34049/bcc.52.B.0015

Influence of press factor and additional thermal treatment on technology for production of eco-friendly MDF based on lignosulfonate adhesives

V. Savov[1*], I. Valchev[2], N. Yavorov[2], K. Sabev[1]

[1] *University of Forestry, 10 Kl. Ohridski Blvd., 1797 Sofia, Bulgaria*
[2]*University of Chemical Technology and Metallurgy, 8 Kl. Ohridski Blvd., 1756 Sofia, Bulgaria*

Received: May 11, 2020; Revised: September 11, 2020

A major shortcoming of medium density fibreboards (MDF) as a material for furniture production is the emission of formaldehyde from the boards. To solve the problem of formaldehyde emissions, an especially perspective direction is the use of lignosulfonates as natural adhesives. A major disadvantage of the lignosulfonates compared to the presently used synthetic binders is their lower reactivity. This leads to the need for an extended duration of the hot-pressing and to the worse water-resistance of the panels. This report presents a study on the influence of the duration of hot-pressing and the additional thermal treatment on the properties of eco-friendly MDF. Panels are produced in laboratory conditions with lignosulfonate as adhesive without any formaldehyde-based synthetic binders. Six types of panels were produced with variation of the press factor from 30 to 60 s.mm^{-2} with and without additional thermal treatment. The properties of the obtained boards were compared with values in EN standards and with a control board obtained with 10% urea formaldehyde resin. The obtained panel properties fully satisfy the relevant EN standards on mechanical properties of boards. A comparative analysis was carried out, with corresponding conclusions and recommendations, on the influence of the press factor and the additional thermal treatment on the efficiency of the eco-friendly technology for MDF production based on lignosulfonate adhesives.

Keywords: eco-friendly MDF, lignosulfonate adhesives, press factor, additional thermal treatment

INTRODUCTION

In view of the shortage of large-sized wood raw material [8], the main challenge facing the woodworking industry is the utilization of small-sized, lower-quality wood [4]. One of the main industries using this type of raw material is the production of fibreboards [13]. The production of dry-processed fibreboards is more than 80% of the global production of this type of wood-based panels [23]. In this type of production, as a part of the wood and furniture industry, the issue of environmental friendliness of the production and of the product itself [11] is actual. A major drawback, from an environmental point of view, of the use of urea formaldehyde resins in the industrial production of MDF is the formaldehyde emission from the boards [5]. A major problem for the future development of medium density fibreboards (MDF) technology is the release of formaldehyde from the boards. To the present moment MDF should meet the requirements for Class E_1 formaldehyde emissions, but companies like IKEA have significantly stricter requirements and are in the process of introducing a new class E_0 for formaldehyde emissions.

To reduce the emissions of free formaldehyde in wood-based panels, there are currently four major areas of global concern: reducing the levels of free formaldehyde in resins, while maintaining their adhesive properties [12]; addition of acceptors in order to reduce formaldehyde release from the panels [7]; and use of alternative binders that do not significantly impede the production of panels while maintaining their properties [1].

The latter direction to solve the problem of formaldehyde emissions is the use of so-called green binders, with a view to obtaining eco-friendly boards [2]. Of these binders, wood lignin-based products are the most promising ones [3]. Particularly suitable for binders in the production of MDF, due to the nature of the fiber connections, are lignosulfonates. The latter contain 12 ÷ 19% phenolic OH, ≈16% alcohol OH, ≈3% carbonyl and ≈1% carboxyl groups [6], by which the fiber elements in the panels can be bonded. There have also been a number of successful attempts to obtain, under laboratory conditions, lignosulfonate-based MDFs [9] with partial [14, 15] or complete [11, 16] substitution of synthetic (phenol formaldehyde or urea formaldehyde) resins. A major disadvantage is the relatively large press factor: 60 s.mm^{-1} with partial replacement of phenol formaldehyde and urea formaldehyde resins and 90 s.mm^{-1} in the obtaining of MDF only with the involvement of lignosulfonate as a binder. Previous studies by team members have shown that when using lignosulfonates, hot-pressing temperatures should be above 200 °C [11, 16].

* To whom all correspondence should be sent:
E-mail: victor_savov@ltu.bg

EXPERIMENTAL

For the production of the panels industrially produced wood pulp was used with the following composition: beech - 57%, oak 35%, poplar - 8%. The pulp was dried to a water content of 11%. Bulk density was 29 kg.m^{-3}.

As a binder for the experiments magnesium lignosulfonate was used. Lignosulfonates are residues in the production of lignocellulosic fibrous materials by the sulfite method. As a result of the ongoing delignification, lignosulfonates are released, which may be based on Na or Mg. The solution also contains sugars and products from the decomposition of carbohydrates and their concentration after evaporation reaches about 50% dry matter.

The concentration of lignosulfonate used for the experiments was determined by a weight method and was 51.5%. Magnesium content was 6%. The acid factor of the solution was pH 4 ± 1. The content of lignosulfonate in absolutely dry fibres was 15%.

Panels were produced with press factors of 30 s.mm^{-1}, 45 s.mm^{-1} and 60 s.mm^{-1} with and without additional thermal treatment. The secondary heat treatment was carried out at a temperature of 160 °C and duration of 45 min.

Blending was carried out on a high-speed (850 rpm) needle blade blender. For hot-pressing a laboratory press type RMC ST 100, Italy, was used. The hot-pressing temperature was 220 °C. The relatively high pressing temperature applied was for the purpose of using an accelerated pressing cycle and because of the high moisture content of the pressed material. The panels were with a set density of 850 kg.m^{-3} (type heavy MDF) and a thickness of 6 mm. Control MDF with 10% urea formaldehyde resin (UFR) content was also manufactured at a press factor of 30 s.mm^{-1} and a hot-pressing temperature of 200 °C. The properties of the panels were determined in accordance with the requirements of the European standards [17-21].

RESULTS AND DISCUSSION

The summarized results for the physical and mechanical properties of the produced MDF are presented in Tables 1 and 2.

The density of MDF varies from 844 to 858 kg.m^{-3}, or a deviation of 1.7% is observed in this basic property. Since the deviation is significantly less than the allowed 5%, this main property should not affect the others physical and mechanical properties of the panels and therefore their deviations are due to the change in the studied factors.

Table 1. Physical properties of eco-friendly MDF in dependence of press factor and additional thermal treatment

№	Press factor *c*, s.mm^{-1}	Additional thermal treatment *τ*, min	Density *ρ*, kg.m^{-3}	Water absorption *A*, %	Swelling in thickness *Gt*, %
1.	30	0	856	135.21	101.06
2.	45	0	850	132.00	77.63
3.	60	0	851	121.34	71.00
4.	30	45	855	123.26	71.77
5.	45	45	847	88.07	44.69
6.	60	45	844	79.55	37.59
Control MDF (with 10% urea formaldehyde resin)					
7.	30	0	858	80.65	35.44

Table 2. Mechanical properties of eco-friendly MDF in dependence of press factor and additional thermal treatment

№	Press factor *c*, s.mm^{-1}	Additional thermal treatment *τ*, min	Bending strength *fm*, N.mm^{-2}	Modulus of elasticity *Em*, N.mm^{-2}
1.	30	0	31.7	3130
2.	45	0	23.1	2610
3.	60	0	15.4	1750
4.	30	45	33.5	3410
5.	45	45	31.5	3540
6.	60	45	25.6	3230
Control MDF (with 10% urea formaldehyde resin)				
7.	30	0	27.2	2280

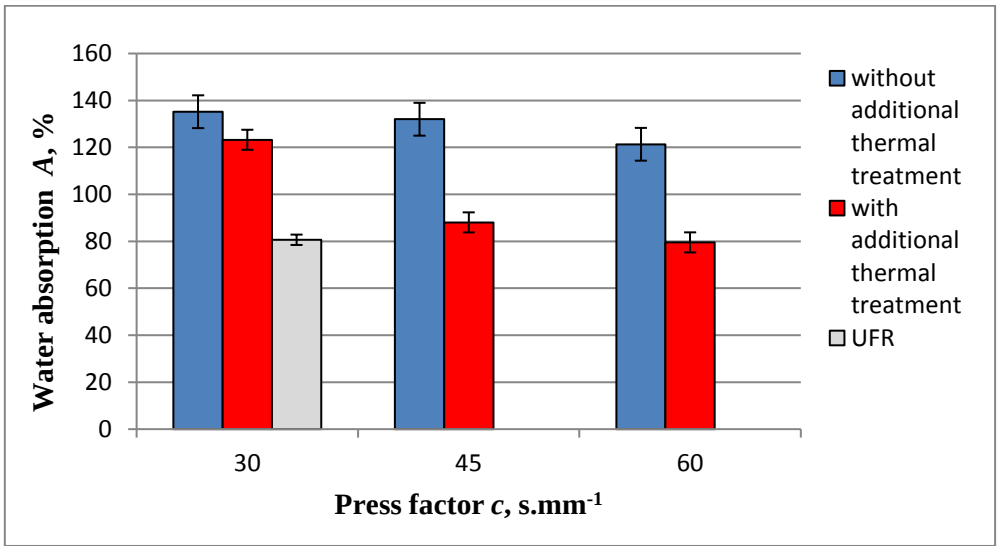

Fig. 1. Water absorption of eco-friendly MDF

In graphic form, the change of the water absorption as a result of the change in press factor and the additional thermal treatment is shown in Figure 1. The chart also shows the value of the control MDF made with urea formaldehyde resin. Under the conditions of the experiment, the water absorption of the obtained eco-friendly MDF varied from 135.2 to 79.6% and the value of the property of the control panels obtained with the urea formaldehyde resin was 80.7%. In general, the panels obtained with lignosulfonate as binder, without additional thermal treatment, exhibit poor water resistance. Of the panels without additional thermal treatment, the MDF obtained at a press factor of 60 s.mm^{-1} was the best, with the smallest values of the water absorption. However, the difference with the worst value of this group of panels at a press factor of 30 s.mm^{-1} was 14% or the improvement in the property with an increase in the press factor from 30 to 60 s.mm^{-1} was only 1.12 times.

The additional thermal treatment had a much stronger influence on the property. At press factors of 45 and 60 s.mm^{-1}, when additional thermal treatment was applied, a significant improvement in the water absorption of the panels was observed. The corresponding improvements in comparison with the MDFs without additional thermal treatment were from 1.53 to 1.5 times.

The MDF obtained at a press factor of 60 s.mm^{-1} and additional thermal treatment had a water absorption value similar to that of the control panel obtained with urea formaldehyde resin. The MDF obtained at a press factor of 30 s.mm^{-1}, despite the additional thermal treatment, displayed high values of water absorption.

In graphic form the change in the swelling of the thickness of the MDF, as a result of the change in press factor and the additional thermal treatment, is shown in Figure 2.

The swelling of the thickness of the MDF obtained with lignosulfonate varied from 101 to 37.6%. This property showed the same tendency as in the case of water absorption - an improvement, respectively a decrease in the values of the property with the increase of the press factor and a significant improvement with the application of additional thermal treatment. In panels without additional thermal treatment, the improvement by increasing the press factor from 30 to 60 s.mm^{-1} was from 101 to 71% or 1.42 times. With the application of additional thermal treatment, the improvement was in the range of 1.88 times, again with a press factor of 60 s.mm^{-1} and additional thermal treatment, the values of the property were similar to those of the control panel obtained with urea formaldehyde resin. In graphical form, the change in bending strength of MDF as a result of the change in the press factor and the additional heat treatment is presented in Fig. 3. The bending strength of the MDFs with lignosulfonate varies from 15.4 to 33.5 N.mm^{-2}. This property, in contrast to the water absorption and swelling in thickness of the panels, shows better, more evident values, with the decrease of the press factor. This can be explained by the relatively high (220° C) hot-pressing temperature, which, with the increased press factor, respectively the increased pressing time, affects the hemicelluloses and cellulosic complexes in the wood, which leads to the fragility (reduced strength) of the panels. However, all panels except those obtained without additional thermal treatment and at a press factor of 60 s.mm^{-1} meet the requirements for general purpose MDF

[22]. The MDF obtained with a press factor of 30 s.mm^{-1}, even without additional thermal treatment, meet the requirements of MDF for load-bearing structures. The additional thermal treatment also gives good results in the bending strength of the panels, with a much greater improvement when the press factor is 45 and 60 s.mm^{-1}. The panels obtained with a press factor of 30 s.mm^{-1} have even better values than the control MDF obtained with urea formaldehyde resin. The results for this property are very encouraging, since the press factor is commensurate with that used in industrial conditions, producing environmentally friendly MDFs with good mechanical strength, which can be used for structural purposes in the manufacture of furniture and others in dry environments. The change in the modulus of elasticity of resulting from the change in the press factor and the additional thermal treatment is presented in graphical form in Fig. 4.

The modulus of elasticity of MDF obtained with lignosulfonate varies from 3540 to 1750 N.mm^{-2}. All panels with the exception of the panel obtained at a press factor of 60 s.mm^{-1} without further thermal treatment, have a modulus of elasticity better than that of the control panel obtained with 10% urea formaldehyde resin. All panels obtained with additional heat treatment meet the most stringent requirements for the property, namely MDF for load-bearing structures.

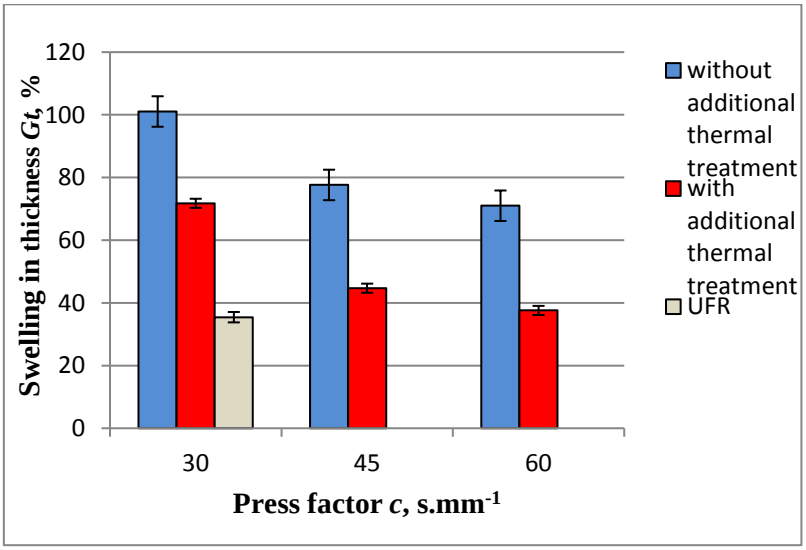

Fig. 2. Swelling in thickness of eco-friendly MDF

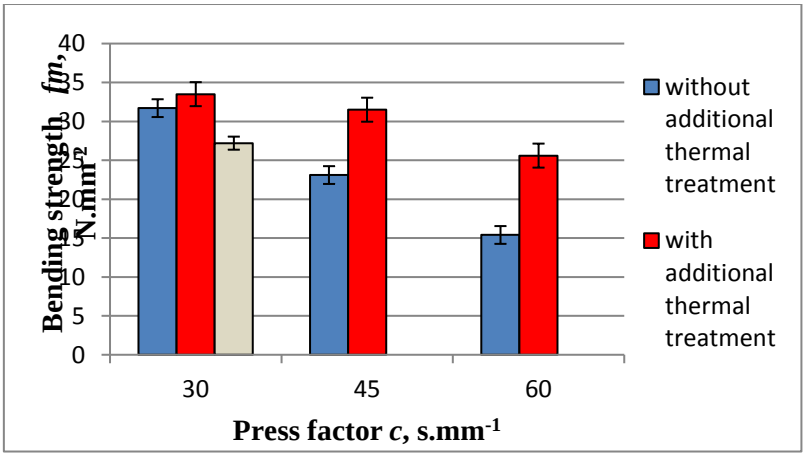

Fig. 3. Bending strength of eco-friendly MDF

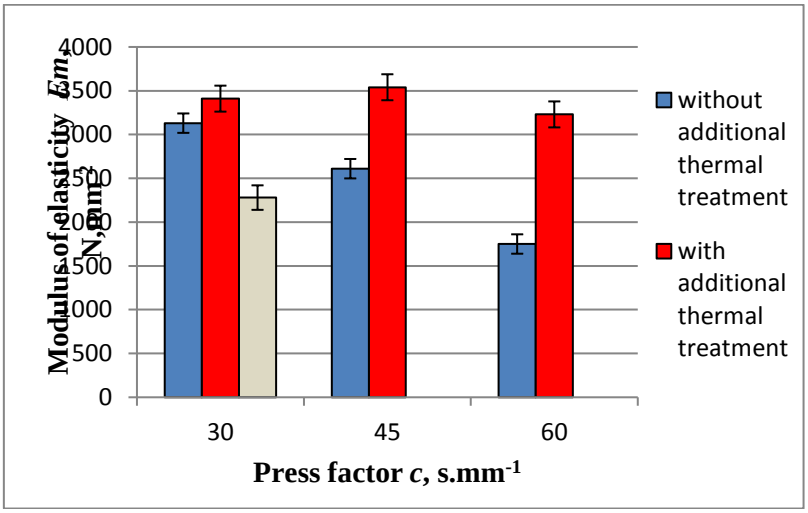

Fig. 4. Modulus of elasticity of eco-friendly MDF

CONCLUSIONS

As a result of the study it was found that eco-friendly MDFs can be successfully produced by applying lignosulfonate adhesives at press factors of hot-pressing similar to industrial ones when urea formaldehyde resins are used.

No significant darkening of the boards was observed as a result of the use of lignosulfonate, their color being similar to that of control MDF produced with urea formaldehyde.

The produced MDFs have mechanical properties similar to, and in some regimes even better than, the control board obtained with 10% urea formaldehyde.

It was found in this study that one of the major disadvantages of using lignosulfonate adhesives in an accelerated cycle of hot-pressing - the water resistance of the boards, can be overcome by applying additional thermal treatment after the hot pressing. By such additional treatment the boards improve by reducing nearly twice their swelling in thickness.

Acknowledgement: *This research was supported by the project № KP-06-KOST/1 funded by the National Science Fund.*

REFERENCES

1. A. Pizzi, Marcel Dekker Inc., New York, 2003.
2. E. Athanassiadou, European Network of Bioadhesion Expertise (ENBA), 2017, p.16.
3. E. Nordström, D. Demircan, L. Fogelström, F. Khabbaz, E. Malmström, Intehopen Books, p.71, dx.doi.org/10.5772/intechopen.72072.
4. J. Mihailova, B. Iliev, T. Todorov, R. Grigorov, Proceedings of Scientific Conference "Innovations in the Wood Industry and Engineering Design", Iundola, Bulgaria, 2008, p. 93,78-954-323-538-4.
5. L. Carvalho, F. Magalhães, F. João, researchgate.net/publication/236273710, 2012, p. 44.
6. L. Dumitrescu, I. Manciulea, S. Patachia, D. Perniu, Annals of DAAAM for 2009 & Proceedings of the 20th International DAAAM SymposiumVienna, Austria, 2009, p 289.
7. M. Valyova, Y. Ivanova, D. Koynov, *International Journal – Wood, Design & Technology*, **6(**1), 72 (2017).
8. N. Tritchkov, P. Antov, Proceedings of COST Action 44th Conference Broad Spectrum Utilization of Wood, BOCU, Vienna, Austria, 2005, p 131.
9. N. Yotov, I. Valchev, St. Petrin, V. Savov, *Bulg. Chem. Commun*., **49(**Special Issue L), 92 (2017),
10. P. Antov, T. Pancheva, Proceedings of Management and Sustainable Development Conference, 2017.
11. P. Antov, I. Valchev, V. Savov, IWBLCM Proceedings, Cordoba, Spain, 2019, p. 104.
12. S. Sepahvand, K. Doosthosseini, H. Pirayesh, B. K. Maryan, *Drvna Iindustria*, **69**(3), 215 (2018).
13. V. Savov, Proceedings of Conference "Management and sustainable development", Jundola, 2007, p. 373.
14. V. Savov, J. Mihajlova, International Conference "Wood Science and Engineering in the Third Millennium" – ICWSE, 2017, p. 348
15. V. Savov, J. Mihajlova, Proceedings of International Conference "Wood Science and Engineering in the Third Millennium" – ICWSE, 2017, p. 353
16. V. Savov, I. Valchev, P. Antov, IWBLCM Proceedings, Cordoba, Spain, 2019, p. 165.
17. EN 310:1999 Wood-based panels - Determination of modulus of elasticity in bending and of bending strength.
18. EN 316:2009 Wood fibre boards - Definition, classification and symbols.
19. EN 317:1998 Particleboards and fibreboards - Determination of swelling in thickness after immersion in water.
20. EN 322:1998 Wood-based panels - Determination of moisture content.
21. EN 323:2001 Wood-based panels - Determination of density.
22. EN 622-5:2010 Fibreboards - Specifications - Part 5: Requirements for dry process boards (MDF).
23. http://www.fao.org/forestry/statistics/ (last accessed 04.2019).

Bulgarian Chemical Communications, Volume 52, Special Issue B (pp. 53-60) 2020 DOI: 10.34049/bcc.52.B.0018

Investigation on the barrier and antibacterial properties of packaging papers with blend fillers of chitosan and rice starch

D. Todorova[1], U. Vrabič Brodnjak[2]

[1] *University of Chemical Technology and Metallurgy, Department of Pulp, Paper and Printing Art, St. Kliment Ohridski 8, 1756 Sofia, Bulgaria*

[2] *University of Ljubljana, Faculty of Natural Sciences and Engineering, Department of Textiles, Graphic Arts and Design, Snežniška 5, SI-1000 Ljubljana, Slovenia*

Received: November 30, 2019; Accepted: September 15, 2020

Bio-based materials or biomaterials fall under the broad category of bio-products or bio-based products which includes materials, chemicals and energy derived from renewable biological resources. Paper and cellulose fibers are the first materials in this list. Therefore, the usage of bio-based additives in paper production would have an increased application in the future years. In the present experiment, packaging paper with blend fillers of chitosan and rice starch were made with blended mixtures of different concentrations of chitosan and rice starch. Investigations were made in order to evaluate the effect on the barrier and antibacterial properties of the obtained paper samples. The goal of our research was to improve paper properties and to make paper sheets, which will be suitable as packaging paper. To evaluate the effect of the bio based fillers, air permeability, grease resistance, moisture, water absorptiveness and antibacterial activity were determined. The research showed that the barrier properties of the obtained packaging paper towards air, water and grease improved but the used chitosan mixtures had no antibacterial activity against *Escherichia coli* K12. The results showed that blend fillers of chitosan and rice starch are effective paper fillers in the preparation of cellulose mixtures for bio based papers. Therefore, preparing paper using a combination of chitosan and rice starch blend fillers is an improved and convenient procedure to enhance many properties of such papers.

Keywords: chitosan, rice starch, pulp, paper additives, bio polymers, modified paper

INTRODUCTION

Paper is one of the main materials used for food packaging that provides preservation and protection for the final product till reaching the consumer without compromising the quality. There are many types of paper for food packaging such as sulfite paper, kraft paper, grease-free paper, paperboards and laminated paper among others. Improving barrier properties of paper for food packaging is essential since the presence of oxygen or water vapor is a key factor that limits shelf life of foodstuffs. The reason for that is the effect of oxidation on taste, color and odor. Moreover, presence of oxygen facilitates the growth of microorganisms and insects. Therefore, removal of oxygen and increasing barrier properties of the packaging material has been the main target for food packaging researchers [1]. Protection of foodstuffs largely depends on the barrier properties of the packaging material that can be enhanced by several ways.

Latest tendencies show that packaging materials, with which producers reduce environmental pollution, are based on bio polymers and increase their consumption due to their biodegradable, nontoxic and environmentally friendly nature, as well sufficient barrier properties. [2-4]. According to the Pro Carton "Consumer attitude survey" - a major independent study of 7000 European consumers in seven countries, 90% of the responding shoppers in all surveyed countries said, they'd like information about the environmentally-friendliness of packaging and four out of five consumers (81%) said that, given the choice, they would choose paper/carton board packaging over plastic [5]. The research also reveals that Europeans have a good working understanding of different packaging forms, highlighted by the fact that 52% of all Europeans believe paper/cardboard to be the most environmentally-friendly packaging – a result broadly echoed across each country. Glass came in second with 32% of the Europe-wide vote. Some 9% of Europeans believe plastic is the most environmentally-friendly form of packaging, whereas only 5 % chose tin so it still appears that there's an education job to be done [5]. The primary packaging function is to protect its content, but in the last years, the technical performance, promotion of the product, costs and other characteristics have been inferior to recyclability. In recent years, the materials

* To whom all correspondence should be sent:
E-mail: todorova.dimitrina@uctm.edu

used in the packaging of goods, such as fruit, vegetables, bakery products or flowers, have improved in developing recyclable packaging from waste or abundant materials.

As far as packaging materials containing paper are considered, such as paper-polyethylene terephthalate (PET) and paper-aluminium laminates, the quality of the commodity paper is decisive for the microbiological quality of the final product, since paper usually contains a certain microbial load that is not completely eliminated during the production process. Compared to other materials such as metals, glass or plastics, rather low temperature treatment is applied to those laminates [6]. Therefore, from practical point of view an important focus should be set on the prevention of microbiological activity to ensure sufficient barrier and antibacterial packaging paper properties.

Bio-based polymers are polymers which can be directly extracted from biomass (polysaccharides, proteins and lipids), polymers which are synthesized from bio-derived monomers (polylactic acid – PLA or other polyesters) or polymers which are produced directly by microorganisms (polyhydroxyalkanoates – PHA, bacterial cellulose, xanthan, pullulan and curdlan). They can be used alone or in combination. Bio based polymers are usually coated on papers and cardboards, applied with different coating techniques (solution coating, surface sizing, curtain coating or compression molding) [7-9].

Polysaccharides mostly used are chitosan, starches (rice, wheat, maize, corn and potato), cellulose and alginates. They are nontoxic, widely used and available in the market also as waste materials. With high gas, aroma and grease barriers, such coatings have great potential in packaging materials. Because of their hydrophilic nature, polysaccharides exhibit poor water vapour barrier [7-9].

However, additives to paper packaging, such as polysaccharides enhance mechanical strength and barrier properties of the final product. Moreover, polysaccharides such as chitin and starch are belonging to green chemicals and characterized by their availability, renewability and biodegradability [1].

Chitosan, which is a linear copolymer of β-(1,4)-2-acetoamido-2-deoxy-D-glucopyranose units and β-(1,4)-2-amino-2-deoxy-D-glucopyranose units, is one of the most widespread natural polysaccharide. It exhibits excellent oxygen-barrier properties due to its highly crystallinity and hydrogen bonds between molecular chains [10]. The $–NH_2$ group present transforms into a polycation in dilute acidic solution. Therefore, the cationic character causes stronger adsorption by electrostatic interactions to the paper pulp, which has an anionic character [11]. Chitosan interacts in combination with cellulose, which causes improved tensile properties and promotes good printability of paperboard [12]. Blends of different cellulose and chitosan in papermaking processes have been studied and presented earlier [13-19]. Laleg and Pikulik reported that chitosan additives increased the strength of wet paper towels, disposable diapers, and grocery bags [13]. Li *et al.* found that chitosan was absorbed onto the surface of the cellulosic fibres, which was caused due to cationic amino groups and electrostatic interactions between the chitosan and cellulose pulp [14]. Chitosan in combination with polyvinyl alcohol and starch was studied by Mucha and Miskiewicz. They determined strong ionic interactions between the fillers and increase of the paper tensile properties [15]. Nada *et al.* found that chitosan, cyanoethyl and carboxymethyl chitosan enhanced the strength properties of aged and un-aged paper sheets [16]. Fernandes *et al*. studied the distribution of chitosan onto the paper sheets, using a fluorescent derivative [17]. Their results have proven that chitosan and its modifications could be used as a probe to understand the deposition of chitosan onto the paper.

Numerous researchers published investigations on the antibacterial properties of coated paper with bio-based polymers like starch [20], chitosan [21, 22], E-poly-L-lysine in combination with carboxymethyl cellulose [23] and others.

Few studies are currently available on the application potential of chitosan derivatives in papermaking. Nevertheless, several papers demonstrate the efficiency of chitosan derivatives as process and functional additives. Although scarce, the experimental data available on this subject provide promising results, which validate the versatility and multifunctionality of chitosan derivatives as papermaking additives [19].

The aim of our research was to make paper sheets, which will be suitable as packaging paper and to improve its properties by using two different bio polymers as fillers (chitosan and rice starch). The literature shows no record of previous research done on the blend of rice starch and chitosan as paper fillers. The purpose of our research was to investigate different ratios of blends to evaluate the barrier - air permeability, grease resistance, moisture, water absorptiveness and antibacterial activity of the obtained paper. The chemistry of the preparation process of these paper sheets is fully environmentally friendly and paper is characterized with improved properties, compared to the classic type of papers.

EXPERIMENTAL

Materials

The used softwood pulp was bleached sulfate kraft cellulose from pine and spruce trees, delivered by SCA, Sweden with: breaking length of 3300 m, acc. to ISO 1924/2; tensile index of 26 N.m/g acc. to ISO 1924-2; burst index of 1.5 kPa m^2/g acc. to ISO 2758; tear index of 18.8 $mN.m^2$ /g acc. to EN 21974 and 80% brightness acc. to ISO 3088.

The used hardwood pulp was bleached hardwood kraft pulp from beech trees, delivered by Svilosa AD, Bulgaria. The kraft pulp is placed on the market under the registered trade mark SVILOCELL®. The properties include; breaking length of 1900 m, acc. to ISO 1924/2, tensile index of 18 N.m/g acc. to ISO 1924-2, burst index of 0.75 kPa m^2/g acc. to ISO 2758, tear index of 2.3 $mN.m^2$ /g acc. to EN 21974 and 80% brightness acc. to ISO 3088.

Both chitosan and acetic acid (99%) were purchased from Sigma Aldrich (Austria). The chitosan is with molecular weight lower than 20 kDa and deacetylation degree higher than 85%.

Rice starch was obtained from Farmalabor Srl (Italy) and had 14% of moisture content, 1% of proteins and 0.6% of ashes. Modified cationic polyacrylamide was delivered by Kemira, Finland and is with molecular weight of 11.10^6 g/mol, charge density of 1.05 meq/g, viscosity (Brookfield) 700 $cP_{(0.5\%,25°C)}$ and conductivity 66.6 $\mu S_{(0.5\%)}$.

Methods

Preparation of the pulp. Two types of kraft pulp - softwood and hardwood - were used in our experiment, which were refined by a laboratory Jokro mill method with six refining units, acc. to ISO 5264-3:21979. The refining concentration in each unit was 6% (16 g o.d.f in 267 ml of water). The two celluloses were separately refined. The Schopper Riegler value (ISO 5267-1/AC:2004) of the softwood pulp was 20 ºSR and of the hardwood pulp 42ºSR. After mixing the pulps the Schopper Riegler value of the suspension was 29 ºSR.

Preparation of pulp suspensions. Paper suspensions were prepared using 6 combinations of pulp suspensions, bio polymers (chitosan and rice starch) and retention additive. Pulp suspension was prepared with 50% of softwood (pine and spruce) and 50% of hardwood (beech). Chitosan solution was prepared by dissolving chitosan in acetic acid in order to prepare a 5% and a 7.5% solution. The solution was mixed for 10 min at 85°C and then cooled to room temperature. Rice starch was also separately prepared by dissolving rice starch in distilled water. It was mixed until it gelatinized (85°C for 10 min), then was cooled to room temperature. The chitosan-rice starch solution was prepared by mixing the same amounts of rice starch and chitosan solution (5% or 7.5%). The procedure of mixing pulp and other additives was as follows: firstly 23.5 g o.d.f. were stirred in tap water (2000 ml), then the chitosan and rice starch were added. The mixing proceeded and after that the retention additive was added. The preparation was followed with mixtures:

1) Only pulp (P);
2) Pulp and 0.05% retention additive (PR);
3) Pulp, 5% chitosan, 0.05% retention additive (5% CH);
4) Pulp, 5% rice starch and chitosan, 0.05% retention additive (5% CHR);
5) Pulp, 7.5% chitosan, 0.05% retention additive (7.5% CH);
6) Pulp, 7.5% of rice starch and chitosan, 0.05% retention additive (7.5% CHR).

Preparation of paper sheets. The papermaking process was simulated by using a laboratory paper-sheet machine. All samples were prepared on a paper laboratory machine (Rapid-Kothen, Germany) acc. to ISO 5269-2:2005, with a grammage of 80 g/m^2, with drying conditions of - 90°C and duration of 7 min.

Characterisation of the samples

Grammage, density, specific surface, thickness. It was necessary to determine the grammage of all samples. Grammage was determined in accordance with the ISO 536 standard, 10 samples of each paper were cut into size 10 × 10 cm and weighed. The thickness of the samples was measured with a precision digital micrometre Mitutoyo Corporation, Japan, to the nearest 0.0001 μm at 10 random locations on each paper. Density and specific surface volume were calculated from grammage and thickness, as described in the standard method ISO 534.

Moisture, water absorptiveness (Cobb value), determination of capillary rise (Klemm method). Moisture content was determined according to ISO 287 by measuring weight loss after drying in a laboratory oven at 105 ± 1 °C until constant weight. Five samples of each paper were tested and the results were expressed in percentage. Water absorptiveness was determined with the Cobb value, as described in the standard method ISO 535, where a given amount (100 ml) of water was in contact with the paper for 60 sec and weight differences were compared. For each paper, five sample tests were made. The capillary rise of the paper samples was determined by the Klemm method, as described in

ISO 8787. Two samples of each paper were tested and the results were expressed in mm, as height of water uptake after 10 min in distilled water.

Smoothness, air permeability and grease resistance. Smoothness and air permeability were determined according to standard TAPPI T460 and ISO 8791-2. Grease resistance of all sample paper sheets was determined using a modified TAPPI test -507, which was presented by Park *et al.* [24]. Smaller stained areas per hour on paper indicated greater grease resistance.

Surface (SEM). The SEM micrographs of paper surfaces were taken with a scanning electron microscope (JSM-6060 LV). The instrument operated at 10 kV and magnification 1000×.

Antibacterial activity. The potential antibacterial activity of the obtained paper materials against *Escherichia coli* K12 was evaluated on the basis of the inhibition-zone size. The cultures were grown, sub-cultured and maintained in Luria-Bertani (LB) medium and stored at 4 ºC. For the experiment a single colony of each organism was inoculated into 50 ml of LB broth and incubated overnight (24 h) at 37 ºC for *E. coli* K12 under shaking at 200 rpm. 100 µL of the bacterial suspension with concentration of 1×10^6 CFU mL^{-1} were seeded in agar plates with solid LB medium by the pour plate technique. After 10 min, 10 mg of pressed test materials were placed on the plates. Inhibition zones were measured after incubation overnight at 37 ºC for *E. coli* K12. The formation of a clear zone (restricted bacterial growth) around the tested paper samples is an indication of antibacterial activity for the obtained materials.

RESULTS AND DISCUSSION

Basic properties

To evaluate the effect of bio based components onto the barrier and antibacterial properties of the paper, it was essential to obtain paper samples with the same grammage. Therefore, the paper sheets were prepared with the grammage 80 g/m^2. The beating degree of a pulp, hardwood fibers, dimensions of the fibers and addition of the fillers have influence on the thickness of the paper. As expected, the thickness of the samples had mostly the same values (Table 1). Paper with only pulp, combination of softwood and hardwood fibers with no additives, had the lowest thickness (0.0084 mm). With addition of the retention additive and fillers, the thickness of all other paper sheets increased.

Changes were also detected for specific surface and density, where sample P, with only pulp and no additives, had the highest density, compared to other tested papers.

Barrier properties

It is known that paper has a certain grade of moisture, which depends on relative humidity, types of used pulp, degree of refining and types of used coatings. For packaging materials, it is very important to have excellent barrier properties. Among moisture, absorption ability and capillary rise, which are presenting water barriers, are also gas and grease barriers important for this kind of paper.

As expected and seen in Table 2, the decrease of moisture was noticed for samples with the retention additive and fillers. With increasing amount of fillers, the moisture decreased.

Table 1. Basic properties of all paper samples

	Samples					
	P	PR	5% CH	5% CHR	7.5% CH	7.5% CHR
Grammage, g/m^2	80	80	80	80	80	80
Thickness, mm	0.084	0.095	0.091	0.090	0.095	0.096
Specific surface, m^3/g	0.0011	0.0012	0.0011	0.0011	0.0012	0.0012
Density, g/m^3	952.38	842.11	879.12	888.89	842.11	833.33

Table 2. Water barrier properties of all tested samples

	Samples					
	P	PR	5% CH	5% CHR	7.5% CH	7.5% CHR
Cobb value, g/m^2	30,04	28,82	27,63	24,21	20,27	20,24
Moisture, %	10	9,9	7	6,8	6,7	6,50
Capillary rise, mm	47	40	10	15	10	9

Ability of fluids to penetrate the structure of paper is a highly significant property to the use of packaging paper. Resistance towards the penetration of water was measured by $Cobb_{60}$ values acc. to ISO 535. From the obtained results it is seen that the addition of chitosan-rice starch decreased water absorptiveness, i.e. $Cobb_{60}$value (Table 2). The higher the filler content, the higher resistance towards water penetration was detected. For the paper with 7.5 % of chitosan and rice starch, the water absorptiveness decreased by 33%, compared to paper with only pulp. For samples, where 5% of fillers were used, 8% (5% CH) and grease barrier properties were affected by the fillers and additives in paper samples. In the first hour, for all samples with fillers, lower percent of stained area was detected, compared to paper with only pulp and retention additive (Figure 1). Chitosan has a high grease barrier ability, compared to rice starch. The grease migration for papers with fillers is also due to open surface (pores) between the paper fibers, where grease could permeate through the paper [25]. There is also an important factor of beating degree of the pulp, where highly beaten papers have smaller pores [26]. Our grease permeability analyses showed that fillers and additive filled and reduced pore sizes, which was also proven with scanning electron microscope analysis. It is visible from the graph (Fig. 1) that chitosan and rice starch samples have no significant grease permeation, which proves that such type of bio-based fillers are suitable for packing of products (food or technical details) for long lasting periods.

19% (5% CHR) decrease was detected. It was also proven that retention additive had an influence on paper structure and properties. The same trend was detected for capillary rise. With addition of chitosan and rice starch, the resistance towards water capillarity increased. With higher concentration of bio polymer components, the capillary rise decreased. The most significant change was detected for the sample with 7.5 % of chitosan and rice starch. The decrease was from 80% (7.5% CHR) to 68% (5% CHR). Chitosan is insoluble in water while rice starch has a hydrophilic nature. Therefore, the sample, where only chitosan was used, achieved higher values, but still much lower than paper sheet, where only pulp and pulp with retention additive was used.

Smoothness, air permeability and grease resistance

Paper is a highly porous material composed of a felted layer of fibers and the additives could cause variation of many properties. Some of the affected properties are for sure smoothness and air permeability. Chitosan and rice starch, included in the paper sheets, filled the pores and holes. The open surface of paper sheets decreased with increasing amount of the mentioned polymers.

Smoothness was better for samples with chitosan and rice starch. When the amount of bio polymers increased, the smoothness improved as well. As expected and seen from the results in Table 3, the air permeability was worse for paper with pulp included. With the addition of bio polymers and retention additive, the structure of the paper became more even and filled, therefore the properties improved. The best air permeability achieved was for the paper with 7.5% CHR, where only 1186 ml/min was measured.

Table 3. Smoothness and air permeability of all sample papers

	Samples					
	P	PR	5% CH	5% CHR	7.5% CH	7.5% CHR
Smoothness, ml/min	417	410	345	350	340	303
Air permeability, ml/min	1411	1309	1260	1238	1221	1186

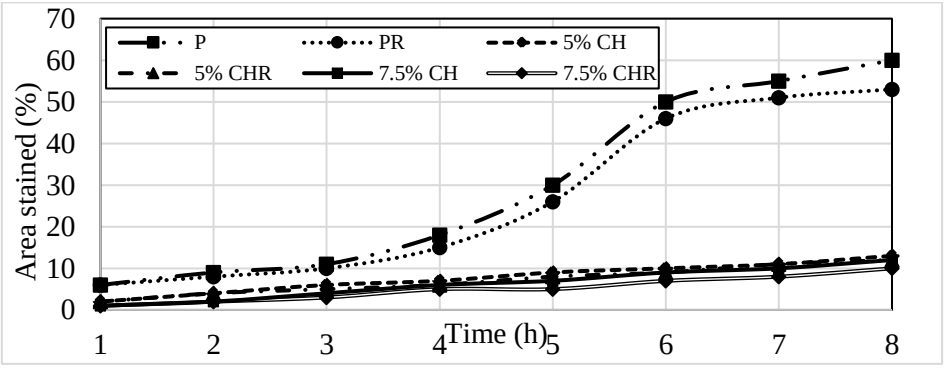

Fig. 1. Grease permeation of sample papers.

After 5 hours of the test, the grease migration increased for all samples, being the highest for the samples P and PR, where it increased from 6 to 30% of stained area. As expected, there was a slight increase for papers with fillers, from approx. 2 to 9% (sample 5% CH). After 8 hours, the same trend as before was detected for all tested samples. As predicted, the analysis showed that for the paper with no fillers, more stained areas were detected.

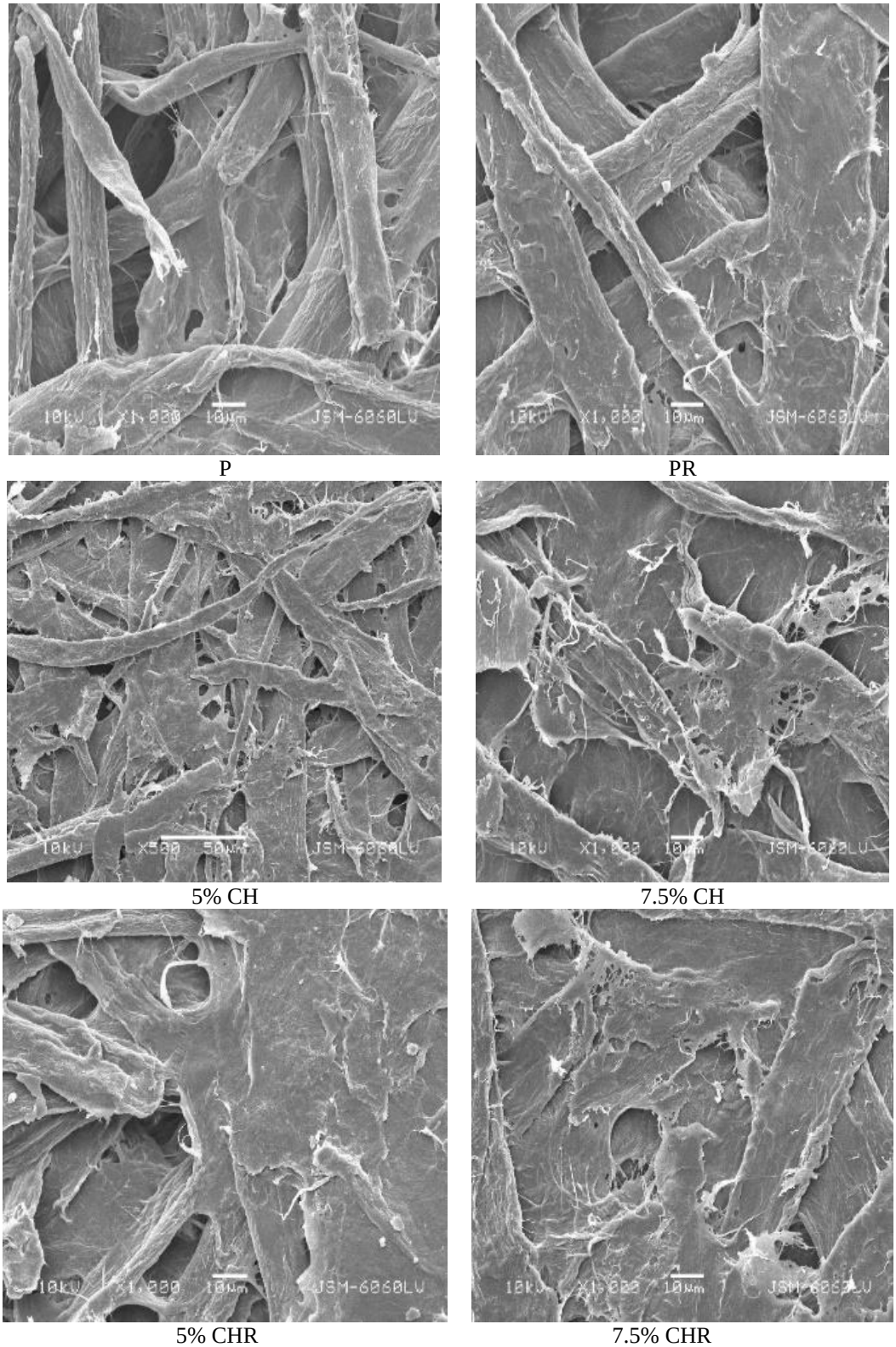

Fig. 2. SEM micrographs of all samples taken at 1000× magnification and operating at 10 kV voltage.

Surface texture

The distribution of chitosan and rice starch onto the paper sheets was evaluated by scanning electron microscopy (SEM).

The micrographs (Figure 2) show that the fillers covered the fibers and closed the pores and open areas in the base paper due to the increased fiber bonding and probable film-like covering process, which most likely occurs in the drying process of the paper samples where the drying temperature is above 95 °C and also increased due to the lower molecular weight of the used chitosan.

The surface of the sample papers was smoother and more even for paper with fillers (Figure 4) 7-5%CH, 5% CHR, 7.5% CH and 7.5% CHR), compared to the samples with no fillers (P and PR). A comparison between paper sheets with fillers of different concentrations proved their effect which is consistent with the improved mechanical, grease and water barrier properties. The absorption, thickness, moisture and roughness of the papers with fillers, have great influence on the properties of chemical structures, types of the fillers. If the fillers are uneven distributed in the fiber paper composition, many properties can worsen and this can influence not only the barrier but the printing properties.

Antibacterial activity

The antibacterial activity of the obtained paper samples was determined after a 24-hours stay in *Escherichia coli* K12 environment. Figure 3 presents the plate of *Escherichia coli* K12 for the obtained paper samples. As a zero probe paper samples with retention additive (PR) were used.

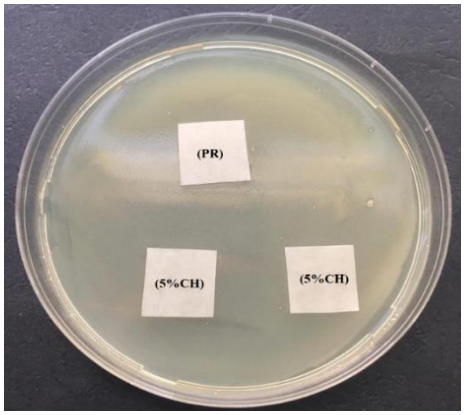

5% CH

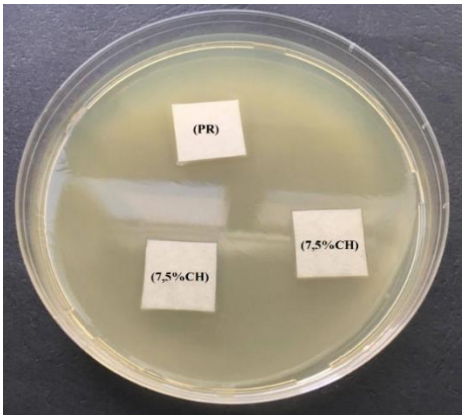

7.5% CH

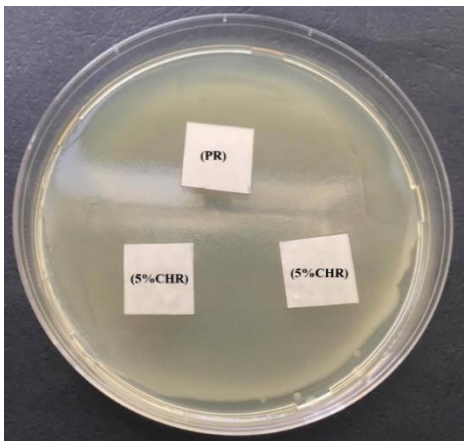

5% CHR

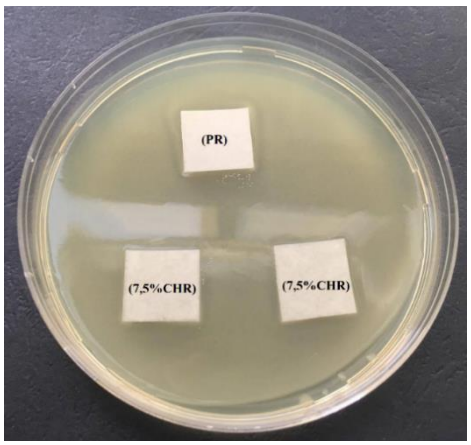

7.5% CHR

Fig. 3. Antibacterial activity of all samples against *Escherichia coli* K12

Chitosan has an inhibition effect due to the presence of amine group and its water-binding ability which cause a dry environment surrounding bacteria, not suitable for bacteria growth. A previous study reported that chitosan generally showed stronger antibacterial effects against Gram-positive bacteria than Gram-negative bacteria [21]. However, antibacterial activity also depends on the molecular weight and degree of deacetylation of chitosan. The molecular weight of chitosan used in this study is 20

kDa which is low. Chitosan of lower molecular weight possesses stronger antibacterial activity against Gram-negative bacteria. However, the filled packaging paper with chitosan and rice starch showed no inhibition zone, correspondingly, there is no antibacterial activity of the obtained packaging paper filled with chitosan and rice starch blends, probably due to the blocking of the amine groups by the OH-groups of cellulose in the paper suspension preparation process. This proved that chitosan and rice starch blends are efficient for water and grease resistance. In cases were antibacterial activity of packaging paper is needed, chitosan and rice starch blends could be used as a coating application solution.

CONCLUSION

The results showed that blend fillers of chitosan and rice starch are effective paper fillers in the preparation of pulp mixture for bio based papers. Such paper sheets have better moisture resistance. The research showed that the water absorptiveness and the resistance toward capillary rise improved for the 7.5% blend mixture of chitosan and rice starch. For paper, where 7.5 % of chitosan and rice starch were used, the water absorptiveness decreased by 33%, compared to paper with only pulp. Grease resistance of papers with fillers improved up to 88%. Furthermore, smoothness and air permeability improved for papers with chitosan and rice starch. Chitosan and rice starch blends provided water and grease resistance, but not antibacterial activity against *Escherichia coli* K12. Therefore, preparing paper using a combination of chitosan and rice starch blend fillers is an improved and convenient procedure to enhance many properties of such papers.

Acknowledgements: *The authors would like to thank COST Action FP1405 (ActInPak) for financial support. We are also thankful to the University of Ljubljana, Faculty of Natural Sciences and Engineering in Ljubljana, Slovenia and the University of Chemical Technology and Metallurgy, Department of Pulp, Paper and Printing in Sofia Bulgaria.*

REFERENCES

1. M. A. El-Samahy, S. A. A. Mohamed, M. H. Abdel Rehim, M. E. Mohram, *Carbohydrate Polymers*, **168**, 212 (2017) https://doi.org/10.1016/j.carbpol.2017. 03.041.
2. R. P. Babu, K. O'Connor, R. Seeram, *Progress in Biomaterials*, **2** (2013), doi:10.1186/2194-0517-2-8.
3. U. Siripatrawan, W. Vitchayakitti, *Food Hydrocolloids*, **61**, 695 (2016).
4. I. Leceta, M. Peñalba, P. Guerrero, K. de la Caba, *European Polymer Journal*, **66**, 170 (2015).
5. Pro carton Consumer attitude survey, https://www.procarton.com/publication/consumer-attitude-survey/, **10**, 2018.
6. M. Feichtinger, U. Zitz, H. Fric, W. Kneifel, K. J. Domig, *Food Control* **50**, 548 (2015) https://doi.org/10.1016/j.foodcont.2014.10.002
7. V. Rastogi, K. Samyn, *Coatings*, **5**, 887 (2015).
8. W. Zhang, H. Xiao, L. Qian, *Carbohydrate Polymers*, **101**, 401 (2014).
9. N. Bordenave, S. Grelier, V. Coma, *Biomacromolecules*, **11**, 88 (2010).
10. H. Kjellgren, M. Gällstedt, G. Engström, L. Järnström, *Carbohydr. Polym.* **6**, 454 (2006).
11. H. Li. Y. Du, Y. Xu, *Appl. Polym. Sci*. **91**, 2642 (2004).
12. M. Gällstedt, M. S. Hedenqvist, *Carbohydr. Polym*. **63**, 46 (2006).
13. M. Laleg, I. I. Pikulik, *Nord Pulp Pap. Res*. **7**, 174 (1992)
14. H. Li, Y. Du, Y Xu, *J. Appl. Polym. Sci.* **91**, 2642 (2004).
15. M. Mucha, D. Miskiewicz, *J. Appl. Polym. Sci*. **77**, 3210 (2000).
16. A. M. A. Nada, M. El-Sakhawy, S. Kamel, M. A. M Eid, A. M. Adel, *Carbohydr. Polym.* **63**, 113 (2006).
17. S. C. M. Fernandes, C. S. R. Freire, A. J. D. Silvestre, C. P. Neto, A. Gandini, J. Desbriéres, S. Blanc, R. A. S. Ferreira, L. D. Carlos, *Carbohydr. Polym.* **78**, 760 (2009).
18. H. J. Park, S. H. Kim, S. T. Lim, D. H. Shin, S. Y. Choi, K. T. Hwang, *JAOCS*, **77,** 269 (2000).
19. T. Balan, C. Guezennec, R. Nicu, F. Ciolacu, E. Bobu, *Cellulose Chem. Technol*., **49**(7-8), 607 (2015).
20. S. Butkinaree1, T Jinkarn, R. Yoksan, *Journal of Metals, Materials and Minerals*, **18,** 219 (2008).
21. S. Zakaria, Ch. H. Chia, W. H. W. Ahmad, H. Kaco, S. W Chook, Ch. H. Chan, *Malaysian J. Anal. Sci.*, **44**(6) 905 (2015).
22. S. Kopacic, A. Walzl, A. Zankel, E. Leitner, W. Bauer, *Coatings*, **8**, 235 (2018) doi:10.3390/ coatings8070235
23. H. Li, R. Cui, L. Peng, Sh. Cai, P. Li, T. Lan, *Polymers*, **10**, 15 (2018) doi:10.3390/ polym10010015.
24. H. J. Park, S. H. Kim, S. T. Lim, D. H. Shin, S. Y. Choi, K. T. Hwang, *JAOCS*, **77**, 269 (2000).
25. L. Dai, Z. Long, *Zhe Jiang Zao Zhi*, **35**, 11 (2011).
26. J. M. Krochta, C. De Mulder-Johnston, *Food Technology*, **51**, 61 (1997).

Bulgarian Chemical Communications, Volume 52, Special Issue B (pp. 61-67) 2020 DOI: 10.34049/bcc.52 B 8

Investigation on differences in peel strength of the printed laminated paperboard

M. Pál[1], D. Novaković[1], N. Kašiković[1], S, Dedijer[1*], V. Zorić[1], I. Spiridonov[2], R. Boeva[2]

[1]*University of Novi Sad, Faculty of technical sciences, Department of graphic engineering and design, Novi Sad, Serbia*
[2]*University of Chemical Technology and Metallurgy, Department of Printing Arts, Pulp and Paper, Sofia, Bulgaria*

Received: November 30, 2019; Revised: October 13, 2020

Lamination process is one of the major surface enhancement techniques for print protection against mechanical surface damage, such as rubbing, tearing, scratching. Thus, the lamination process and its quality control are an active field of research, because it is significant for overall printed product quality assurance. The aim of the study is to investigate the differences in adhesive bond strength, i.e. peel strength of laminated printed sheets, depending on the used laminating film, printing color and employed digital printing machine tested via 180° peel adhesion testing. The samples were made from matte coated paperboard, printed by three different digital printing machines in full tone with the four process colors and laminated with two different polymer films (matte and gloss). The obtained results showed differences in peel strength caused not only by printing machine but also by laminating film, while a comprehensive statistical analysis proved that ink color had only partially influence on overall peel strength of laminated samples.

Keywords: peel strength, laminated paperboard, digital printing

INTRODUCTION

The lamination process, as one of the main surface enhancement techniques in the printing industry, is providing protection against stains, smudges and spills, fingerprints, grease, dirt, moisture or mechanical surface damage by applying a thin layer of polymer to paper or paperboard sheets. In general, lamination can be applied by heat or adhesion. Since the thermal application can provide a stronger and more durable bond than adhesion lamination, it is the most commonly used technique [1-3]. Lamination adds strength and stiffness to the printed substrates, improves their visual appearance by deepening and brightening the ink colors, making the printed images stand out more, while it does not impair or blemish the printing in any way. In addition, the lamination process is highly recommended for printed products with frequent use (for example: educational materials, book and brochure covers, business and membership cards, etc.). It increases the durability and protection from the wear and tear of everyday practices, such as creasing, tearing, scratching or sun damage, so they can withstand high levels of daily use [3, 4]. Other printed materials (such as operating instructions, safety signage, reusable tags, etc.), which have to be completely protected against dirt or moisture in damp or similar environment, usually get that laminating polymer film on both sides. The applied polymer films then often extended beyond the edge of the substrate, where the films can bond with each other. Thereby the printed substrate becomes totally enclosed in the polymer film, providing in that way, a tight seal which protects the printed material from dirt, moisture and other contaminants [5]. There are two basic types of thermal lamination foils, matte and gloss, but nowadays a new type of adaptable, silky finish foil is also present on the market. Along the proper protection, all these foils provide clear covering and make the printed text and illustration completely visible. However, due to the differences in the light reflection (matte foils absorb light, while gloss foils reflect it, and the silky ones are somewhere between them), these foils give different appearances to the printed substrates, so they should be selected accordingly to the required final look [4, 6]. Regardless of their surface characteristics, in general, thermal laminating foils are similarly constructed of a layer of the base film (polyester, nylon, polypropylene, vinyl, etc.) that is bonded to an adhesive layer [6].

The lamination process has been widely used on a broad range of substrates printed with conventional printing techniques (offset, rotogravure or flexography), but with the growing digital printing market, it is gaining importance in that field too, especially for the short-run high-quality graphic products. Digital printing technologies are increasing in popularity, mostly because of their effectiveness in short-run jobs at low costs and easy operational process. Electrophotography printing is one of the major digital printing technologies today, often called laser printing, since it is based on

* To whom all correspondence should be sent:
E-mail: dedijer@uns.ac.rs

electrostatic charges on photoconductor drum caused by a light source, most commonly a laser.

In this printing technique the inks are toner-based and after the creation of latent image on photoconductor drum, the image is transferred and permanently fixed to the surface of the substrate using heat and pressure mechanism (hot roll fuser) or radiant fusing technology (oven fuser). This way they melt and bond the toner particles into the printing substrate. The derived printing quality is excellent and in order to extend the image life on printed products, especially with frequent use, the lamination process is applied [3, 7-10].

When it comes to quality of lamination, good adhesion is a prime consideration. Adhesion strength or bond strength is one of the main properties of a laminate structure, and its quality assessment is mandatory, because a laminated film, which does not adhere to the printed substrate has no commercial value [11]. The peel test is a commonly used testing method for objective evaluation of adhesion strength or bond strength in thin and flexible laminates or flexible-bonded-to rigid specimen. In general, the procedure consists of a laminate bonded to a thick substrate (or another laminate) and the test is conducted by pulling the laminate off of the substrate at defined angle while recording the peeling force during debonding. It is usually performed on tensile testing machines in several different ways using various commercially available fixtures [12].

The adhesion strength between lamination film and printed materials is influenced by factors related to the printing process, such as printing method, the type of color, the amount of applied ink, and factors related to the lamination process and conditions, such as temperature, speed or nip pressure [11]. While, the factors of lamination process could be adjusted to the certain printed project based on the foil manufacturer's` recommendation, factors of printing process heavily depend on graphic design, selected substrate, printing technique, etc. which are related to a given product type.

In this light, an investigation was done on the adhesive bond strength (peel strength) of two laminating foils adhered to substrate printed with three different digital printing machines in full tone of the four process colors. The conducted research was aiming to explore the changes in adhesive bond strength of applied laminating foils depending on the ink color and the employed digital printing system, and the results are presented in this paper.

Materials and methods

For the purpose of this investigation, a commercially available, matte, double side coated paperboard has been chosen (NEVIA CS2 Art Board, Hainan Jinhai Pulp & Paper Co, China) with basis weight of 300 g/m^2. The selected paperboard is commonly used for fine printed products such as book and magazine covers, advertising materials, calendars, catalogues, postcards, etc. Its dimensional stability, surface properties and good ink absorption allow trouble-free printing not just with conventional printing techniques (offset, rotogravure, flexography, letterpress), but with digital printing techniques as well. The basic properties of selected paperboard are presented in Table 1 [13].

Table 1. Basic properties of selected paperboard

Parameter	Value
Basis weight [g/m^2]	300±9
Thickness [µm]	285±8
Roughness [µm]	≤2.5
Gloss [%]	30±5
Opacity [%]	98.5±1.5
Brightness [%]	89.5±1.5

For the laminating process a gloss and a silky matte thermal laminating foil was selected from the same manufacturer (Cosmo Films Limited, India). Both foils are BOPP based and have extrusion coated surfaces with low temperature melting resin, which enables the lamination of the film to paper products by heat and pressure. They are applicable with all kinds of printed and unprinted paper and paperboards like book covers, magazines, diaries, brochures, manuals, folders, photo albums etc. Their basic characteristics are given in Table 2 [14,15].

Table 2. Basic properties of selected thermal gloss and matte foils

Properties	BOPP Gloss	BOPP Matte
Product reference number	24 PCT-2(DL)	27 PCT-2(M-SIL) DL
Thickness [µm]	24	27
Unit weight [g/m^2]	22	22.5
Yield [m^2/kg]	45.4	44.4
Surface tension (min.) Ex-coated/Uncoated side [dynes/cm]	42/38	40/40
Gloss (45°) - Uncoated side [gardner]	>58	17-25
Lamination temperature [°C]	100 - 120	100 - 120

In order to investigate the effect of different printing machines, colors and foil types on the peel strength (bond strength) of laminated paperboard, a simple test form was prepared based on [11]. It included a blank, non-printed area, used as a referent area with no color (0%) and four printed patches covered in maximum density for each primary process color (100% C, 100% M, 100% Y i 100% K). The dimensions of printed and non-printed areas were determined based on the specimen`s parameters defined by FINAT standard FTM 1 Peel adhesion (180°) at 300 mm per minute [16]. It defines a 25 mm wide specimen with a minimum length of 175 mm in the direction of traction displacement. The dimensions of a single specimen and the design of complete test form are presented on Figure 1. Printing of the prepared test form was done on the following three digital printing machines: Xerox DocuColor 252 (hereafter referred to as Machine 1 or M1), Xerox Versant 80 (Machine 2 or M2), Konica Minolta C6000L (Machine 3 or M3).

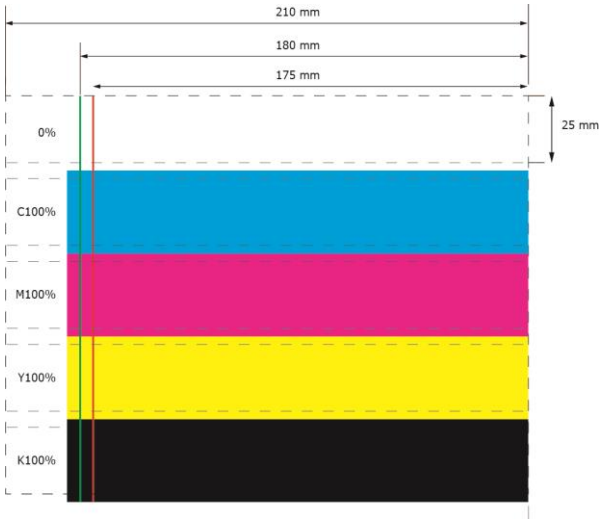

Fig. 1. The dimensions of a single specimen and the design of complete test form.

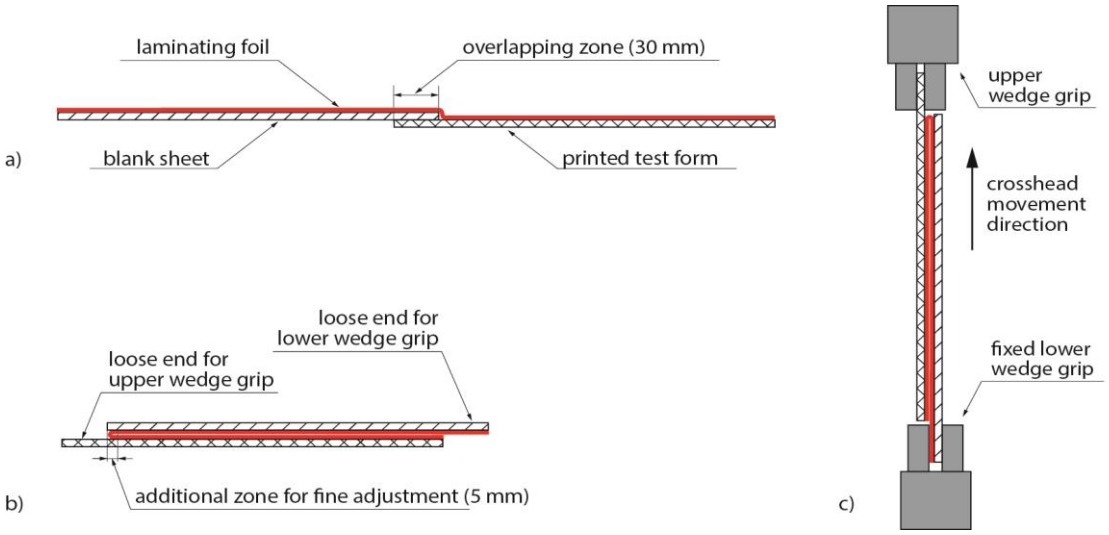

Fig. 2. Schematic overview of the sheet and foil placement (a), the final form of the prepared specimen (b) and its appearance during the peel testing (c)

The 180° peel test was conducted for all prepared laminated samples on a universal testing machine (Shimadzu EZ-LX table top, single column) using high-precision load cell (capacity of 500N, ISO 376 accuracy class 00) and non-shift wedge tensile grips (capacity of 5kN). The speed of traction displacement was constant at 300 mm/min, clamp length 175 mm, sampling frequency of 10 msec, break detection at 50% of maximum load. The testing was controlled and monitored via TRAPEZIUM X software (version 1.4.2, Shimadzu, Japan) in Single mode, peel test. During the peel test all the specimens were first placed into upper grip. After that, the starting line has been finely adjusted by separating manually the laminated foil from the substrate in the zone of additional fine adjustment (see Figure 2b). Afterwards, the specimens were placed into the lower grip. All the specimens had interfacial failure and the surface of the laminating foil looked clean after peeling. None of the specimens had paper failure (paper delamination, fiber tearing off, surface picking, etc.). All measurements were conducted in a controlled environment (at room temperature and standard relative air humidity) and the samples were conditioned for more than 48 hours prior to testing. 20 specimens were prepared for each printing machine, color and laminating foil combination.

Peel resistance is defined as the average force per unit of test specimen width, measured along the bond

line that is required to separate progressively two adherend layers of a bonded joint**.** According to the corresponding standards [20-22], the 180° peel strength is determined by using the following equation:

$$\text{Peel strength} = F/w \quad (1)$$

where F is the average peel force (N) and w is the width of the specimen (mm), however, in this paper the [N/25mm] unit was used due to the very low strength values.

Mean values and standard deviations of obtained peel strength values have been calculated for each specimen combination. In order to determine the statistical significance of the differences in the gained peel strength depending on the various sample characteristics (machine type, color and laminating foil), detailed statistical analyses were done by three-way ANOVA with additional two- and one-way ANOVA and the corresponding post hoc tests (Dunnett's T3 post hoc and Welsh and Brown-Forsythe test). Preliminary analyses were performed to ensure no violation of the assumptions of normality, linearity and homogeneity. All the statistical analyses were done using IBM SPSS statistics software (version 20), with an initial significance level of $p < 0.05$. Beside statistical significance, the effect sizes (the practical significance) were also determined for each post hoc test using partial eta squared [23].

RESULTS AND DISCUSSION

The obtained results were analyzed in three stages. First, the derived peel force versus distance curves were examined. In the second stage, the peel strength was analyzed regarding to different printing machines, printing colors and laminating foils, while the third stage was dealing with statistical analysis of differences in the obtained peel strength results. In the following section, results are presented in that manner.

Figure 3 shows a typical example of peel force versus distance curves of one set of investigated parameters (100% of cyan, laminated with matte foil and printed with machine M2). The chart contains 20 individual curves and the average curve, marked with bold red line.

From the presented chart, a couple of remarks can be noticed. First of all, there is no significantly higher peel force at the beginning of the curves. In other word no static strength (peak force to initiate failure) is detected, which suggests that the laminating structure had similar amount of melted resin or copolymer as adhesive over the entire surface of the specimens [24]. Secondly, the noisy, but approximately constant peel curves are referring to the interfacial or adhesive bond failure during peel test. Usually, that kind of bond failure is associated with lower peel rate (24, 25], however in this case, a peel rate of 300 mm/min also resulted in a clean foil delamination from the printed surface. It has to be noted, that although the length of tested specimens was 175 mm, the separation process doubled the overall stroke length, resulting in that excessively long distance or stroke value. Moreover, in some cases a slight foil elongation was noticed during peel test, thus adding more distance in that way to displacement of the measuring head. Furthermore, a comment had to be addressed to the sharp peel force value drop and raising near the end of peel curves, which are correlated to the sheet overlapping during the lamination process. For proper analysis of obtained results, we excluded these extremely high and low peel forces by cropping the peel force-displacement curve from 5 mm to 285 mm (see green bold line in Figure 3).

The obtained mean values of peel strength [N/25 mm] with corresponding standard deviation values for all specimen combination are presented on Figure 4a and b, grouped by laminating foils (gloss and matte), respectively.

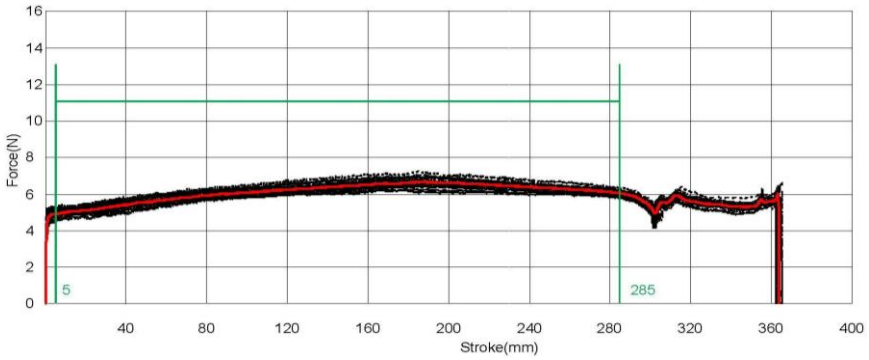

Fig. 3. An example of obtained individual peel curves (dotted black lines) and average peel curve (solid red line) for sample printed with 100% of cyan on machine M2 and laminated with matte foil

a)

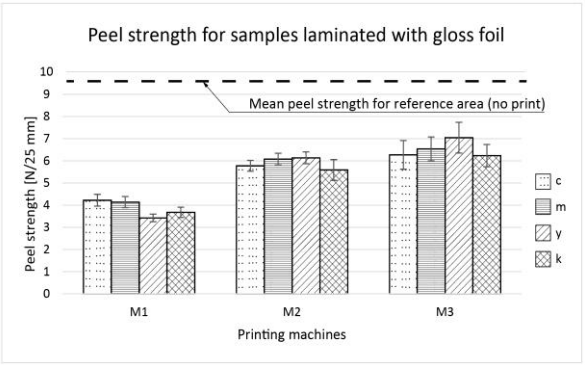

b)

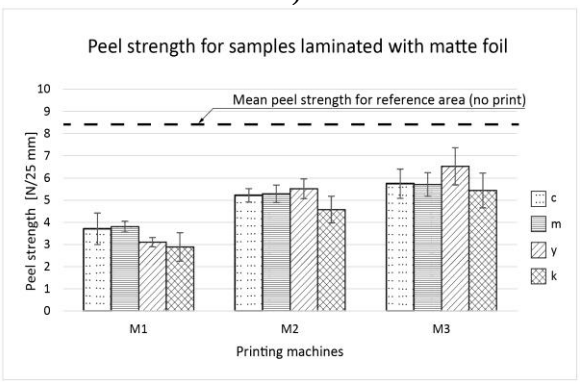

Fig. 4. Mean values of peel strength [N/25mm] with corresponding standard deviation values grouped by gloss (a) and matte laminating foil (b)

As it can be easily noticed from the presented figures, printing machine M1 gained far lower mean peel strength values that the other two printing machines, regardless of the laminating foil. The differences between the mean peel values between machine M2 and M3 were not that significantly expressed for any of the colors, especially cyan and magenta, however there are differences in favor of machine M3, for both laminating foils. By comparing the mean peel strength value of non-printed reference area (9.56 N/25 mm for gloss and 8.43 N/25mm for matte foil), all the observed specimen combinations give visibly lower peel strength values. The lowest mean peel strength value was 65.83% lower, while the highest one was 26.35% lower as well. Since all three printing machines are based on the same principles of electrophotography printing, similar outcomes were expected, which clearly was not the case.

Regarding the process colors, results have varied in relatively narrow range for both laminating foils. For machine M1, mean peel strength values were from 3.42 N/25 cm up to 4.22 N/25 cm for gloss foil and from 2.88 N/25 cm to 3.80 N/25 cm for matte foil. Machine M2 delivered values from 5.58 N/25 cm to 6.13 N/25 cm for gloss foil and from 4.57 N/25 cm to 5.51 N/25 cm for matte foil, while machine M3 had similar range with values of 6.23 N/25 cm ÷ 7.04 N/25 cm for gloss foil and 5.44 N/25 cm ÷ 6.53 N/25cm for matte foil. The low values of standard deviations indicate high consistency of measured values. The corresponding CV values were in most cases less than 10% or slightly above, except two samples for matte foil, printed with M1 machine, where the CV values were around 20%. Furthermore, it can be observed that black color delivered the lowest adhesive bond strength for almost all machines and foil combinations. The exception was the yellow color printed on machine M1 and laminated with gloss foil (3.42 N/25mm). Besides that, the yellow color from the same machine laminated with matte foil derived just slightly higher mean peel value that the black color. Unlike these results, in all other cases, yellow color made the laminate foils adhered the most, especially in the case of machine M3. In addition, it can be also noticed that cyan and magenta delivered very close peel strength values for all printing machines and foil combinations. On the one hand, these typically low values for black ink, and similar values for cyan and magenta, may suggest that the ink composition of applied printing colors could have an influence on the adhesive bond strength in the lamination process. However, on the other hand, the narrow range of obtained results indicates that the applied printing color had less influence on the peel strength than the printing machine or laminating foil.

Comparing the results by the laminating foils, it is showed that gloss foil delivered higher peel strength values for all samples, printed with any color on any machines, without exception. These results could be correlated with the literature findings, according to which gloss foils are more durable and provide a higher level of protection than matte ones [4].

Albeit, the presented graphs can deliver useful information about the differences in peel strength, but they do not set out whether these differences are statistically significant or not. In order to determine the statistical significance of the differences in the gained peel strength values depending on various printing and laminating parameters, statistical analyses were done by three-way ANOVA, with the additional set of two two-way and four one-way between-groups analysis of variance and corresponding post hoc test.

A three-way between-groups analysis of variance (at alpha level of .05) was used to explore the impact of laminating foil (gloss and matte), color (four process colors - cyan, magenta, yellow and black) and printing machine (M1, M2 and M3) on the mean peel strength value.

Statistically significant main effect (p value of .000) was established for all three factors, confirmed by large effect size (above .25). An interaction effect was also statistically significant in case of color and machine, color and foil as well as machine and foil (p value of .000, .000 and .002, respectively). On the other hand, a three-factor interaction effect (machine, foil and color) did perform statistically insignificant result (p value of .078 with small effect size - partial eta squared of 0.024) and observed power of 0.603, which cannot be treated as strong. Thus, significance value being just above the bound of .05 and knowing that the power of a test is very dependent on the size of the sample (individual group size was 20), where insignificant result can be a consequence of small group size, resulted three-factor interaction insignificant effect is recommended to be taken with caution.

When significant result for interaction effect is obtained, follow-up tests are needed in order to explore the relationships more in detail. The first performed test was a two-way between-groups analysis of variance (at alpha level of .05), which was used to explore the impact of laminating foil (gloss and matte) and color (cyan, magenta, yellow and black) on the mean peel strength value for each printing machine (M1, M2 and M3) separately. In case of each printing machine, there was a statistically significant main effect for laminating foil as well as color, with following large effect size: machine M1: laminating foil [F(1, 152)=66.91, p=.000, partial eta squared=0.31], color [F(3, 152)=44.95, p=.000, partial eta squared=0.47]; machine M2: laminating foil [F(1, 152)=324.07, p=.000, partial eta squared=0.68], color [F(3, 152)=60.33, p=.000, partial eta squared=0.54]; machine M3 laminating foil [F(1, 152)=86.73, p=.000, partial eta squared=0.36], color [F(3, 152)=34.48, p=.000, partial eta squared=0.40]. An interaction effect reached statistical significance in case of machines M1[F(3, 152)=5.36, p=.002, partial eta squared=0.96] and M2 [F(3, 152)= 16.24, p=.000, partial eta squared=0.24] while in case of machine M3 [F(3, 152)=0.5, p=.68, partial eta squared=.01] an interaction effect did not perform statistically significant result, but the observed power was extremely low (0.15), thus reached statistical insignificance must be taken with precaution.

According to literature findings [23], when significant result for interaction effect is obtained, which was our case, it is advisable to run follow-up tests to explore this relationship further. Thus, in order to get better insight into each machine and thus color impact on peel strength of laminated material, we have applied broadly used statistical test one-way ANOVA, for each printing machine and each laminating foil. In this analysis we adjusted the alpha level to .10, instead of the traditional .05 level, based on the finding that the power of a test is very dependent on the size of the sample, where the group size of 20 is characterized as small and can lead to wrong conclusion (non-significant result may be due to insufficient power) [23]. As a post hoc tests, we have used Dunnett's T3 post hoc test and Welsh and Brown-Forsythe test.

A one-way between-groups analysis of variance indicated a statistically significant difference at the $p<0.1$ level in mean peel strength of laminated material in case of all three printing machines (for all 4 process colors) and both laminating materials. In the case of gloss foil, the actual difference in mean scores between the groups was large [23]: the effect size, calculated using eta squared, was above 0.14: 0.81, 0.39 and 0.44 for machines M1, M2 and M3, respectively. Post-hoc comparisons using Dunnett's T3 post hoc test indicated that in the case of machine M1, only the mean value of peel strength for cyan process color (M=4.22, SD=0.18) did not differ significantly from mean value for magenta (M=4.13, SD=0.17). In case of machine M2, the mean value of peel strength for cyan process color (M=5.77, SD=0.19) did not differ significantly from mean value for black (M=5.58, SD=0.26) as well as magenta (M=6.07, SD=0.17) and yellow (M=6.13, SD=0.21). For machine M3, the mean value of peel strength for cyan process color (M=6.26, SD=0.47) did not differ significantly from mean value for black (M=6.23, SD=0.36) and magenta (M=6.53, SD=0.28) as well as magenta (M=6.53, SD=0.28) and black (M=6.23, SD=0.36). In all other cases, the mean values differ significantly.

In case of matte foil, the actual difference in mean scores between the groups was also large [23]: the effect size, calculated using eta squared, was above 0.14: 0.40, 0.66 and 0.39 for M1, M2 and M3, respectively. Post-hoc comparisons using Dunnett's T3 post hoc test indicated that in the case of machine M1, only the mean value of peel strength for cyan process color (M=3.70, SD=0.72) did not differ significantly from mean value for magenta (M=3.80, SD=0.25) as well as yellow (M=3.10, SD=0.13) and black (M=2.89, SD=0.65). In case of machine M2, only the mean value of peel strength for cyan process color (M=5.21, SD=0.18) did not differ significantly from mean value for magenta (M=5.28, SD=0.41). For machine M3, the mean value of peel strength for cyan process color (M=5.74, SD=0.49) did not differ significantly from mean value for black (M=5.44, SD=0.65) and magenta (M=5.70, SD=0.68) as well

as magenta (M=5.70, SD=0.68) and black (M=5.44, SD=0.65). In all other cases, the mean values differ significantly.

CONCLUSIONS

The lamination process is an excellent surface enhancement technique for print protection against grease, dirt, stains or different type of surface damage, like scratching, rubbing, tearing. Adhesive bond strength or bond strength is one of the main properties of a laminate structure, and its quality assessment is mandatory. This paper is dealing with differences in adhesive bond strength, i.e. peel strength of laminated printed sheets, depending on the used laminating film (gloss and matte), printing color (four process colors, cyan, magenta, yellow and black) and employed digital printing machine. The obtained results showed statistically significant difference at the $p<0.1$ level in mean peel strength of laminated samples in case of all three printing machines (for all four process colors) and both laminating foils. For both laminating foil, gloss and matte, the actual differences in mean peel values between the groups were large (all eta squared values were above 0.14), while according to the performed corresponding post hoc tests (Dunnett's T3), cyan color can stand out as one which does not differ significantly from other color or colors, regardless of printing machines or used foils. Based on the obtained results, it is clear that in order to get more insight into the nature of changes in peel strength values, additional and expanded investigation is needed. This subsequent investigation would include different substrates, papers and paperboards with different surface characteristics, printing techniques, ink compositions, tone values, etc., as influencing factors of printing process, but also different laminating machine set-up parameters.

Acknowledgement: *This work was supported by the Serbian Ministry of Science and Technological Development, Grant No.: 35027 "The development of software model for improvement of knowledge and production in graphic arts industry".*

REFERENCES

1. H. Chen, B. Jiang, Z-Q. Cai, *Polym. Adv. Technol*., **26**, 1065 (2014).
2. H. Kipphan, Handbook of Print Media - Technologies and Production Methods, Springer, 2001.
3. https://kaizenprint.co.uk/inspire-support/print-finishing-lamination/
4. https://www.printivity.com/insights/2019/07/09/comparing-matte-vs-gloss-lamination-for-printing/
5. https://www.formaxprinting.com/blog/2011/07/laminated-printing-the-many-benefits-and-uses-of-print-lamination/.
6. https://www.fespa.com/en/news-media/features/the-ultimate-laminating-guide-films-and-applications
7. M. Ataeefard, *Prog. Org. Coat*., **77**, 1376 (2014).
8. M. Ataeefard, *Pigm. Resin. Technol*., **44**(4), 232 (2015).
9. Đ. Vujčić, B. Ružičić, *J. Graph. Eng. Des*. **7**(2), 31 (2016).
10. I. Jurič, D. Ranđelović, I. Karlović, I.Tomić, *J. Graph. Eng. Des.* **5**(1), 17 (2014).
11. https://www.astm.org/Standards/ASTM F2296 - 04 (2012)
12. N. Padhye, D. M. Parks, A. H. Slocum, B. L. Trout, *Rev. Sci. Instrum*. **87**, 085111 (2016).
13. http://khushboopackaging.com/products/paper-boards/printing-papers-boards.html
14. https://www.cosmofilms.com/uploads/products/PCT-2%20(DL).pdf
15. https://www.cosmofilms.com/uploads/products/PCT-2%20(M-SIL)%20DL.pdf
16. http://www.adhesivetest.com/resources/docs/FinatTestMethods.pdf
17. https://www.office.xerox.com/latest/D60BR-01.PDF
18. https://www.office.xerox.com/latest/V80BR-01U.pdf
19. https://vipimex.com/files/files/bizhub_PRO_C6000L_General_Brochure.pdf
20. https://www.iso.org/standard/ISO 8510-2:2006
21. https://www.iso.org/standard/ISO 29862:2018
22. S.-H. Lee, S.-W. Yang, E.-S. Park, J.-Y. Hwang, D.-S. Lee, *Coatings*, **9**(1), 61 (2019).
23. J. Pallant, A step by step guide to data analysis using SPSS for Windows (Version 12), Allen & Unwin, 2005.
24. B. Zhao, R. Pelton, *J. Adhes. Sci. Technol*. **17**(6), 815 (2003)
25. B. Zhao, R. Pelton, *Tappi*, **3**(7), 3 (2004).

Instructions about Preparation of Manuscripts

General remarks: Manuscripts are submitted in English by e-mail The text must be typed on A4 format paper using Times New Roman font size 11, normal character spacing. The manuscript should not exceed 15 pages (about 3500 words), including photographs, tables, drawings, formulae, etc. Authors are requested to use margins of 2 cm on all sides

Manuscripts should be subdivided into labelled sections, e.g. **Introduction, Experimental, Results and Discussion**, *etc*. **The title page** comprises headline, author's names and affiliations, abstract and key words. Attention is drawn to the following:

a) **The title** of the manuscript should reflect concisely the purpose and findings of the work. Abbreviations, symbols, chemical formulas, references and footnotes should be avoided. If indispensable, abbreviations and formulas should be givenin parentheses immediately after the respective full form.

b) **The author**'s first and middle name initials and family name in full should be given, followedby the address (or addresses) of the contributing laboratory (laboratories). **The affiliation** of the author(s) should be listed in detail by numers (no abbreviations!). The author to whom correspondence and/or inquiries should be sent should be indicated by asterisk (*) with e-mail address.

The abstract should be self-explanatory and intelligible without any references to the text andcontaining not more than 250 words. It should be followed by key words (not more than six).

References should be numbered sequentially in the order, in which they are cited in the text. The numbers in the text should be enclosed in brackets [2], [5, 6], [9–12], etc., set on the text line. References are to be listed in numerical order on a separate sheet. All references are to be given in Latin letters. The names of the authors are given without inversion. Titles of journals must be abbreviated according to Chemical Abstracts and given in italics, the volume is typed in bold, the initial page is given and the year in parentheses. Attention is drawn to the following conventions:a) The names of all authors of a certainpublications should be given. The use of "*et al*." inthe list of references is not acceptable.b) Only the initials of the first and middle names should be given. In the manuscripts, the reference to author(s) of cited works should be made without giving initials, e.g. "Bush and Smith [7] pioneered...". If the reference carries the names of three or more authors it should be quoted as "Bush *et al*. [7]", if Bush is the first author, or as "Bush and co-workers [7]", if Bush is the senior author.

Footnotes should be reduced to a minimum. Each footnote should be typed double-spaced at thebottom of the page, on which its subject is first mentioned.**Tables** are numbered with Arabic numerals on the left-hand top. Each table should be referred to inthe text. Column headings should be as short as possible but they must define units unambiguously.The units are to be separated from the preceding symbols by a comma or brackets. Note: The following format should be used when figures, equations, *etc*. are referred to the text (followed by the respective numbers): Fig., Eqns., Table, Scheme.

Schemes and figures. Each manuscript should contain or be accompanied by the respective illustrative material as well as by the respective figure captions in a separate file (sheet).As far as presentation of units is concerned, SI units are to be used. However, some non-SI units are also acceptable, such as °C, ml, l, etc.The author(s) name(s), the title of the manuscript, the number of drawings, photographs, diagrams, etc., should be written in black pencil on the back of the illustrative material (hard copies) inaccordance with the list enclosed. Avoid using more than 6 (12 for reviews, respectively) figures in the manuscript. Since most of the illustrative materials are to be presented as 8-cm wide pictures, attention should be paid that all axis titles, numerals, legend(s) and texts are legible.

The authors are required to submit the text with a list of three individuals and their e-mail addresses that can be considered by the Editors as potential reviewers. Please, note that the reviewers should be outside the authors' own institution or organization. The Editorial Board of the journal is not obliged to accept these proposals.

The authors are asked to submit **the final text** (after the manuscript has been accepted for publication) in electronic form by e-mail. The main text, list of references, tables and figure captions should be saved in separate files (as *.rtf or *.doc) with clearly identifiable file names. It is essential that the name and version of the word-processing program and the format of the text files is clearly indicated. It is recommended that the pictures are presented in *.tif, *.jpg, *.cdr or *.bmp format.

The equations are written using “Equation Editor” and chemical reaction schemes are written using ISIS Draw or ChemDraw programme.

EXAMPLES FOR PRESENTATION OF REFERENCES

REFERENCES

1. D. S. Newsome, *Catal. Rev.–Sci. Eng*., **21**, 275 (1980).
2. C.-H. Lin, C.-Y. Hsu, *J. Chem. Soc. Chem. Commun*., 1479 (1992).
3. R. G. Parr, W. Yang, Density Functional Theory of Atoms and Molecules, Oxford Univ. Press, New York, 1989.
4. V. Ponec, G. C. Bond, Catalysis by Metals and Alloys (Stud. Surf. Sci. Catal., vol. 95), Elsevier, Amsterdam, 1995.
5. G. Kadinov, S. Todorova, A. Palazov, in: New Frontiers in Catalysis (Proc. 10th Int. Congr. Catal., Budapest,(1992), L. Guczi, F. Solymosi, P. Tetenyi (eds.), Akademiai Kiado, Budapest, 1993, Part C, p. 2817.
6. G. L. C. Maire, F. Garin, in: Catalysis. Science and Technology, J. R. Anderson, M. Boudart (eds), vol. 6, SpringerVerlag, Berlin, 1984, p. 161.
7. D. Pocknell, *GB Patent* 2 207 355 (1949).
8. G. Angelov, PhD Thesis, UCTM, Sofia, 2001, pp. 121-126.
9 JCPDS International Center for Diffraction Data, Power Diffraction File, Swarthmore, PA, 1991.
10. CA **127**, 184 762q (1998).
11. P. Hou, H. Wise, *J. Catal.*, in press.
12. M. Sinev, private communication.
13. http://www.chemweb.com/alchem/articles/1051611477211.html.

Texts with references which do not match these requirements will not be considered for publication!!!

Selected papers from the 10th Jubilee National Conference on Chemistry, Sofia, September 26-28, 2019

CONTENTS